

UNCLASSIFIED

AD NUMBER

ADB004162

LIMITATION CHANGES

TO:

Approved for public release; distribution is unlimited.

FROM:

Distribution authorized to U.S. Gov't. agencies only; Test and Evaluation; DEC 1974. Other requests shall be referred to Air Force Flight Dynamics Laboratory, Wright-Patterson AFB, OH.

AUTHORITY

AFFDL ltr, 27 Dec 1977

THIS PAGE IS UNCLASSIFIED

THIS REPORT HAS BEEN DELIMITED
AND CLEARED FOR PUBLIC RELEASE
UNDER DOD DIRECTIVE 5200.20 AND
NO RESTRICTIONS ARE IMPOSED UPON
ITS USE AND DISCLOSURE,

DISTRIBUTION STATEMENT A

APPROVED FOR PUBLIC RELEASE;
DISTRIBUTION UNLIMITED,

AD B 004162

AFFDL-TR-74-137



**ANALYSIS/THEORY OF CONTROLLED
CONFIGURED STRUCTURES**

VOUGHT SYSTEMS DIVISION
LTV AEROSPACE CORPORATION

Bo

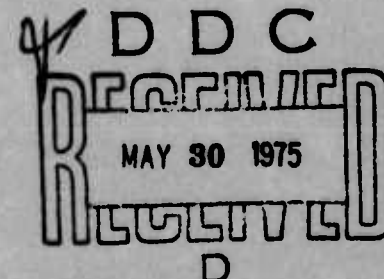
AD No.
DDC FILE COPY

TECHNICAL REPORT AFFDL-TR-74-137

DECEMBER 1974

FINAL REPORT FOR PERIOD MAY 1974 - DECEMBER 1974

Distribution limited to Government agencies only; test and evaluation data;
December 1974. Other requests for this document must be referred to
AFFDL (FBS), Wright-Patterson Air Force Base, Ohio 45433.



AIR FORCE FLIGHT DYNAMICS LABORATORY
AIR FORCE SYSTEMS COMMAND
WRIGHT-PATTERSON AIR FORCE BASE, OHIO 45433

ACCESSION for	
NTIS	White Section <input type="checkbox"/>
DDC	Buff Section <input checked="" type="checkbox"/>
UNANNOUNCED	<input type="checkbox"/>
JUSTIFICATION.....	

NOTICE

BY.....
DISTRIBUTION/AV.

Dist. AVAIL

3

When Government drawings, specifications, or other data are used for any purpose other than in connection with a definitely related Government procurement operation, the United States Government thereby incurs no responsibility nor any obligation whatsoever; and the fact that the government may have formulated, furnished, or in any way supplied the said drawings, specifications, or other data, is not to be regarded by implication or otherwise as in any manner licensing the holder or any other person or corporation, or conveying any rights or permission to manufacture, use, or sell any patented invention that may in any way be related thereto.

This technical report has been reviewed and is approved for publication.

George T. Estill

George T. Estill
Aerospace Engineer
Structures Development
and Integration Group

Francis V. Janik, Jr.

Francis V. Janik, Jr.
Chief, Structural Development Branch
Structures Division

Copies of this report should not be returned unless return is required by security considerations, contractual obligations, or notice on a specific document.

UNCLASSIFIED

SECURITY CLASSIFICATION OF THIS PAGE (When Data Entered)

REPORT DOCUMENTATION PAGE		READ INSTRUCTIONS BEFORE COMPLETING FORM
1. REPORT NUMBER AFFDL-TR-74-137	2. GOVT ACCESSION NO.	3. RECIPIENT'S CATALOG NUMBER
4. TITLE (and Subtitle) ANALYSIS/THEORY OF CONTROLLED CONFIGURED STRUCTURES.		5. TYPE OF REPORT & PERIOD COVERED Final Report 23 May 1974 - 23 Dec 74
7. AUTHOR(s) J. G. Williams		6. PERFORMING ORG. REPORT NUMBER 2-534437
9. PERFORMING ORGANIZATION NAME AND ADDRESS Vought Systems Division LTV Aerospace Corporation P. O. Box 5907 Dallas, Texas 75222		8. CONTRACT OR GRANT NUMBER(s) F33615-74-C-3088
11. CONTROLLING OFFICE NAME AND ADDRESS Air Force Flight Dynamics Laboratory Wright-Patterson AFB, Ohio		10. PROGRAM ELEMENT, PROJECT, TASK AREA & WORK UNIT NUMBERS AF-1368 136802
14. MONITORING AGENCY NAME & ADDRESS (if different from Controlling Office) N/A		12. REPORT DATE Dec 1974 13. NUMBER OF PAGES 98
16. DISTRIBUTION STATEMENT (of this Report) Distribution limited to government agencies only; test and evaluation data; December, 1974. Other requests for this document must be referred to AFFDL (FBS), Wright-Patterson AFB, Ohio 45433		15. SECURITY CLASS. (of this report) Unclassified 15a. DECLASSIFICATION/DOWNGRADING SCHEDULE
17. DISTRIBUTION STATEMENT (of the abstract entered in Block 20, if different from Report) N/A		DDC RECEIVED MAY 86 1975 REGULATED D
18. SUPPLEMENTARY NOTES N/A		
19. KEY WORDS (Continue on reverse side if necessary and identify by block number) Structural re-arrangement built-in twist Wing twist induced "kick" loads Load dependent twist control configured structure elastic axis shift		
20. ABSTRACT (Continue on reverse side if necessary and identify by block number) The purpose of this program was to develop an analytical base and define the potential advantages for configuring aircraft wing structure to conform to predetermined displacements and twists when subjected to flight loads. An advanced fighter wing was selected as a baseline and several alternate internal structural arrangements were formulated for a comparison. All work was done using aluminum materials. Comparisons were made between the		

DD FORM 1 JAN 73 1473

EDITION OF 1 NOV 65 IS OBSOLETE
S/N 0102-014-6601

UNCLASSIFIED

SECURITY CLASSIFICATION OF THIS PAGE (When Data Entered)

408116 ✓

UNCLASSIFIED

SECURITY CLASSIFICATION OF THIS PAGE(When Data Entered)

baseline and alternate designs after each was optimized for strength utilizing identical allowable stresses.

This study indicated that Controlled Configured Structure (CCS) does produce desirable wing twist under applied maneuver loading which show an advantage over conventional structure by improving aerodynamic characteristics (lower drag and inboard CP shift). These characteristics were shown to be achievable with essentially no weight or cost penalty and no effective change in flutter speed. The potential of combining passive airload induced twist and camber was projected.

UNCLASSIFIED

SECURITY CLASSIFICATION OF THIS PAGE(When Data Entered)

FOREWORD

This technical report covers all work performed by Vought Systems Division of LTV Aerospace Corporation, Dallas, Texas under contract F33615-74-C-3088, from 23 May 1974 to 23 December 1974. This report was submitted by the authors in December 1974 for publication.

This contract with Vought Systems Division was initiated under AFFDL Project 1368, Task 136802/Work Unit 13680220, "Analysis/Theory of Controlled Configured Structures." It was accomplished under the technical direction of Mr. George Estill (AFFDL/FBS), Air Force Flight Dynamics Laboratory, Wright-Patterson Air Force Base, Ohio.

The program was conducted under the supervision of Mr. G. A. Starr, Director of Engineering Technical R&D for Vought Systems Division. The program Project Engineer was Mr. S. W. McClaren and the Principal Investigator was Mr. J. G. Williams, Structures Applied Research.

The author acknowledges the technical contributions of Messrs. M. A. Bell - Aerodynamics, T. L. Green - Dynamics, S. D. Gratke and R. H. Dyer - Structures Methods, L. M. Wilshire - Value Engineering, C. D. Chumley - Weights, R. N. Rainey - Product Design and M. M. Desens - Technical illustrations. In addition, the technical direction of Mr. W. A. Poindexter and Mr. P. E. Browne is specifically recognized; since Mr. Poindexter can be credited with the initial conceptual ideas related to Control Configured Structures.

TABLE OF CONTENTS

	<u>Page</u>
1.0 INTRODUCTION	1
2.0 DISCUSSION OF CCS THEORY	5
3.0 DEVELOPMENT AND ANALYSIS OF CONCEPTS	9
3.1 Structural Arrangements that Induce Twist	9
3.2 Aerodynamic Analysis and Load Distribution	23
3.3 Aeroelastic Analysis of Center of Rotation Shift	25
4.0 EVALUATION OF CONCEPT PARAMETERS	27
4.1 Structures Evaluations	27
4.2 Aerodynamics Evaluations	41
4.3 Dynamics Evaluations	47
4.4 Cost Comparisons	53
5.0 CONCLUSIONS	57
6.0 RECOMMENDATIONS	59
7.0 REFERENCES	65
APPENDICES	
A. Structural Analysis Methods	67
B. Aerodynamics Analysis Methods	69
i. Parametric Study	69
2. Analysis Methods	95
C. Dynamics Analysis Methods	97

LIST OF ILLUSTRATIONS

<u>No.</u>	<u>Title</u>	<u>Page</u>
1	FLIGHT LOADS REACTED IN CCS WING BENDING MEMBERS	6
2	ILLUSTRATION OF ROTATIONAL AXIS SHIFT IN CCS STRUCTURE VS. CONVENTIONAL STRUCTURE	7
3	MAIN BOX CONFIGURATION FOR BASELINE DESIGN	10
4	ADVANCED FIGHTER WING PLANFORM FOR THIS CCS STUDY	11
5	MAIN BOX CONFIGURATION FOR ALTERNATE DESIGN NO. 1	12
6	MAIN BOX CONFIGURATION FOR ALTERNATE DESIGN NO. 3	13
7	POSITIVE LIMIT (7.5g) LOADS FOR BASELINE DESIGN	15
8	NEGATIVE LIMIT (-2.5g) LOADS FOR BASELINE DESIGN	16
9	POSITIVE LIMIT (7.5g) LOADS FOR ALTERNATE DESIGNS	17
10	NEGATIVE LIMIT (-2.5g) LOADS FOR ALTERNATE DESIGNS	18
11	BUILT IN TWIST FOR BASELINE DESIGN	19
12	MAIN BOX CONFIGURATION FOR ALTERNATE DESIGN NO. 2F	21
13	MAIN BOX CONFIGURATION FOR ALTERNATE DESIGN NO. 2A	22
14	COMPARATIVE TWISTS FOR THE BASELINE DESIGN AND ALTERNATE DESIGNS NO. 1 AND NO. 3	28
15	AVERAGE DEFLECTIONS OF MODELS AT ULTIMATE LOAD	30
16	COMPARATIVE TWISTS FOR ALTERNATE DESIGNS NO. 1, NO. 2A AND NO. 2F (AT ULTIMATE LOAD)	32
17	COMPARATIVE TWISTS FOR THE BASELINE DESIGN AND ALTERNATE DESIGN NO. 2F 4g LOAD AT MACH NO. 1.2	33
18	COMPARATIVE TWISTS FOR THE BASELINE DESIGN AND ALTERNATE DESIGN NO. 2F 4g LOAD AT MACH NO. 0.80	34
19	TWIST VERSUS POSITIVE LOAD FACTOR FOR THE BASELINE DESIGN AND ALTERNATE DESIGN NO. 2F	35
20	COMPARATIVE TWISTS FOR THE BASELINE DESIGN AND ALTERNATE DESIGN NO. 2F (NEGATIVE LOADS AT MACH NUMBER 1.2)	37
21	COMPARATIVE DEFLECTIONS FOR THE BASELINE DESIGN AND ALTERNATE DESIGN NO. 2F (NEGATIVE LOADS AT MACH NUMBER 1.2)	38
22	MATH MODEL WEIGHT TRENDS	40
23	COMPARISON OF STRUCTURAL TWIST FOR A 4g FLIGHT CONDITION WITH FIXED TWIST USED IN STUDY	42
24	EFFECT OF FLEXIBILITY ON LIFT AND PITCHING MOMENT - ALTERNATE DESIGN NO. 2F	43
25	COMPARISON OF DRAG POLARS FOR THE BASELINE DESIGN AND ALTERNATE DESIGN NO. 2F	45

LIST OF ILLUSTRATIONS (CONT'D)

<u>No.</u>	<u>Title</u>	<u>Page</u>
26	FLUTTER SPEED VS DAMPING FOR THE BASELINE DESIGN AND ALTERNATE DESIGNS NO. 1 AND NO. 3	48
27	MODE SHAPES AND FREQUENCIES FOR THE BASELINE DESIGN	49
28	MODE SHAPES AND FREQUENCIES FOR ALTERNATE DESIGN NO. 1	50
29	MODE SHAPES AND FREQUENCIES FOR ALTERNATE DESIGN NO. 3	51
30	EFFECT OF CAMBER ON BASELINE EQUILIBRIUM TWIST 4g CONDITION AT MACH NUMBER 1.20	62
31	CCS TECHNOLOGY DEVELOPMENT SEQUENCE	63
32	FLOW DIAGRAM FOR STRUCTURAL METHODS EMPLOYED IN CCS ANALYSIS	68
33	COMPARISON OF THEORETICAL PREDICTIONS WITH WIND TUNNEL DATA	72
34	NON-LINEAR DRAG POLAR - COMPUTER DATA VS WIND TUNNEL DATA	73
35	COMPARISON OF THEORETICAL PREDICTIONS WITH WIND TUNNEL DATA	75
36	NOMINAL VALUES OF TWIST AND CAMBER USED IN PARAMETRIC ANALYSIS	77
37	WING PLANFORM GEOMETRY	78
38	EFFECT OF SPANWISE TWIST VARIATION ON DRAG POLAR SHAPE	79
39	EFFECT OF TWIST ON DRAG VALUES	80
40	EFFECT OF SPANWISE TWIST VARIATION OF LIFT AND PITCHING MOMENT	82
41	EFFECT OF TWIST AND CAMBER ON ZERO LIFT PITCHING MOMENT	83
42	SPANWISE LOCATION OF PANEL LOADING - MACH NUMBER 0.80	84
43	SPANWISE LOCATION OF PANEL LOADING - MACH NUMBER 1.20	85
44	EFFECT OF CONICAL CAMBER ON DRAG POLAR SHAPE	87
45	EFFECT OF CONICAL CAMBER ON MINIMUM DRAG VALUES	89
46	EFFECT OF CONICAL CAMBER ON LIFT AND PITCHING MOMENT	90
47	EFFECT OF COMBINED CAMBER AND TWIST ON LIFT AND PITCHING MOMENT - MACH NUMBER 0.80	93
48	EFFECT OF COMBINED CAMBER AND TWIST ON LIFT AND PITCHING MOMENT - MACH NUMBER 1.20	94
49	FLOW DIAGRAM FOR AERODYNAMIC METHODS EMPLOYED IN CCS ANALYSIS	96
50	FLOW DIAGRAM FOR DYNAMICS METHODS EMPLOYED IN CCS ANALYSIS	98

LIST OF TABLES

<u>No.</u>	<u>Title</u>	<u>Page</u>
I	DESIRABLE TWIST/CAMBER CHARACTERISTICS	2
II	STATUS AND CHARACTERIZATION OF CONTROL CONFIGURED STRUCTURES (CCS) TECHNOLOGY REQUIREMENTS	4
III	OPTIMIZATION PROCESS ALLOWABLES AND MINIMUMS	14
IV	WEIGHT BREAKDOWN AND COMPARISON FOR ALL DESIGNS	29
V	FLEXIBLE AERODYNAMIC COEFFICIENTS USED IN FLUTTER CALCULATIONS	52
VI	COST COMPARISONS OF CONTROL CONFIGURED STRUCTURE (CCS) MAIN WING BOXES WITH A CONVENTIONAL WING BOX	54
VII	PROJECTED PERFORMANCE IMPROVEMENTS OVER CONVENTIONAL WINGS	61

1.0 INTRODUCTION

Today's aircraft are required to go faster, further and be more maneuverable increasing the need for high performance wings to perform optimally in all phases of the flight envelope. This requires that a wing be thin for high speeds, cambered for increasing lift at low speeds and during maneuvers, and usually requires that built-in twist be utilized to prevent tip stall at high angles of attack. This study addresses wing structural arrangements which produce a desired wing twist "wash out" when maneuver loads are applied. The unique arrangement of the wing spars and stiffeners will induce twist in the wing section in a direction which is advantageous for aerodynamic characteristics in most flight regimes.

This study undertook to rearrange the internal structure of an advanced fighter aircraft wing in a manner to produce desired twist under flight loads. Four alternate structural configurations were studied. Each was optimized for strength at ultimate load and evaluated for aerodynamic payoffs at two "4g" flight conditions. One condition produced a forward aerodynamic center of pressure and the other produced an aft aerodynamic center of pressure location. The results of these evaluations are compared with a baseline conventional structure at the same conditions and the potential payoffs defined.

It should be noted that this study evaluated a very small portion of an advanced fighter envelope ($MN = 0.8$ and 1.2 at $4g$'s symmetrical) and investigated only the twist aspect of the wing. Results indicates that further study at other points of the V-N diagram should be investigated and that the combination of this twist with wing camber can produce aerodynamic advantages much greater than those gained by twist alone.

Table I illustrates desirable characteristics that the structures and aerodynamics engineer strive to obtain. The readers attention is directed to careful study of where twist alone is desirable, where camber alone is of benefit and where twist and camber combinations should be used to multiply individual effects. While Table I describes the overview objective for

TABLE I: DESIRABLE TWIST/CAMBER CHARACTERISTICS

MACH NUMBER		0.4 ————— 0.7	0.85 ————— 1.00	1.00 ————— 1.30	1.30 ————— 2.5
MISSION SEGMENT	LER -	LARGE	MODERATE	MODERATE	SHARP
	t/c	THICK	MODERATE - TO THIN	THIN	THIN
1 "G" FLIGHT	Λ_{le}	NONE	HIGH	HIGH	LITTLE EFFECT UNLESS Λ_{le} IS VERY HIGH
	TWIST	NONE TO SMALL	NONE TO SMALL	MODERATE	MODERATE
	CAMBER	MODERATE	MODERATE	ZERO	ZERO
	TWIST	HIGH	HIGH	HIGH	HIGH
MANEUVER	CAMBER	LARGE	LARGE	LOW TO MODERATE	LOW

LER=LEADING EDGE RADIUS

t/c =THICKNESS RATIO

Λ_{le} =LEADING EDGE SWEEP

performance, Table II illustrates how the study is related to this overview objective. This study focused on structural and aerodynamic characteristics for Control Configured Structures (CCS) for twist only. Table II presents the technology requirements for combining twist and camber benefits and illustrate areas for other in-depth parametric analysis that are needed to establish total design envelope benefits. Completion of work tasks illustrated in Table II would then allow evaluation of total CCS performance values. For example the blocks on Table II that are emphasized in "heavy outline" cover the scope of this contract. The blocks of Table II outlined by a "dashed line" illustrate the general scope for the next proposed CCS effort, while the blocks denoted by "bullets" illustrate efforts that still need evaluation before all the aspects of CCS can be understood.

TABLE II : STATUS AND CHARACTERIZATION OF CONTROL CONFIGURED STRUCTURES
(CCS) TECHNOLOGY REQUIREMENTS

	STRUCTURES CHARACTERISTICS	AERODYNAMIC CHARACTERISTICS	AERODYNAMIC PERFORMANCES	STRUCTURAL * EVALUATION
CCS TWIST ONLY	STUDIED IN CONTRACT F33615-74-C-3088 (POINT DESIGN)	STUDIED IN CONTRACT F33615-74-C-3088 (POINT DESIGN)	WORK REQUIRED ● FLIGHT BOUNDARY PARAMETRICS	WORK REQUIRED ● WEIGHT/COST RESULTS FROM FLIGHT BOUNDARY PARAMETRIC STUDY
CCS TWIST PLUS ACTIVE CAMBER	TWIST AVAILABLE FROM CONTRACT F33615-74-C-3088 (POINT DESIGN)	AVAILABLE FROM VSD IR&D VARIABLE CAMBER EFFORTS (POINT DESIGN)	WORK REQUIRED ● FLIGHT BOUNDARY PARAMETRICS	WORK REQUIRED ● WEIGHT/COST RESULTS FROM FLIGHT BOUNDARY PARAMETRIC STUDY
CCS TWIST PLUS PASSIVE CAMBER	PROPOSED FOR STUDY IN FOLLOW-ON EFFORT (POINT DESIGN)	PROPOSED FOR STUDY IN FOLLOW-ON EFFORT (POINT DESIGN)	WORK REQUIRED ● FLIGHT BOUNDARY PARAMETRICS	WORK REQUIRED ● WEIGHT/COST RESULTS FROM FLIGHT BOUNDARY PARAMETRIC STUDY

DEFINITIONS: CCS-CONTROL CONFIGURED STRUCTURES

ACTIVE-PILOT ACTUATED

PASSIVE-AIRLOAD ACTUATED (NO PILOT INPUT)

*TOTAL VEHICLE EVALUATION

2.0 DISCUSSION OF CONTROL CONFIGURED STRUCTURES (CCS) THEORY

The orientation of the spar/stringer substructure elements is normally parallel to the structural elastic axis for most wing designs. This arrangement allows the primary bending loads to be reacted by the axial elements with very little out of plane "kick" load being generated which induce additional shear loads in the skins. This structural arrangement makes the twist of the wing completely dependent on the local air load center of pressure, the relative stiffnesses of the front and rear spars and wing sweep angle. Consequently, adverse wing twist under flight loading is a definite problem that can be partially relieved only by the addition of structural stiffness with its weight penalty or a built-in twist which decreases cruise efficiency.

The basic proposition of the CCS theory in main wing box structure is that the internal structure be rearranged so that the spars/stringers substructure members are not necessarily parallel to the usual elastic axis, but at some angle to it. This effect induces shear loads into the skins that tend to twist the wing in direct proportion to the applied bending loads and to the angle at which the bending elements intersect the applied load reference axis. In general, the CCS bending elements have more forward sweep than conventional wing bending elements inducing shear loads in the skin which rotate the wing leading edge down under positive loading. Figure 1 illustrates how this loading occurs. This desired rotation tends to reduce the tip stall problem, at higher angles of attack, which is associated with conventional structure. These induced shear loads must be considered when a shear center (elastic axis) calculation is made, thus an apparent shear center is located forward of the usual shear center. This causes the apparent center of rotation to move forward of the wing structural box producing a nose down rotation under positive bending loads as shown in Figure 2. Although not investigated in depth in this study, the benefits derived for positive loading cases would also apply to negative loadings.

In this report, the following definitions are applicable:

- o Control Configured Structure: Structure whose internal arrangement is so oriented to produce displacements and rotations advantageous

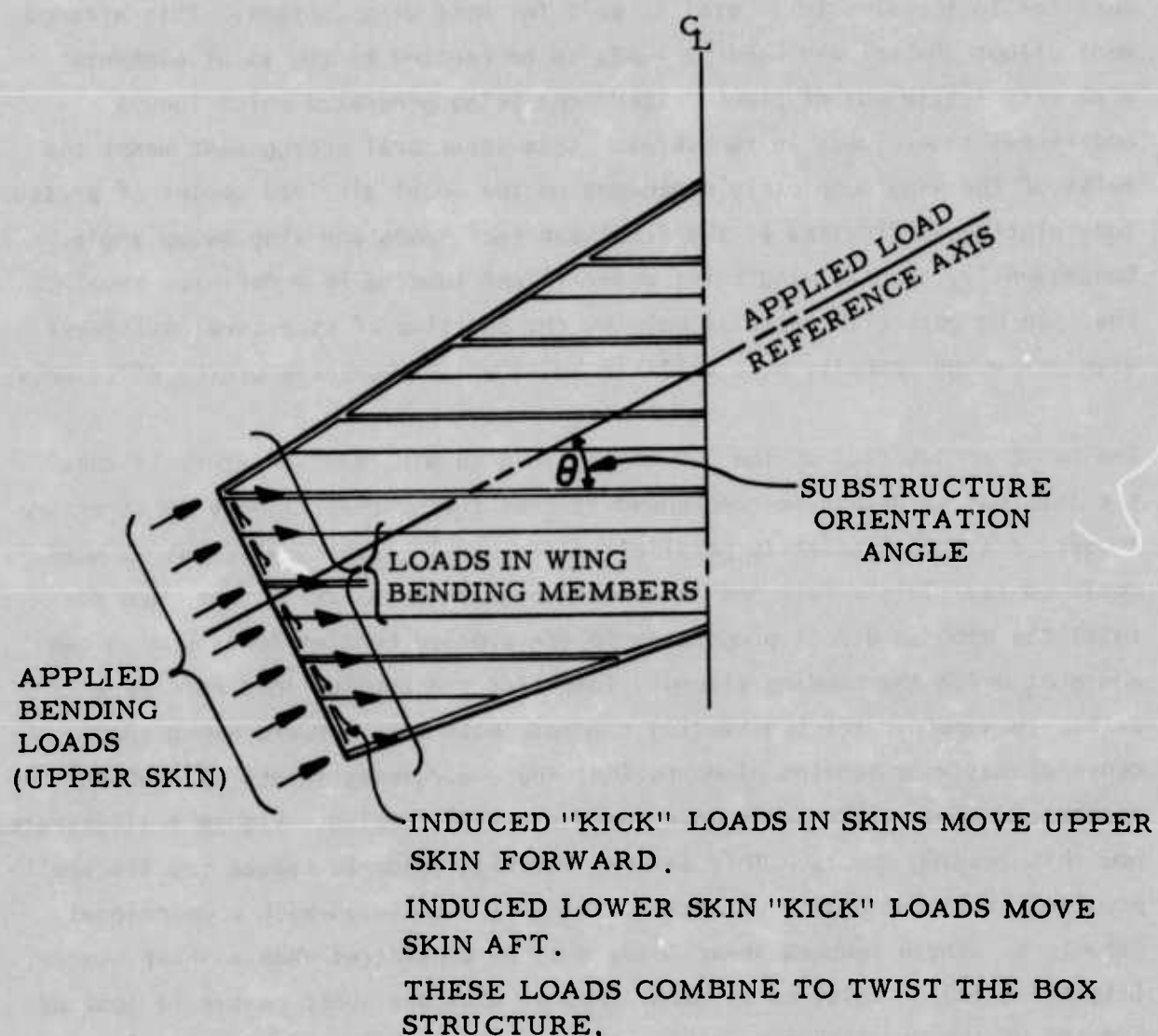
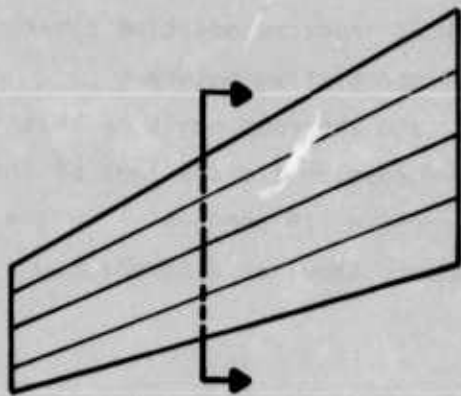
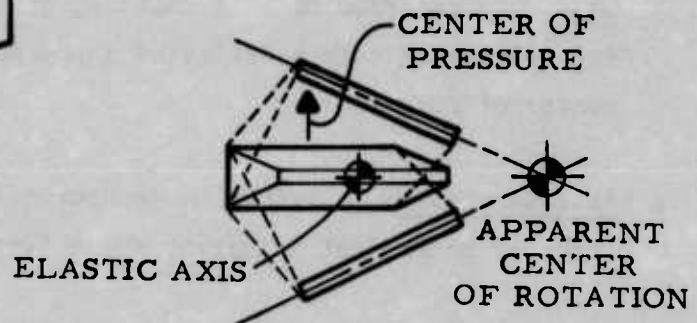


FIGURE 1: FLIGHT LOADS REACTED IN CCS WING BENDING MEMBERS

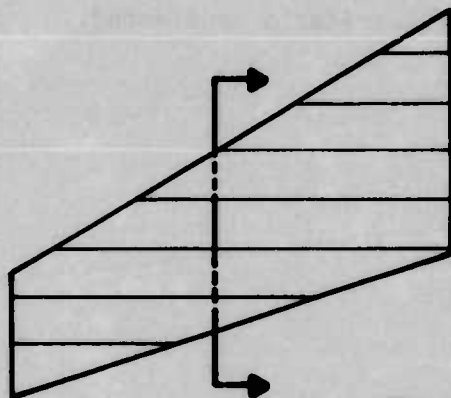
CONVENTIONAL



CONVENTIONAL



C C S



C C S

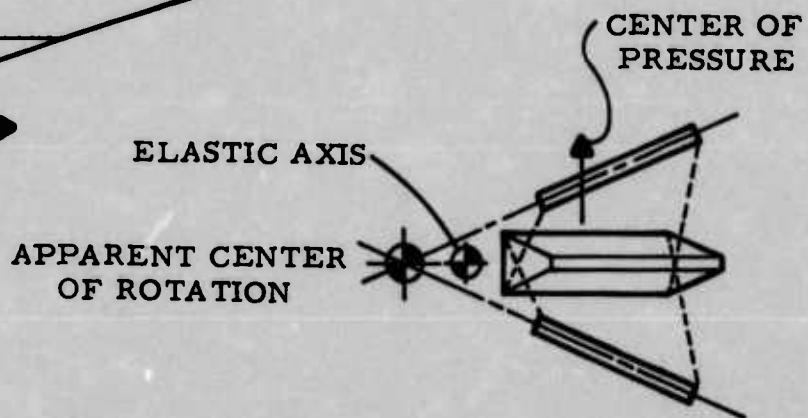


FIGURE 2: ILLUSTRATION OF ROTATIONAL AXIS SHIFT IN C C S STRUCTURE VS. CONVENTIONAL STRUCTURE

to aerodynamic performance as a function of applied loading. The CCS internal structural arrangement is such that a bending load produces both tension or compression in some structural elements and the shear components resulting from this bending load produces additive shear flow that warps the wing main box. In a correlative nature a torsion load produces torsion of the box and the components of this torsion produces relieving tension or compression translations of the box . . . referred to as a coupling of torsion and bending . . . the deformation of such a deflected shape occurs about an apparent new center of rotation.

- o Passive System: A system whose operation is not dependent on pilot input or mechanical actuation but a function of loading.
- o Active System: A system whose operation is dependent on pilot input or mechanical actuation.
- o Strength Design: Sizing of structural elements for strength (allowable stress) only with no stiffness criteria considered.

3.0 DEVELOPMENT AND ANALYSIS OF CONCEPTS

3.1 STRUCTURAL ARRANGEMENTS THAT INDUCE TWIST

The primary objective of this Control Configured Structures (CCS) effort was to achieve leading edge down twist with the wing subjected to positive bending loads. This was accomplished by orienting the sub-structure bending members (spars and stringers) to introduce "kick load" shears into the wing skins which deflected the wing torsionally. The magnitude of this induced torsional twist was a function of the angle at which the bending members intersect the applied load reference axis.

This study used an advanced fighter wing main box design and structural arrangement, shown in Figure 3, as a baseline configuration for comparison to the restructured CCS alternate designs. Figure 4 shows the total wing planform with pertinent data with the main structural box (shaded) which was internally reconfigured. Two alternate structural arrangements were used for the initial structural evaluation: Alternate Design No. 1, shown in Figure 5, which located the spars and stringers at right angles to the aircraft centerline and Alternate Design No. 3, shown in Figure 6, had the bending elements at various angles (45° at the tip to 90° at the root) relative to the aircraft centerline. These two alternate designs and the baseline design were optimized by computer (NASTRAN and peripheral programs, see Appendix A) for strength requirements (no stiffness criteria) at comparable ultimate loading conditions. The allowable stresses and minimum thickness and the area data are shown in Table III and reflect generally applicable limits of fatigue and compression stability stresses and manufacturing/service use minimum areas and thicknesses. The wing loading conditions that were used were those representative of a typical advanced fighter for a balanced symmetrical maneuver. Figures 7 and 8 show the positive and negative limit loads for the Baseline Design. The positive and negative loads for the alternate designs are shown in Figures 9 and 10. The applied loading conditions were not identical, since the Baseline Design incorporated a built-in leading edge down "wash out" (twist) to the degree shown in Figure 11.

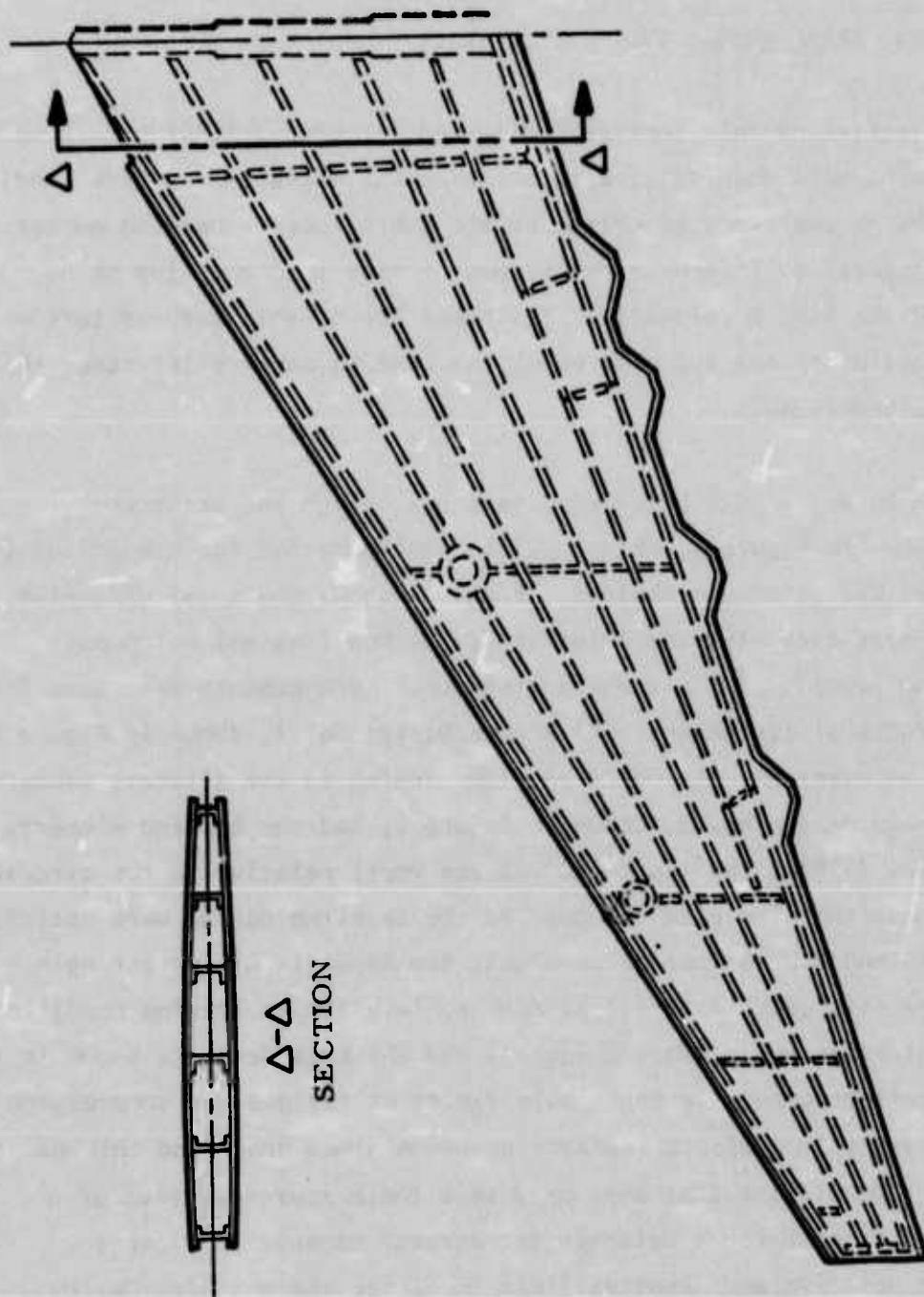


FIGURE 3: MAIN BOX CONFIGURATION FOR BASELINE DESIGN

$$\Lambda_{LE} = 35^\circ$$

$$AR = 3.8$$

$$S = 295 \text{ FT}^2$$

$$b/2 = 200.89 \text{ IN.}$$

$$t/c = .05 \text{ @ ROOT}$$

$$.04 \text{ @ TIP}$$

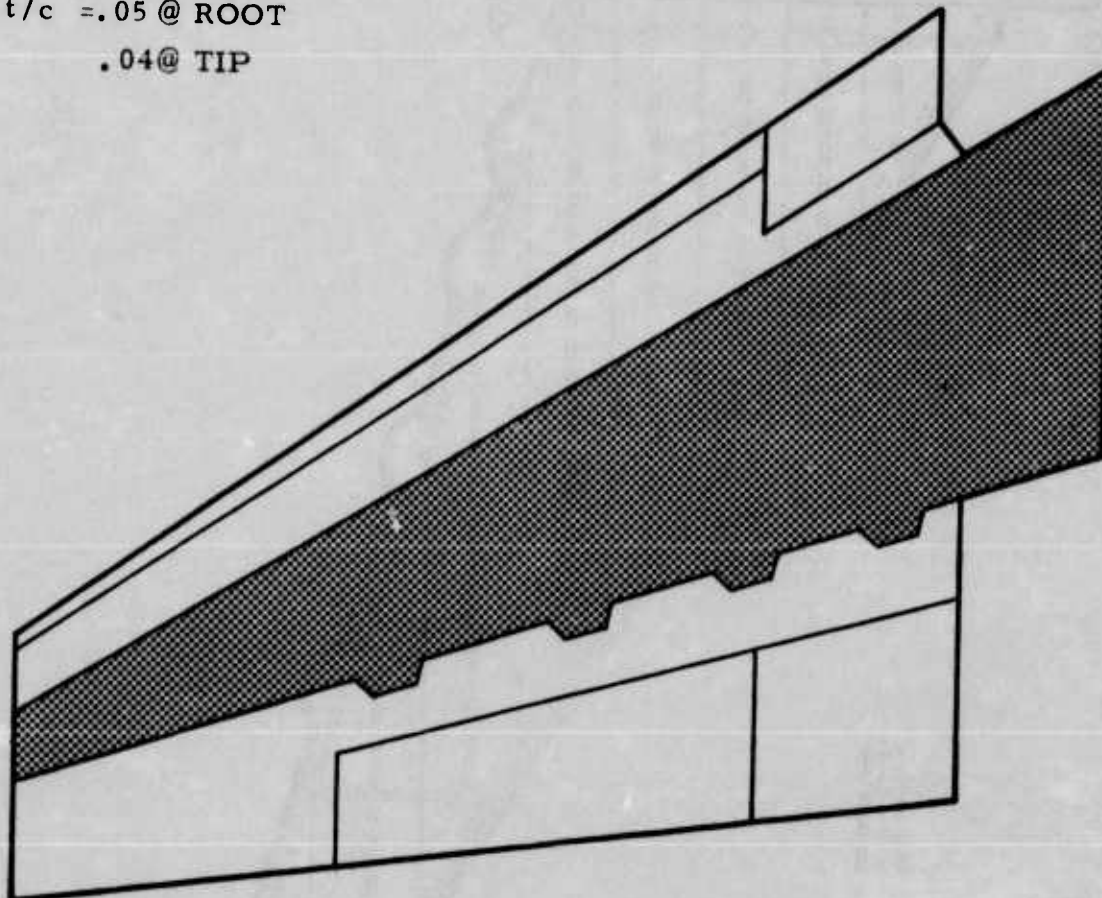


FIGURE 4: ADVANCED FIGHTER WINGPLAN FORM FOR THIS C C S STUDY

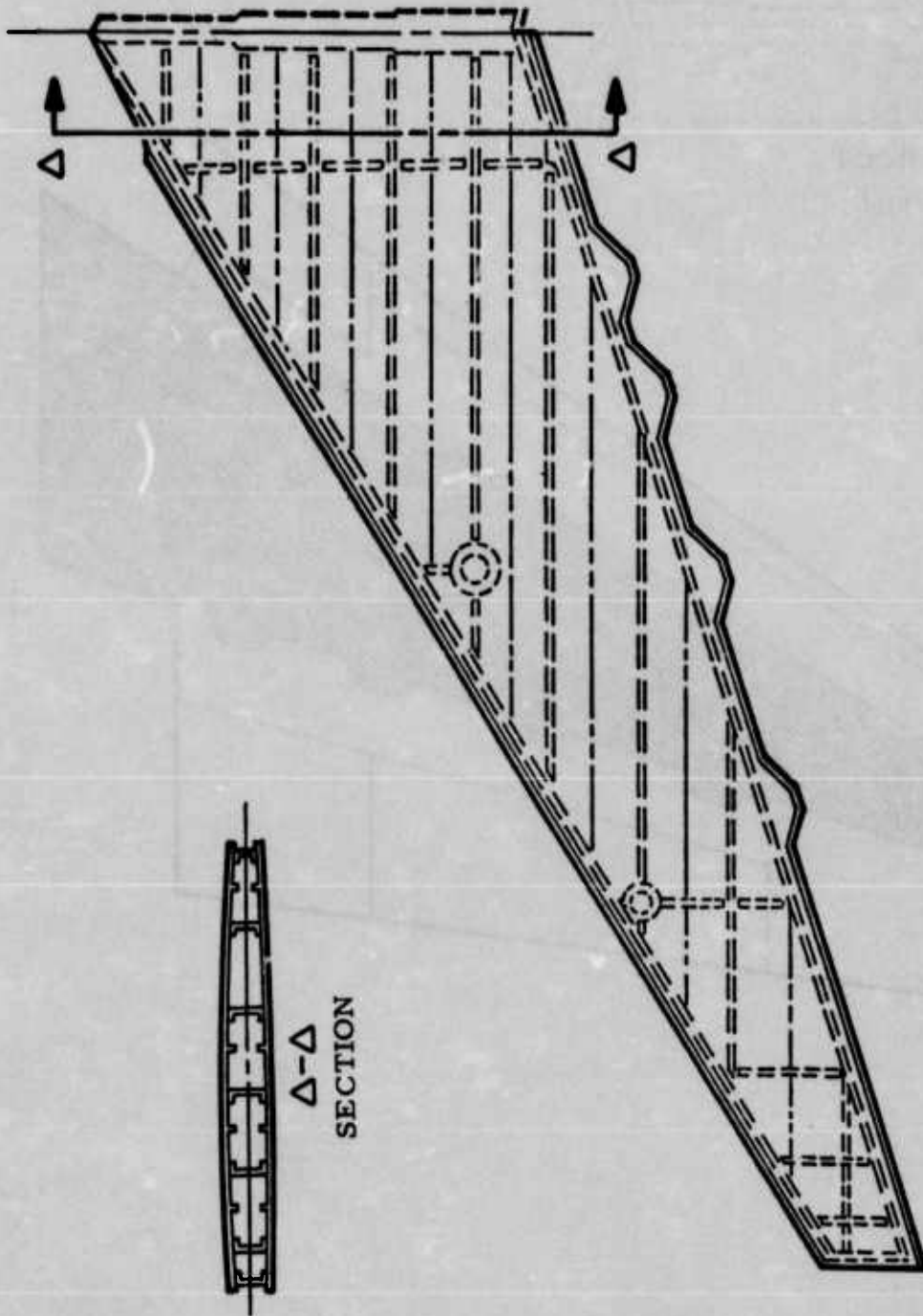


FIGURE 5: MAIN BOX CONFIGURATION FOR ALTERNATE DESIGN NO. 1

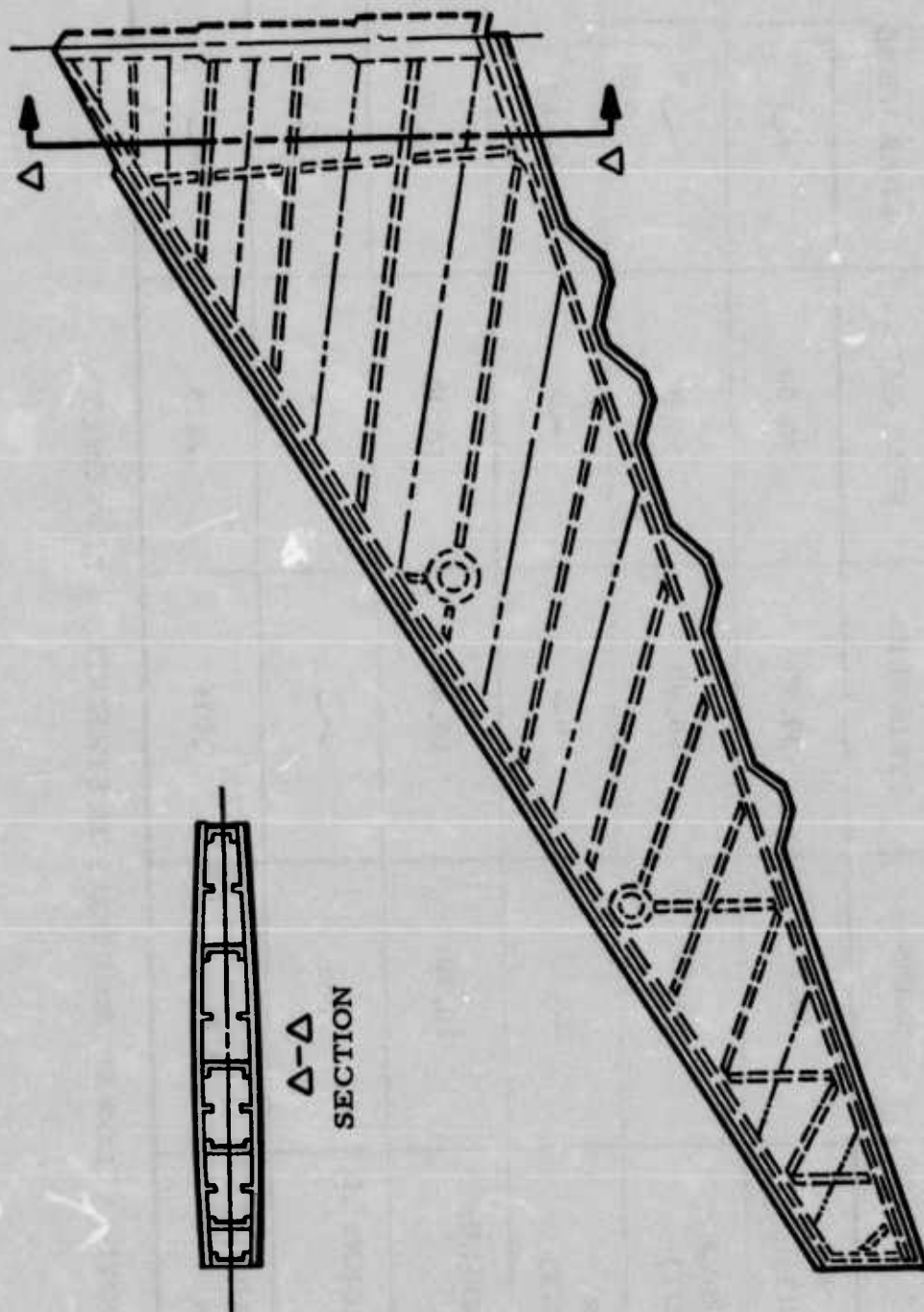


FIGURE 6: MAIN BOX CONFIGURATION FOR ALTERNATE DESIGN NO. 3

TABLE III : OPTIMIZATION PROCESS ALLOWABLES AND MINIMUMS

	SKINS	STRINGERS	SPAR CAPS	SPAR WEBS
TENSION KSI (LIMIT)	30.00	30.00	30.00	~
COMPRESSION KSI (LIMIT)	30.00	30.00	30.00	~
SHEAR KSI (LIMIT)	23.33	~	~	26.67
YOUNGS MODULUS MSI	10.30	10.40	10.40	10.30
MINIMUM THICKNESS IN	.050	~	~	.025
MINIMUM AREA SQ. IN.	~	.075	.075	~

NOTE: ALLOWABLES USED FOR STRENGTH SIZING ONLY

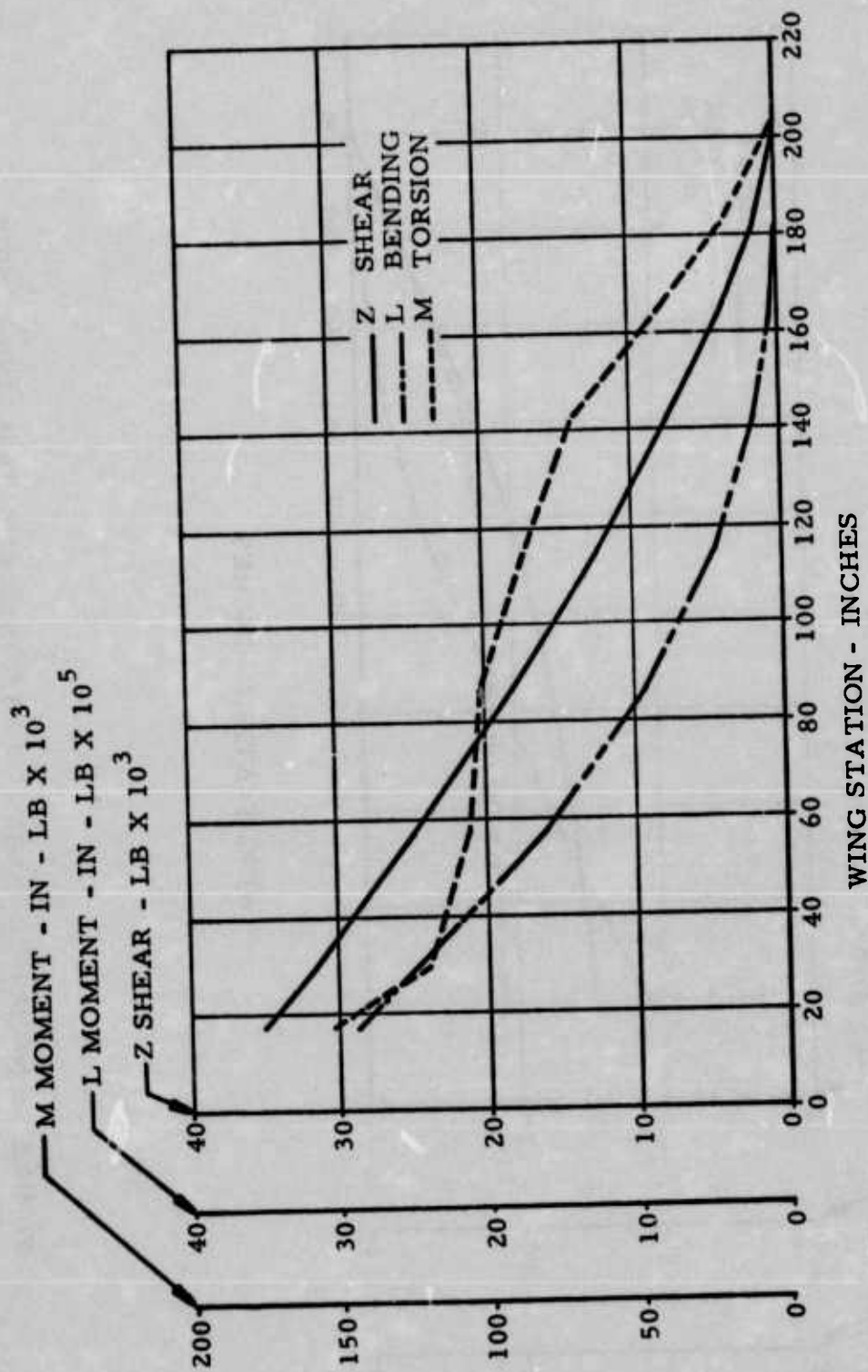


FIGURE 7: POSITIVE LIMIT (7.5g) LOADS FOR BASELINE DESIGN

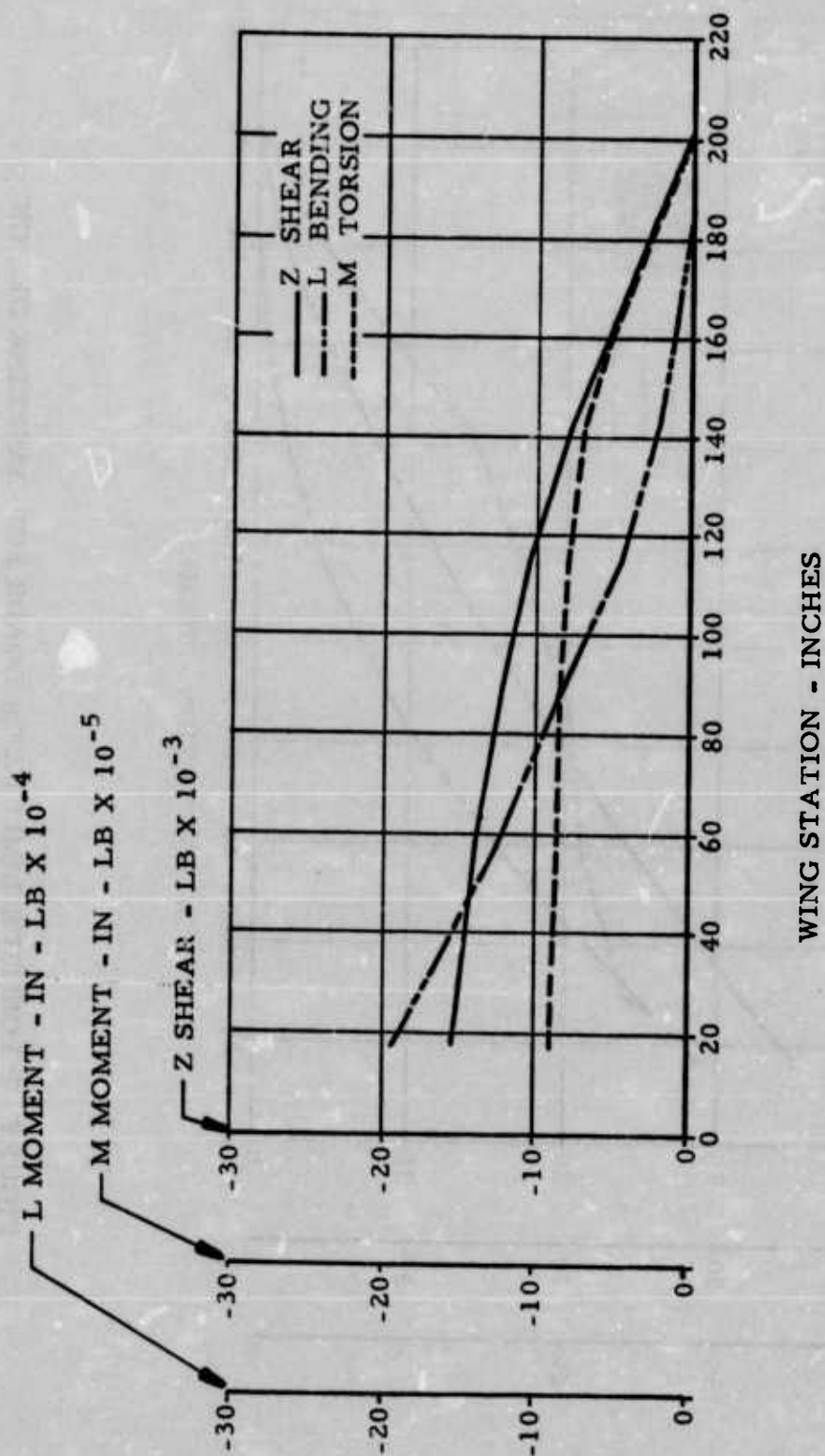


FIGURE 8: NEGATIVE LIMIT (-2.5g) LOADS FOR BASELINE DESIGN

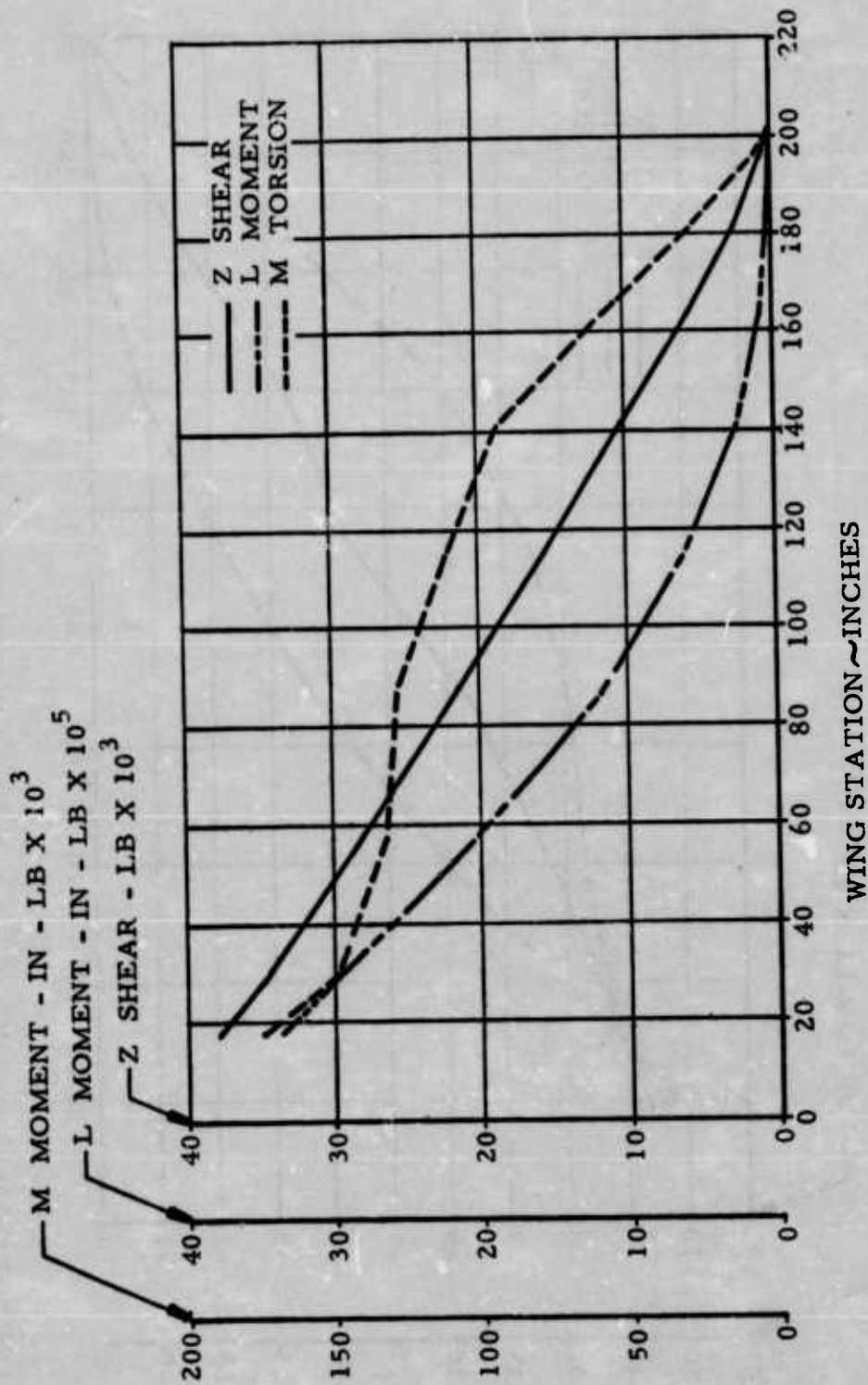


FIGURE 9: POSITIVE LIMIT (7.5g) LOADS FOR ALL ALTERNATE DESIGNS

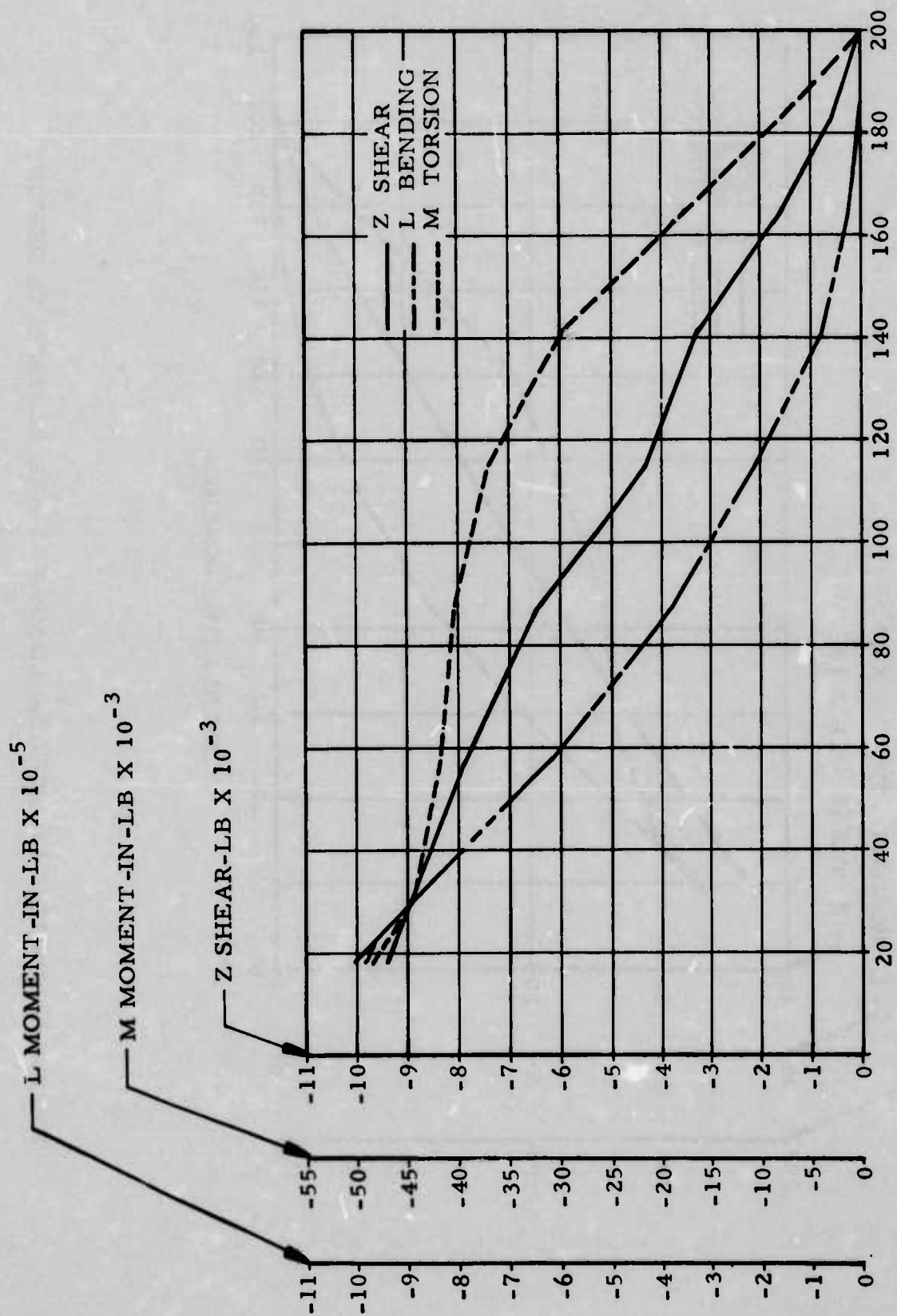


FIGURE 10: NEGATIVE LIMIT (-2.5g) LOADS FOR ALTERNATE DESIGNS

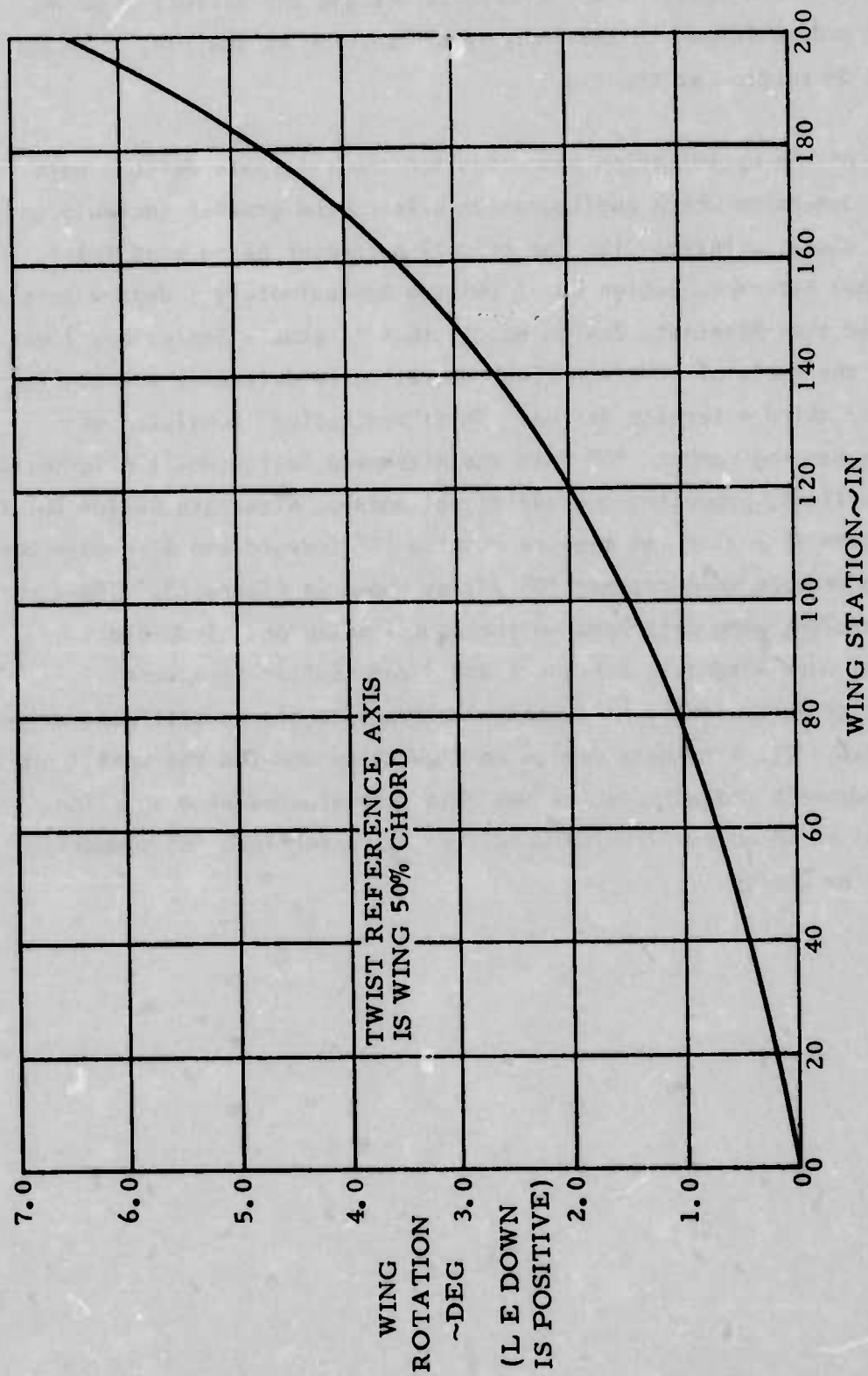


FIGURE 11: BUILT-IN TWIST FOR BASELINE DESIGN

The alternate designs were considered to be "flat" with no initial twist or camber. In both the baseline and alternate designs the airfoil used was symmetrical and conformed to the NACA 65A005 section at the wing root and the NACA 65004 section at the tip.

The results of the optimization processes for the alternate designs were compared to determine which configuration offered the greater increase in aerodynamic characteristics with the primary parameter being wing twist. It was found that Alternate Design No. 1 twisted approximately 1 degree more at ultimate load than Alternate Design No. 3, thus Alternate Design No. 1 was selected as the basis of a "bracketing" operation to determine the configuration of the third alternate design. This "bracketing" consisted of rotating the bending members 10° from the Alternate Design No. 1 orientation in both directions, producing two additional models, Alternate Design No. 2F shown in Figure 12 having its members rotated 10° forward and Alternate Design No. 2A whose members were rotated 10° aft as shown in Figure 13. These two refinement designs were optimized to the same loading and allowable parameters as were Alternate Designs 1 and 3 and similar structural characteristics determined. As in the previous sizings, no stiffness criteria was considered. The alternate design configuration showing the most improvement in aerodynamic characteristics was then re-evaluated at a 4g flight condition for which an equilibrium condition was determined for comparison to the Baseline Design.

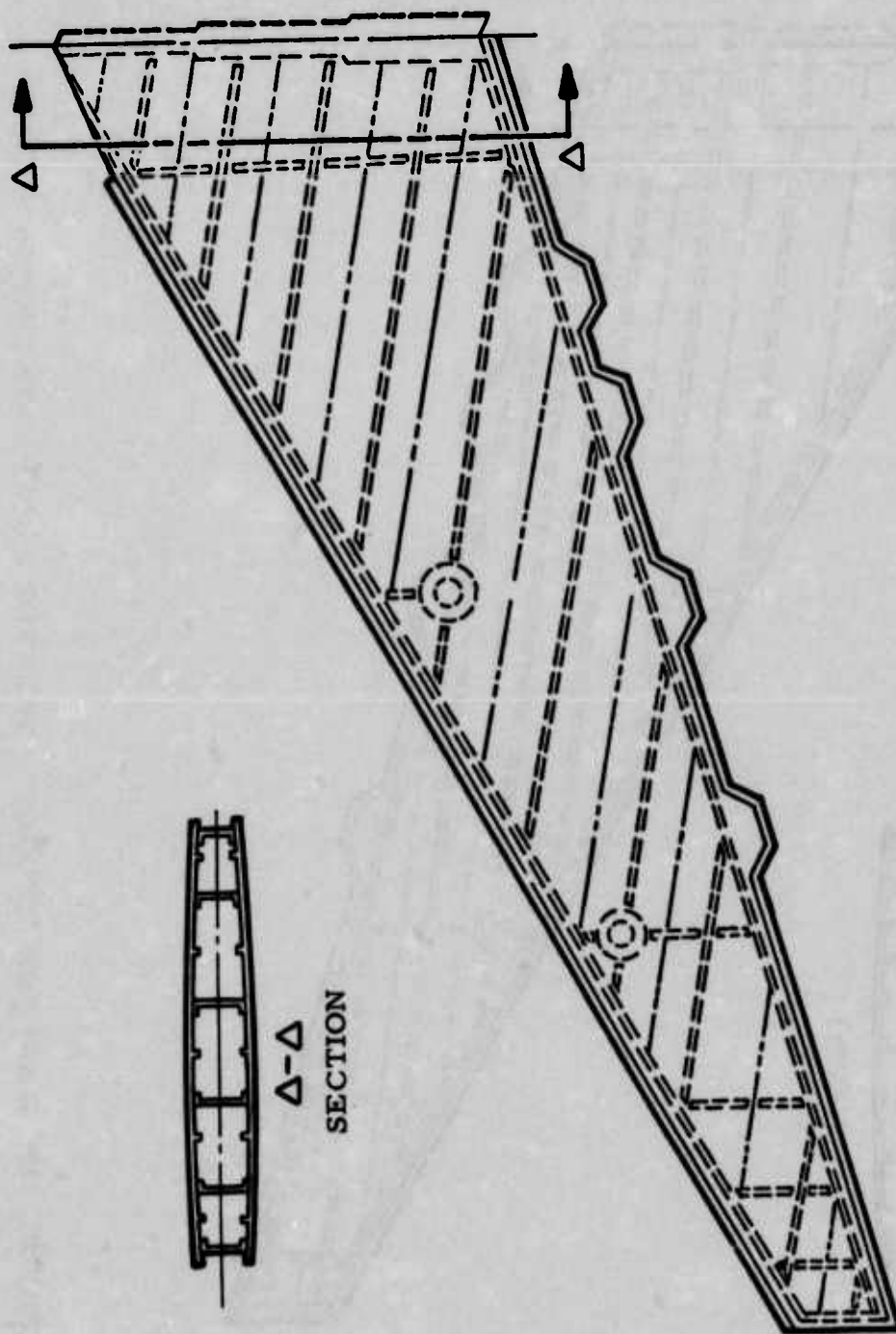


FIGURE 12: MAIN BOX CONFIGURATION FOR ALTERNATE DESIGN NO. 2F

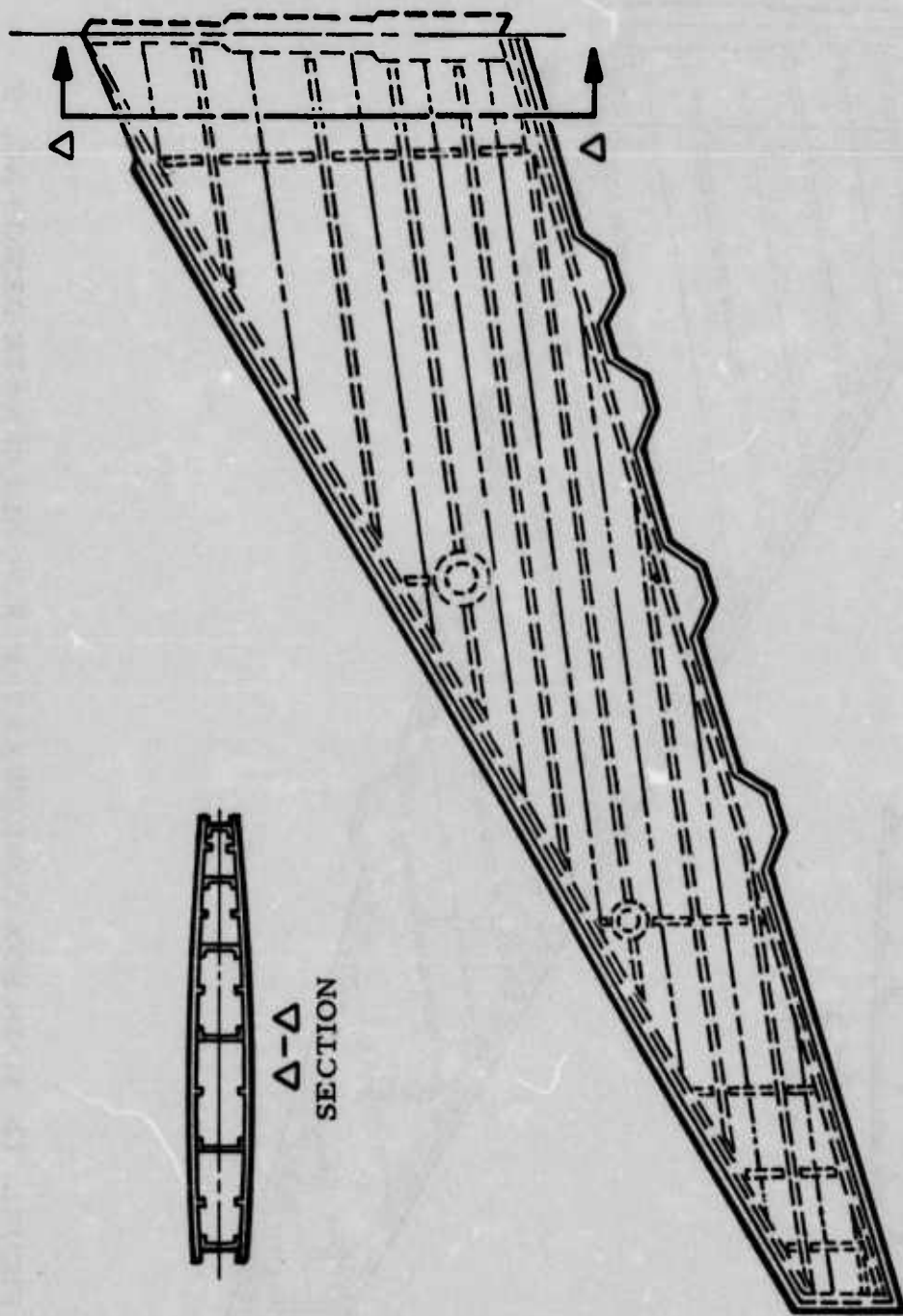


FIGURE 13: MAIN BOX CONFIGURATION FOR ALTERNATE DESIGN NO. 2A

3.2 AERODYNAMIC CHARACTERISTICS AND LOAD DEFINITION

Aerodynamic considerations in conventional wing configuration selection are often focused on specific flight conditions to meet defined mission requirements. The best configuration for these conditions may include wing twist as a means to optimize wing loading and/or camber to obtain best chordwise flow. Because twist and camber are not uniformly beneficial at all Mach numbers and angles of attack, airplane performance is often penalized at off-design conditions. An optimum wing for all flight conditions would require the capability to change wing configuration in flight to conform to the desired combinations of wing geometry for each flight maneuver. Every attempt to achieve this capability mechanically has resulted in excessively heavy and complex (costly) wings. CCS is a concept to approach the optimum wing by properly configuring the wing structural configuration as a function of loading. Because wing loading does vary with angle of attack and Mach number in an orderly manner, there is reason to believe that the desired variation in wing configuration can be shown to vary in a similar order. The purpose of this analysis was to obtain a preliminary evaluation of this potential.

The true potential of the concept cannot be evaluated without considering the aerodynamics of the total airplane. Changes in wing configuration have their effect on aircraft stability, trim requirements and control effectiveness. The CCS concept has an impact on each of these. However, the preliminary nature of this analysis was limited to the investigation of CCS effects on wing performance in a general sense.

The first step in the analysis was to establish the order of magnitude of the effect of various geometric parameters, which could be controlled by use of the CCS concept, on the aerodynamic characteristics of a baseline wing. This study was performed as a parametric analysis (See Appendix B) which was used to provide a preliminary evaluation of the potential benefits of CCS and as a guide in selecting variations in the various structural configurations.

As each structural design alternate or configuration was developed, the aerodynamic characteristics were evaluated and aerodynamic load distributions were developed for a 4 "g" symmetric maneuver at Mach numbers of 0.80 and 1.20 and an altitude of 10,000 feet. These data were developed for an equilibrium twist condition using the structural parameters associated with the particular configuration under consideration.

3.3 AEROELASTIC ANALYSIS OF CENTER OF ROTATION SHIFT

Aeroelastic analyses were performed on the Baseline Design and Alternate Designs No. 1 and No. 3 to determine the aeroelastic effects of moving the center of rotation forward through structural rearrangement.

A NASTRAN analysis was performed to determine the wing main structural box stiffness data, given in the form of an influence coefficient matrix, and the wing box inertial slice data. A transformation was performed to relate the inertial slice data to the dynamic grid points, and the resulting mass matrix was combined with a previously determined mass matrix for the leading and trailing edge structure (aileron, flap, leading edge devices, etc) to form a complete wing mass matrix. The wing mass matrix and the influence matrix were combined and the eigenvalue problem solved resulting in the modal data for each configuration. Aerodynamic analyses were then accomplished for the aircraft at 0.9 Mach number, which from past experience, is considered most critical from a flutter standpoint. Doubiet lattice airforces were then generated and used to determine flexible aerodynamic coefficients. These data were combined with the modal data to perform a flutter analysis for Alternate Designs No. 1 and No. 3 (See Appendix C).

4.0 EVALUATION OF CONCEPT PARAMETERS

4.1 STRUCTURES EVALUATIONS

The primary structures evaluation accomplished in this study was to determine which models demonstrated the best twists and deflections for aerodynamic characteristic improvement. The guidelines set up by the aerodynamics goals was that the wing showing the greatest nose down twist would best tend to improve aerodynamic parameters.

The initial effort was to define and optimize for strength only the Baseline Design and Alternate Design No. 1 and No. 3. From this effort the node point deflections and model element weights were obtained. These node point deflections were used to determine the spanwise wing twist at several points along the wing span and the average wing deflection at these same span locations (average deflection being the average displacement of the front and rear spars at a streamwise cut). The loading condition used for sizing the models was a 7.5g symmetrical flight condition at Mach no. 1.2 ratioed up by an ultimate load factor of 1.5. These respective loads for the baseline and alternate designs were then applied to the models and the elements optimized for strength only. The twists of the models at these ultimate conditions are shown in Figure 14. The indication is that the baseline design twists more than either of the alternate designs, but only from approximately the 87.5% span point outboard, and that being due to the built-in twist present in the baseline design. For a comparison, the twist of the baseline design with the built-in twist subtracted out is also shown and illustrates that the CCS structure does indeed have advantageous twist characteristics over conventional structure. From the data seen in Figure 14 it was decided to expand the analysis of the Alternate Design No. 1 configuration as its twist was 1° greater at its maximum point than that of Alternate Design No. 3. In addition, this ultimate load strength sizing gave the model element weights which are shown in Table IV illustrating that Alternate Design No. 3 was the lighter of the two alternates, but heavier than the baseline by 27 pounds. The average deflections of the models are shown in Figure 15 which gives an indication of the relative bending stiffnesses of each.

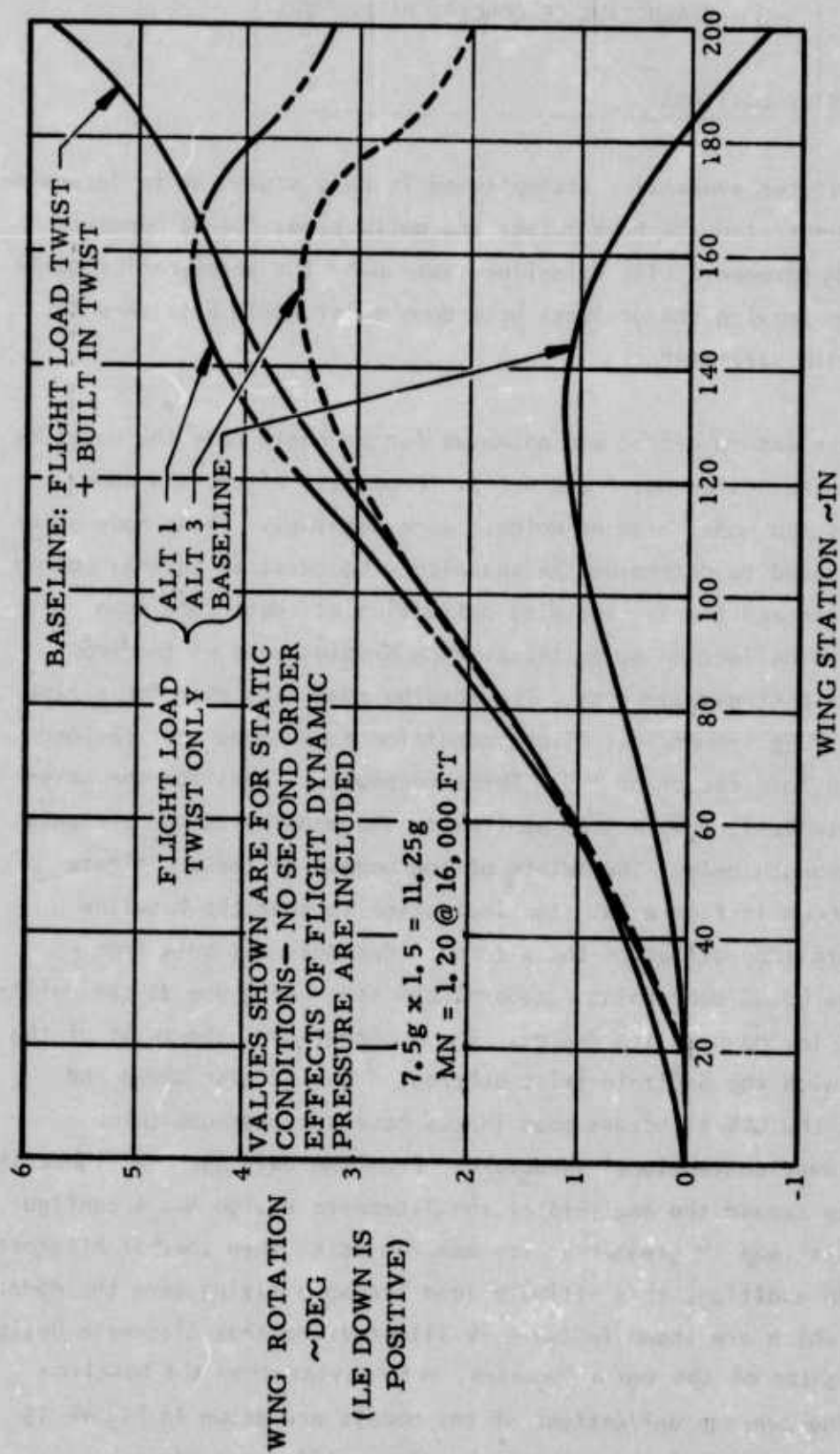


FIGURE 14: COMPARATIVE TWISTS FOR THE BASELINE DESIGN AND ALTERNATE DESIGN NO. 1 AND NO. 3

TABLE IV: STRUCTURAL MATH MODEL WEIGHT BREAKDOWN AND COMPARISON FOR ALL DESIGNS

CONFIGURATION	UPPER SKIN	LOWER SKIN	FRONT SPAR	REAR SPAR	INTER. SPARS	STRINGERS	RIBS	TOTAL
BASELINE	66.17	66.11	13.26	27.53	(4) 103.23	~	10.00	286.30
ALTERNATE DESIGN NO. 1	71.11	70.55	22.87	37.18	(9) 55.95	(9) 49.48	6.81	313.95
ALTERNATE DESIGN NO. 2F	80.73	80.86	26.03	56.80	(11) * 31.78	(9) 24.31	7.60	308.11
ALTERNATE DESIGN NO. 2A	67.45	67.50	20.74	30.16	(8) 110.12	(2) 6.53	8.25	310.76
ALTERNATE DESIGN NO. 3	84.03	83.92	29.63	46.50	(12) 35.74	(9) 25.91	6.73	312.47

NOTES: NUMBER IN PARENTHESES INDICATES NUMBER OF ITEMS IN MODEL.

WEIGHTS BASED ON STRENGTH SIZING ONLY

* ALTERNATE DESIGN NO. 2F TOTAL SPAR LENGTH IS 28% LESS THAN THAT OF THE BASELINE DESIGN

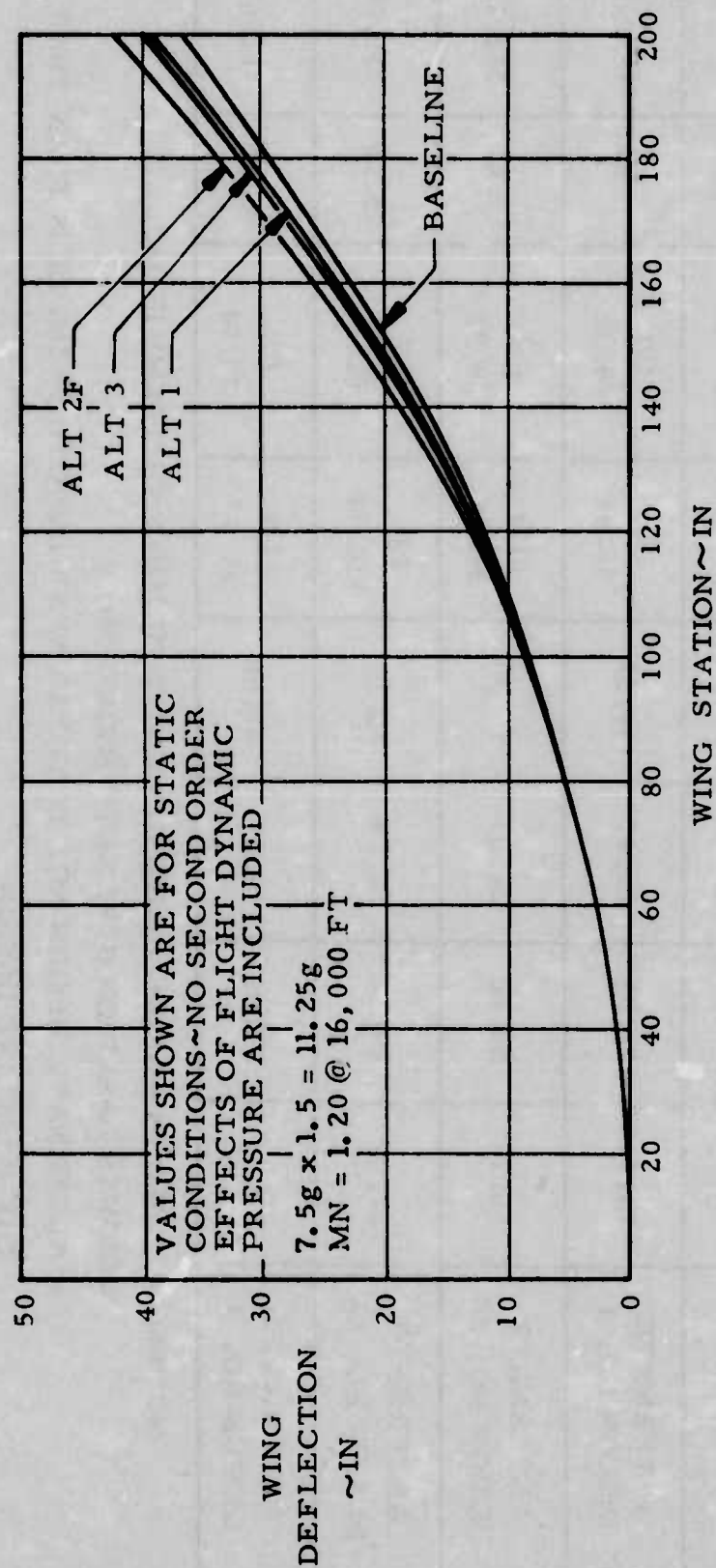


FIGURE 15: AVERAGE WING DEFLECTIONS AT ULTIMATE LOAD (7.5g X 1.5)

In an effort to "bracket" the twist characteristics of Alternate Design No. 1 two additional models were developed and subjected to the same ultimate loading condition. These were Alternate Designs No. 2A and 2F. The twists of these two configurations are compared with that of Alternate Design No. 1 in Figure 16. The indication is that Alternate Design No. 2F experiences more twist for this loading condition than the other two alternates, therefore Alternate Design No. 2F was selected for further comparisons at the 4g equilibrium evaluation conditions.

The baseline and alternate 2F design structural influence coefficients were provided for aerodynamic evaluations which were used to determine an equilibrium condition for each model at two air speeds, Mach number 0.8 to produce a forward C. P. location and Mach number 1.2 for an aft C. P. location.

The loads resulting from these conditions were applied to the two models and their twist distributions determined. These twists are shown in Figures 17 and 18 and again indicate that the absolute twist of the baseline design is greater than that of the CCS design, but only because of its 6.5° built-in twist. The twists due to airloads only demonstrate that the CCS structure has a marked twist advantage over the conventional structure even at a moderate load level. This is illustrated in Figure 19 where the twist characteristics of both configurations are plotted against load factor for the two Mach numbers evaluated. The points plotted are absolute for both Mach numbers at 0g's and 4g's as previously shown in Figures 17 and 18. Since these twists are linear in nature as a function of linear load factor multiples, a straight line extrapolation is shown out to a limit load factor of 7.5g's. A marked advantage in twist is again illustrated by the slopes of the twist curves for the CCS structure at both Mach numbers as compared to the conventional baseline wing without built-in twist.

Structural evaluation of the data obtained from the loadings, twists and deflections of the two models (Baseline Design versus Alternate 2F Design) indicates that the CCS structure does in fact give wing rotations in a direction producing improved aerodynamic characteristics at a greater rate than conventional structure at all normal load factors. This is especially true at negative load factors where the built-in twist of the baseline

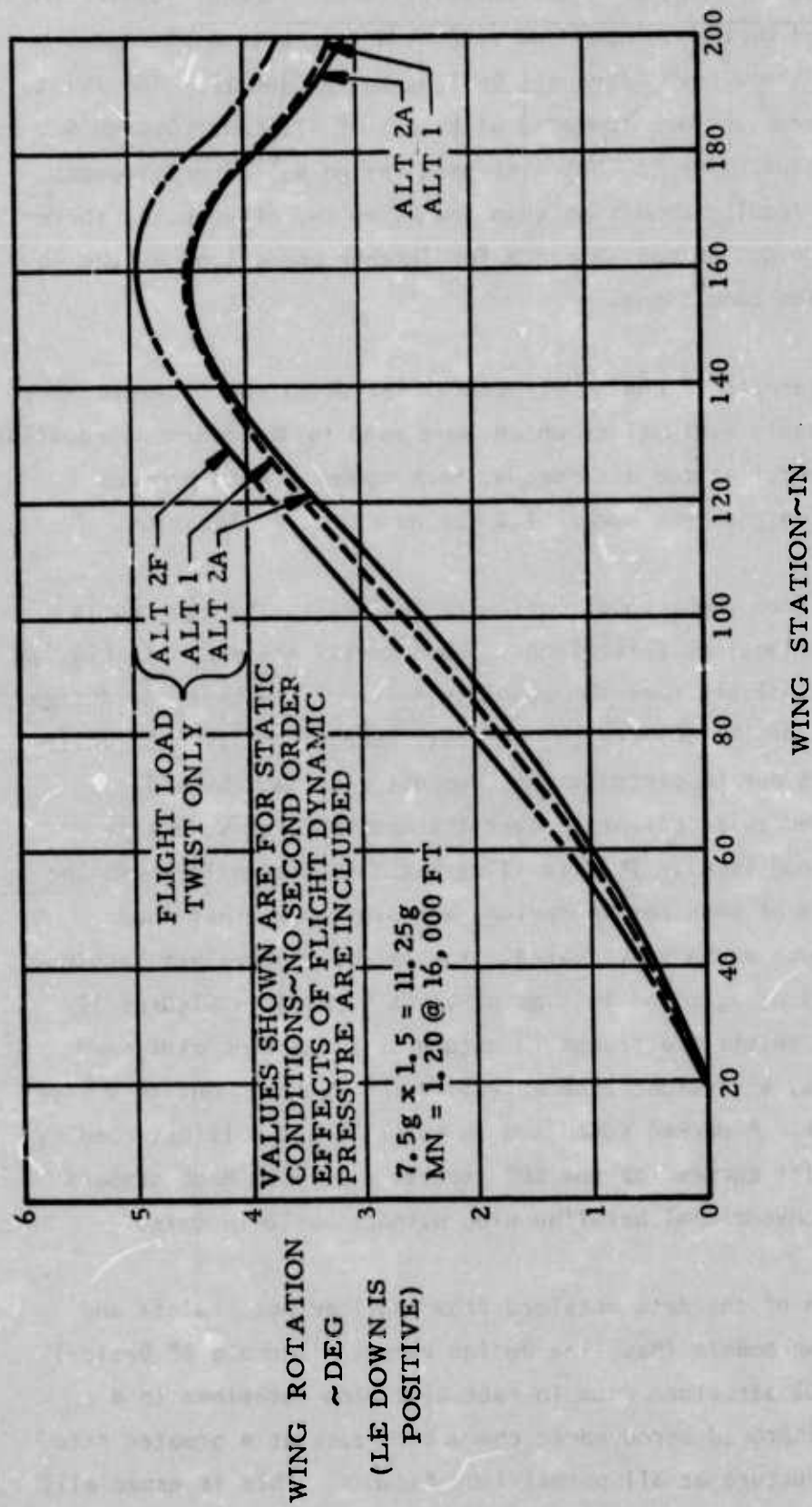


FIGURE 16: COMPARATIVE TWISTS FOR ALTERNATE DESIGNS NO. 1, NO. 2A, AND NO. 2F

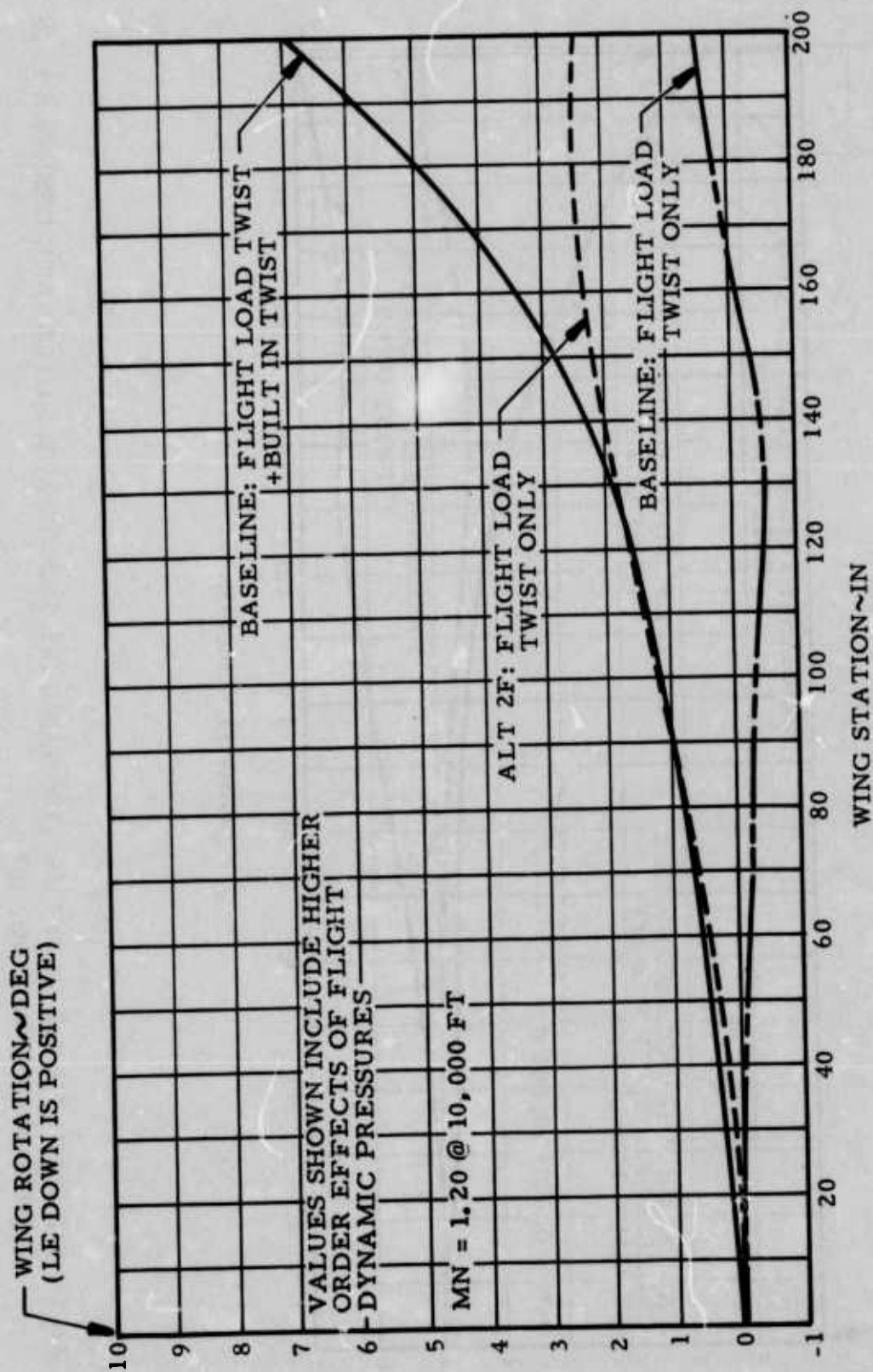


FIGURE 17: COMPARATIVE TWISTS FOR THE BASELINE DESIGN AND ALTERNATE DESIGN NO. 2F
4g LOAD AT MACH NO. 1.20

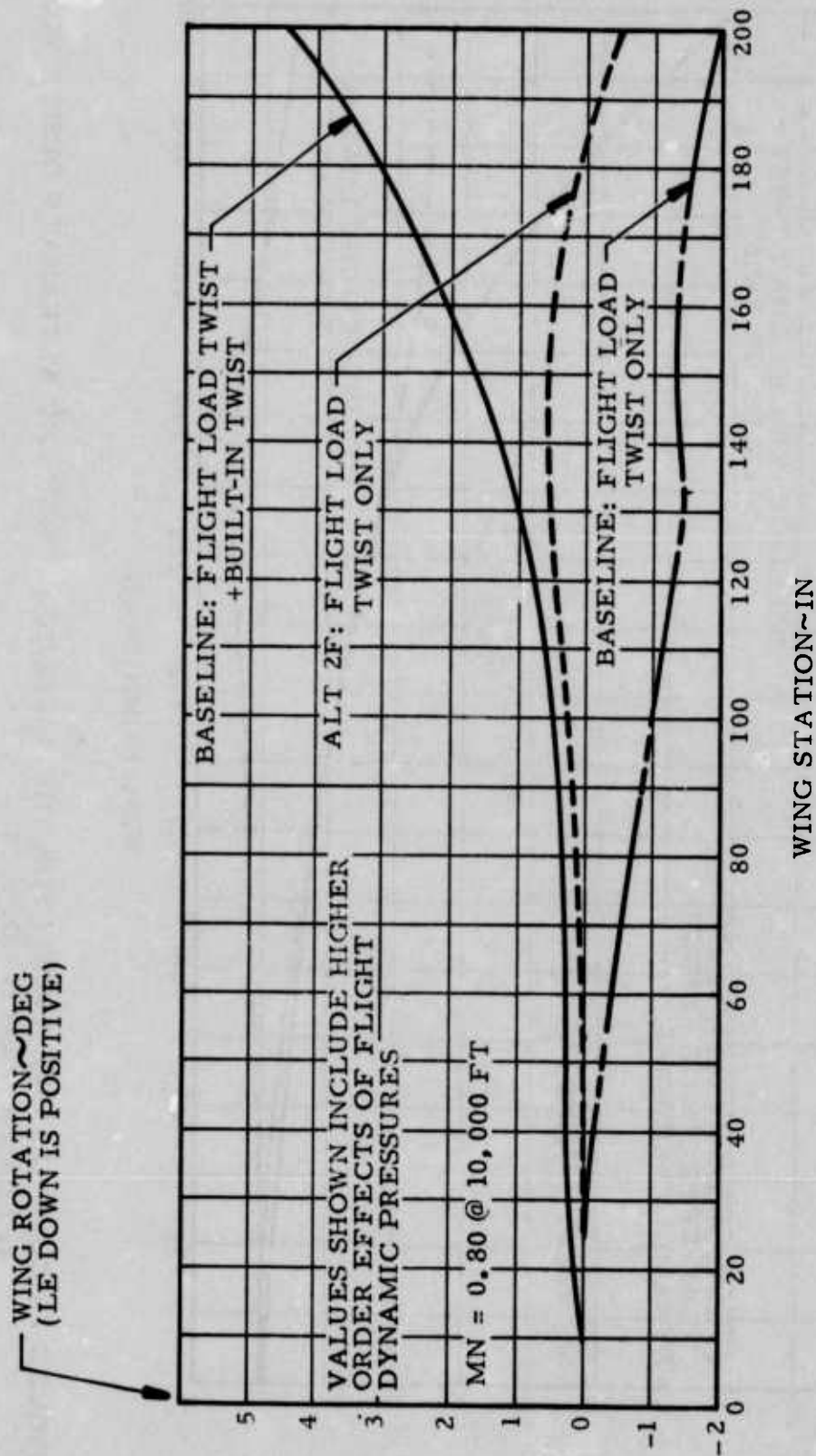


FIGURE 18: COMPARATIVE TWISTS FOR THE BASELINE DESIGN AND ALTERNATE DESIGN NO. 2F
4g LOAD AT MACH NO. 0.80

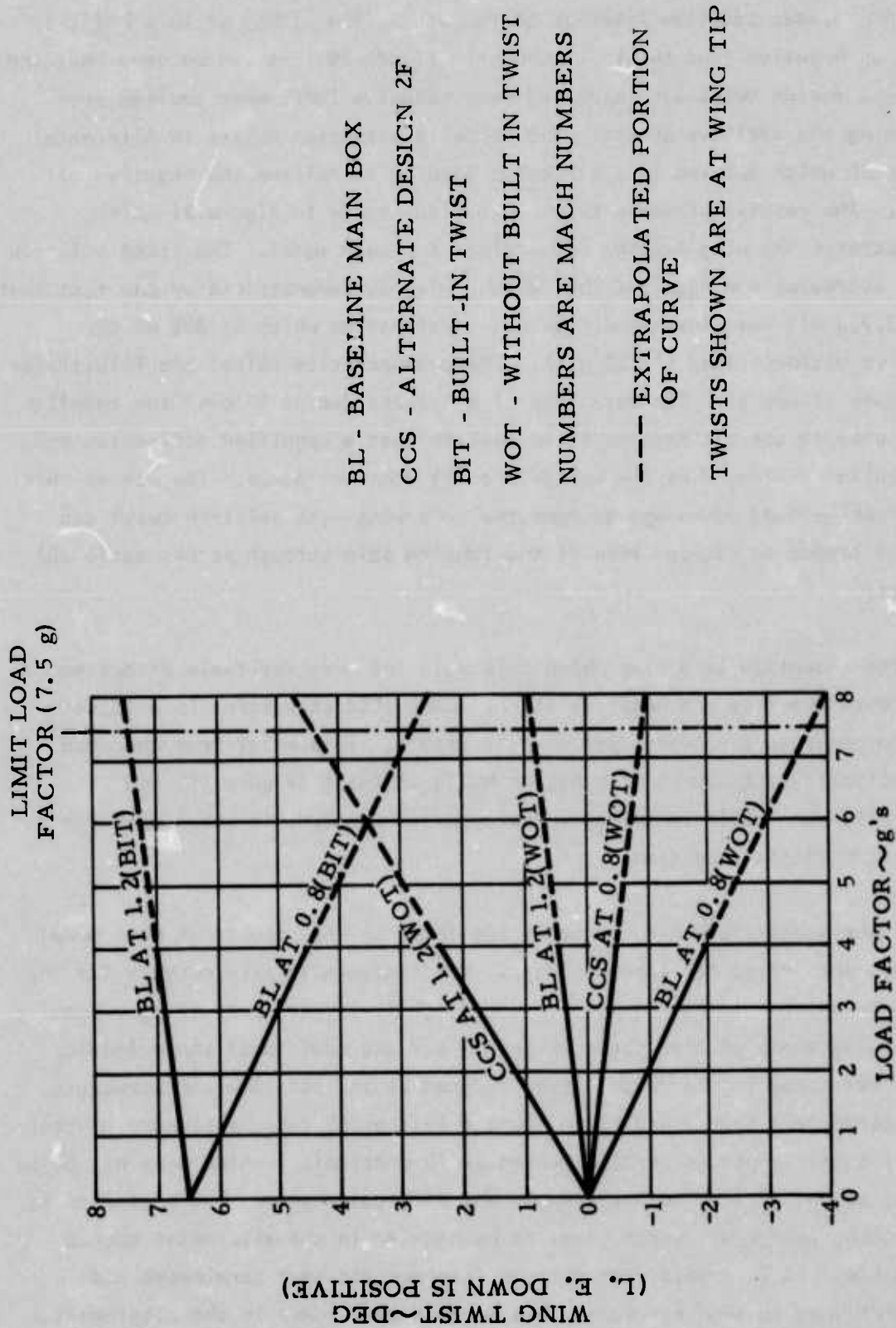


FIGURE 19: TWIST VERSUS POSITIVE LOAD FACTOR FOR THE BASELINE DESIGN AND ALTERNATE DESIGN NO. 2F

design produces additive loadings to the wing. The effect of this built-in twist on negative load twists is shown in Figure 20. It can be seen that the baseline design twist was increased when negative loads were applied thus producing the additive effect. The opposite situation exists in Alternate Design 2F which twisted in a direction tending to relieve the negative air loads. The results of these twists are illustrated in Figure 21 which demonstrates the wing average deflections for each model. The fixed built-in twist increases the negative load on the wing as demonstrated by the fact that the -3.75g ultimate load condition has a deflection which is 86% of the positive ultimate load (11.25 g's). These comparative values are illustrated in Figure 15 and 21. The advantage of alternate design 2F over the baseline as related to the ultimate negative load is that a magnified deflection and load build up induced by the built-in twist does not occur. The use of this CCS negative load advantage as compared to a wing with built-in twist can have an impact on fatigue life of the tension skin through stress ratio (R) effects.

Thus the advantage of a wing which twists in the most desirable direction under both positive and negative flight loads (CCS structure) is evident when compared to a conventional wing structure. This holds true when the conventionally structured wing has no built-in twist (Figure 19) and especially when built-in twist is employed for aerodynamic advantages for a particular flight condition.

The weight numbers given in Table IV are those of the structural math model elements when sized for strength only. The increase in skin weights for the alternate designs is due in part to the slightly larger spar/stringer spacing (especially those of Alternates 2F and 3) and the additional shear loadings in the skins due to the "kick" loads induced by the CCS interior structure. The intermediate spars tend to be lighter in the CCS designs because of their shorter total length (Alternate Design 2F in particular) which does not allow a great amount of load to build up in any particular spar. The exception to this is the rear spar, which tends to be heavier in the alternates due to having its load increased each time an intermediate spar terminates and transfers load to the rear spar. Rib weights were lower in the alternates

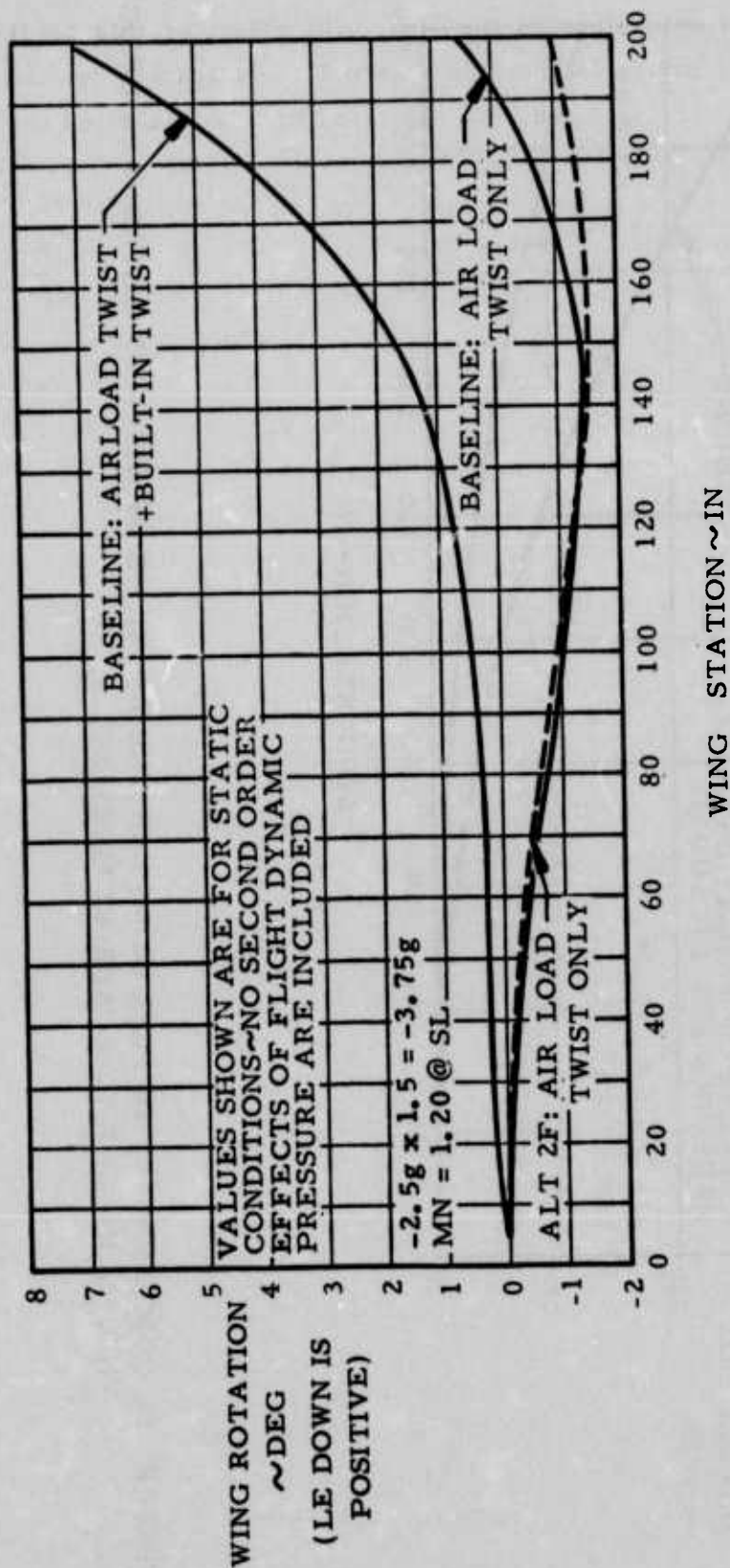


FIGURE 20: COMPARATIVE TWISTS FOR THE BASELINE DESIGN AND ALTERNATE DESIGN NO. 2F
(NEGATIVE LOADS AT MACH NO. 1.20)

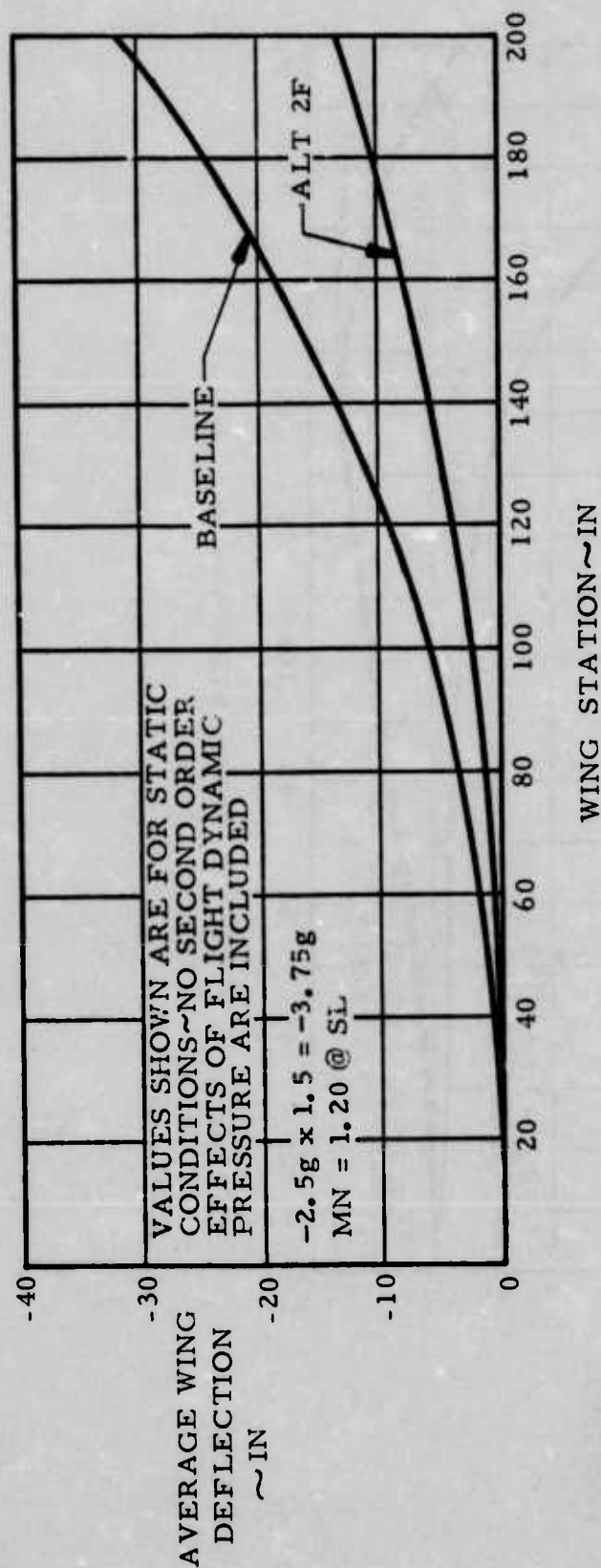


FIGURE 21: COMPARATIVE DEFLECTIONS FOR THE BASELINE DESIGN AND ALTERNATE DESIGN NO. 2F (NEGATIVE LOADS AT MACH NO. 1.20)

because the spars tend to also act as ribs (with the exception of Alternate 2A) and relieve rib requirements. When total math model weights are considered, the increased skin and rear spar weight of the alternate designs tend to be offset by the decrease in intermediate spar weight, so that the overall weight of the CCS main wing box appears to be only slightly sensitive to the internal substructure arrangement. It should also be noted that no studies were made to optimize the spar/stringer spacings for the alternate designs as was done for the baseline in a previous VSD exercise.

The weight trends shown in Table IV and discussed herein are illustrated graphically in Figure 22 as a function of intermediate spar orientation angle. The uppermost curve reflects a projected weight when non-optimum factors such as fasteners and fastener provisions are considered. These indications demonstrate that the weight increase was greater for the baseline design due to the greater weight of its intermediate spars. This increase is a function of spar length and loading characteristics.

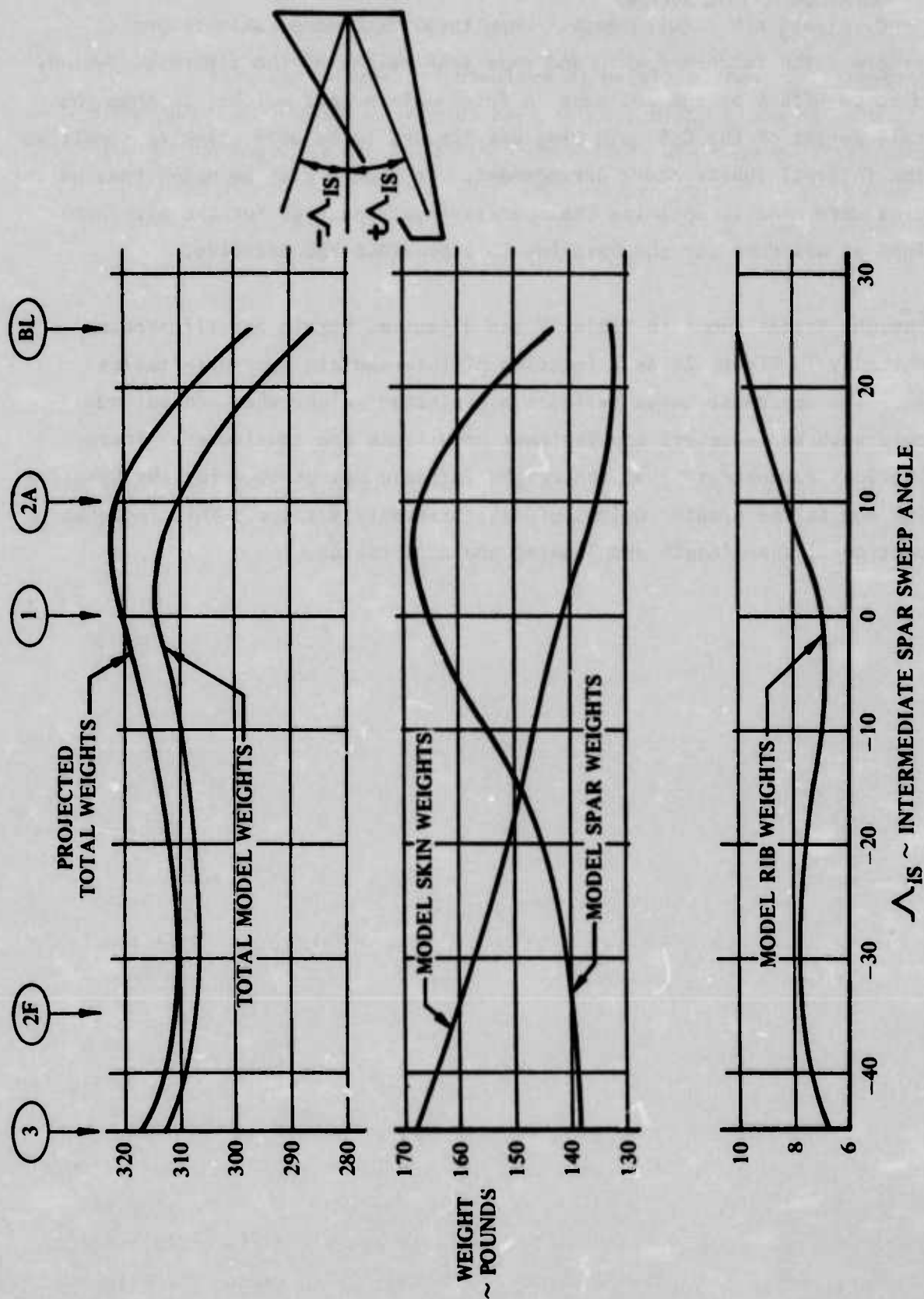


FIGURE 22: MATH MODEL WEIGHT TRENDS

4.2 AERODYNAMIC EVALUATIONS

The present study was initiated to evaluate the advantages of a structure which would deflect under load to provide favorable aerodynamic characteristics over a wide Mach number range. During the course of the program two configuration reviews were made. An initial aerodynamic evaluation was made using the results obtained from a parametric study which was conducted during the early design phases to aid in the selection of the configurations showing the most favorable aerodynamic characteristics. The parametric study discussion and results are presented in Appendix B. This section presents the data used for evaluation of the final configuration design.

The alternate configuration designs were limited to the control of spanwise variations in twist. The baseline wing was designed to provide a fixed 6.5 degrees of twist at the tip. This was desirable in reducing the tail incidence required to trim and is most beneficial at the low supersonic Mach numbers. The data presented in Figure 23 compare this fixed twist to that produced by one of the final alternate designs for a 4 "g" maneuver at Mach numbers of .80 and 1.20 and an altitude of 10,000 feet. The more aft aerodynamic loading at Mach 1.20 shows that a strong trend in the desired direction and degree of twist was developed by the structure. The more forward loading on the wing at Mach .80 resulted in lesser deflection.

The variation of lift and pitching moment with angle of attack for these configurations are shown in Figure 24. This figure illustrates the range of aerodynamic values between the rigid plane and twisted wings and shows the magnitude of the resulting aerodynamic data corresponding to the equilibrium twist conditions of Figure 23. Because the flexed twist distribution at Mach .80 was small, the resulting change in aerodynamic forces between the rigid wing and the flexed plane wing were small. At a Mach number of 1.20 and 4 degrees angle of attack, the differences in spanwise twist between the target fixed values and the resultant equilibrium twist values for the alternate design wing (2F) resulted in small aerodynamic differences in lift and pitching moment. One of the purposes of twist is to reduce the pitching

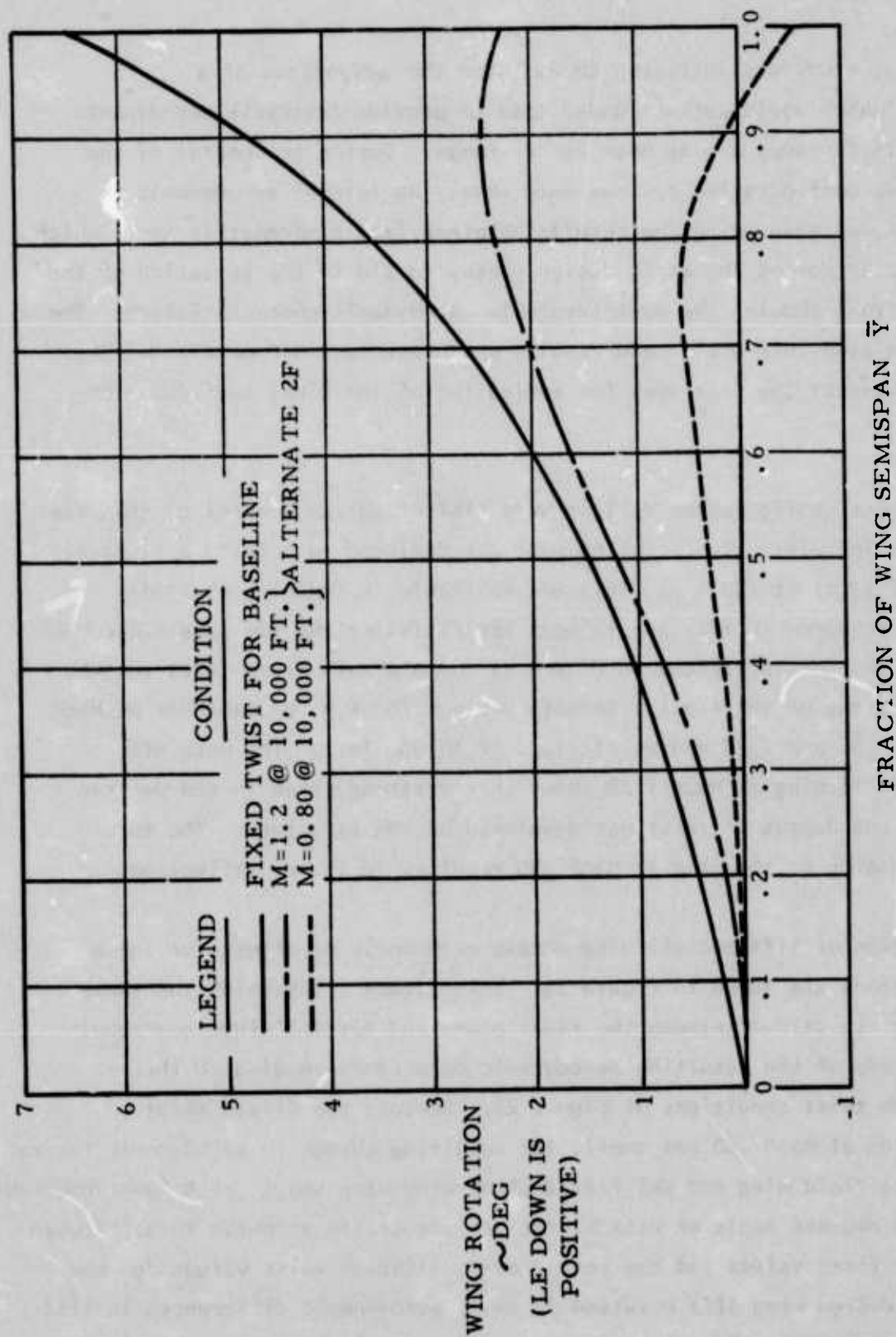


FIGURE 23: COMPARISON OF STRUCTURAL TWIST FOR A 4" g" FLIGHT CONDITION WITH FIXED TWIST USED IN STUDY

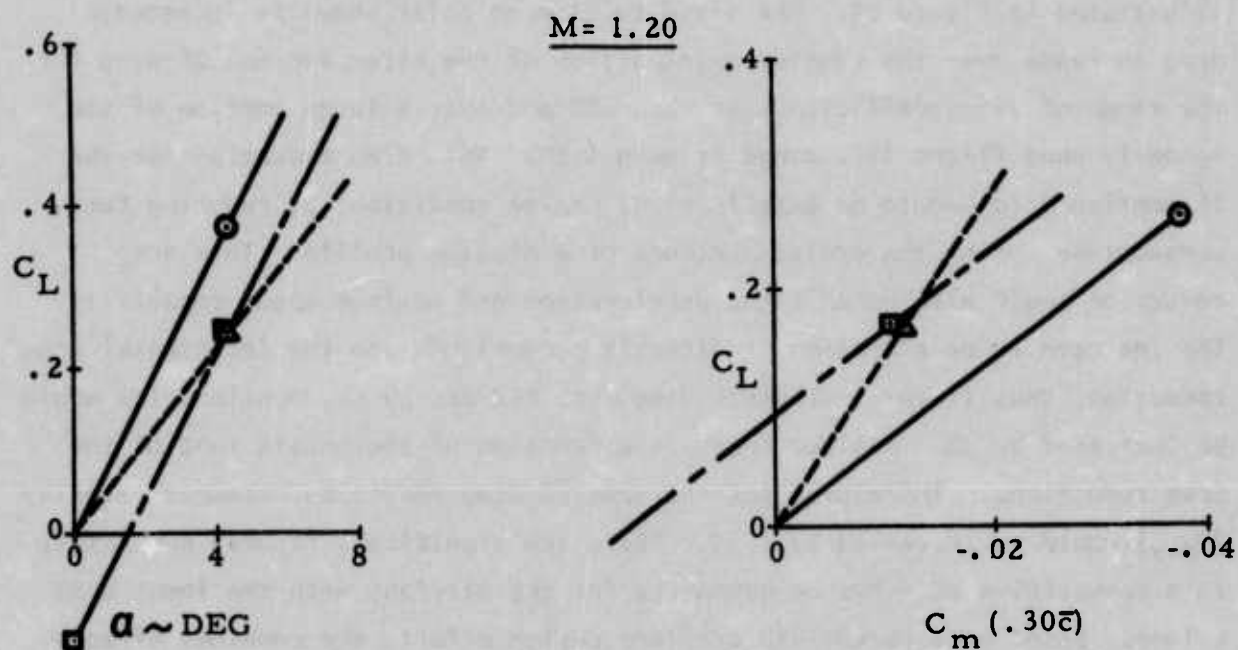
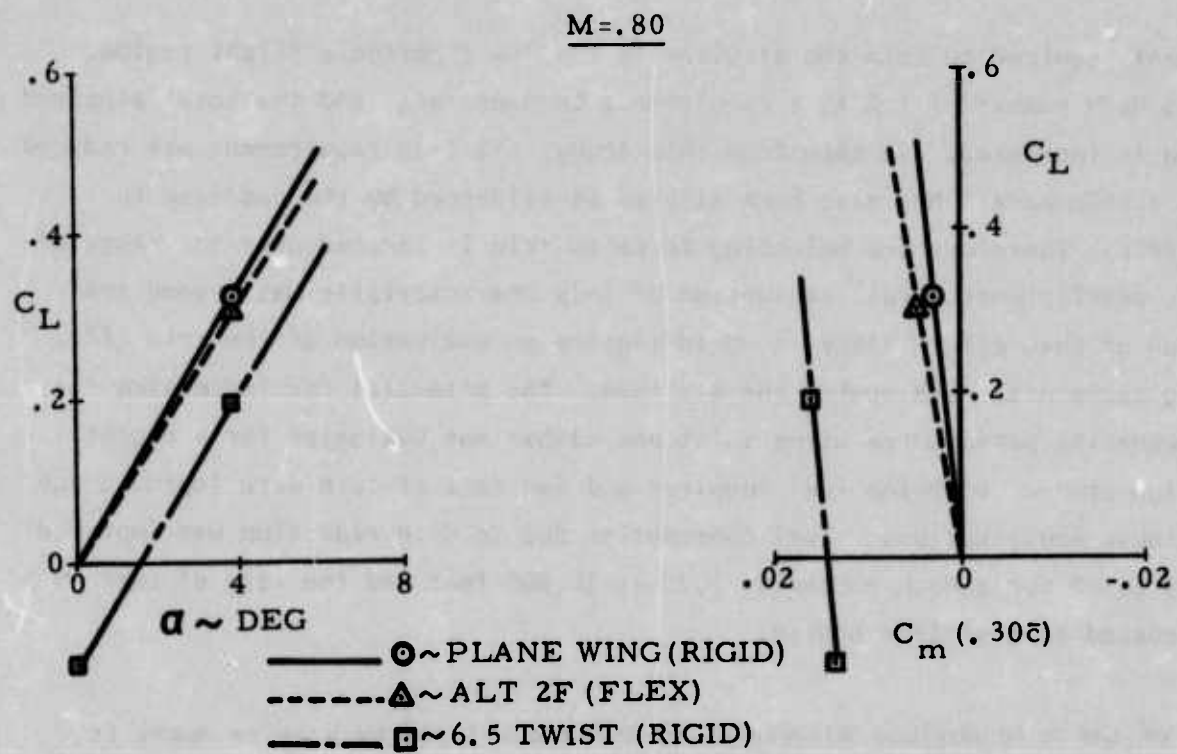


FIGURE 24: EFFECT OF FLEXIBILITY ON LIFT & PITCHING MOMENT -
 ALTERNATE 2F (4g LOADING)

moment required to trim the airplane in the low supersonic flight regime. At a Mach number of 1.2 this requirement becomes large and the total airplane drag is increased. As seen from this study, the trim requirement was reduced. The static margin has also been altered as evidenced by the decrease in dC_m/dC_L . Therefore the balancing force to trim is reduced over the range of lift coefficients. Full evaluation of this characteristic was beyond the scope of this effort since it would require an evaluation of the trim lift/drag ratio with Mach number and altitude. The potential for increasing the maneuvering performance using twist and camber was evaluated for a recent design study. Both the fuel required and the rate of turn were improved due to these modifications. Fuel consumption due to drag reduction was improved by 5 to 6% for a Mach number of 1.20 at 30,000 feet and the rate of turn was increased to a similar degree.

One of the more obvious advantages of twist developed by passive means is illustrated in Figure 25. The fixed twist drag polar shows an incremental drag increase over the passive twist action of the Alternate No. 2F wing for the range of lift coefficients at Mach .80 and over a large portion of the normally used flight lift range at Mach 1.20. This drag reduction for the 2F configuration would be beneficial at cruise conditions by reducing fuel consumption during the cruise portions of a mission profile. This drag reduction would also benefit the acceleration and maximum speed capability. The increase in acceleration is directly proportional to the incremental drag reduction; thus if total airplane drag were reduced by 5%, acceleration would be increased by 5%. Maximum speed is a function of the square root of the drag reductions. Therefore, for the same 5% drag reduction, maximum velocity (V_{max}) would be increased by 2.5%. These are significant figures and result in a competitive performance advantage for the airplane with the lower drag values. Based on a recent VSD airplane design effort, the combined effects of camber and twist resulted in an increase of $C_{D_{min}}$ by 8 to 10%. If CCS could be used to accomplish the same aerodynamic effect without the built-in twist, considerable improvements in acceleration and V_{max} would be realized.

----- Δ ~ ALT 2F FLEX AT 10,000 FT
 ----- \square ~ BASELINE(WITH FIXED TWIST)
 FLEX AT 10,000 FT

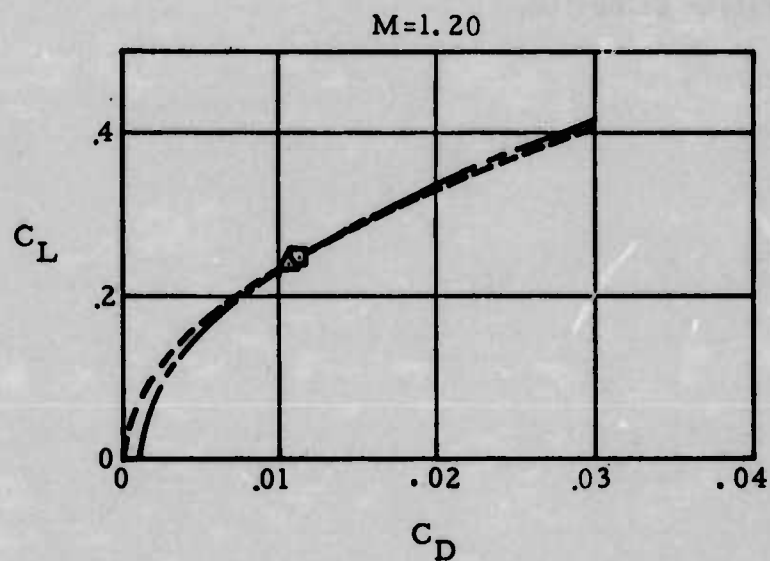
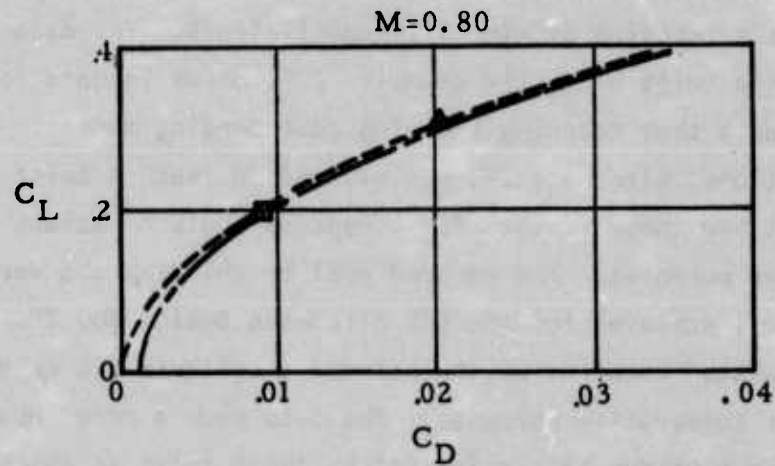


FIGURE 25: COMPARISON OF DRAG POLARS FOR THE BASELINE DESIGN AND ALTERNATE DESIGN NO. 2F

Another of the advantages of built-in twist (baseline) is to reduce the aerodynamic loading with angle of attack of the outer portions of the wing panel. Thus for a given lift value the load distribution is such that the center of pressure (C.P.) of the total wing panel loading is moved inboard. Spanwise loadings for a plane wing (no built-in twist) and a wing having a spanwise variation of twist (built-in twist) as shown in Figure 23 were established as a function of wing lift coefficients. The data shows that for the built-in twist wing, the spanwise C.P. moves inboard for positive lift coefficients thus reducing the wing root bending moment. One of the CCS configurations, Alternate 2F, was allowed to reach a twist equilibrium at 10,000 feet and these results for 4 degrees angle of attack are shown for comparative purposes. The desired goal of shifting the aerodynamic C.P. inboard was achieved for the CCS Alternate Design No. 2F. The equilibrium twisted baseline which included a built-in 6.5 degree twist was calculated for comparative purposes. The data show a more inboard C.P. location of about 4% due to the initial built-in twist at the same lift coefficient. This further reduces the wing root bending moment for a given load, however the drag penalty discussed previously must be considered in final configuration selection.

4.3 DYNAMICS EVALUATIONS

The results of the dynamic flutter evaluation for the baseline and Alternate Design No. 1 and No. 3 are characterized in Figure 26 which is a flutter speed versus damping curve. This figure shows that the baseline flutter occurs at 430 knots, Alternate Design No. 1 flutter at 475 knots and Alternate Design No. 3 flutter at 490 knots. Therefore from a flutter standpoint, Alternate Designs No. 1 and No. 3 show an advantage over the baseline design. However, it should also be noted that these two alternate designs weighed approximately 8-10% more than the baseline design. This is primarily due to the greater skin thicknesses which increased the alternate design stiffnesses. If the baseline were stiffened sufficiently to approach the flutter speeds of the two alternate designs, the weight increase required would be approximately one pound per knot of flutter speed increase. At this rate of weight increase, the baseline would weigh the same as the alternates for the same flutter speed. It can be concluded that from a flutter viewpoint, neither degradation nor improvement would result from use of Alternate Designs No. 1 and No. 3. Figures 27, 28, and 29 present the first four mode shapes and their associated frequencies for these three design configurations. Table V presents the flexible aerodynamic coefficients used to obtain these flutter comparisons. It can be observed that these coefficients are essentially the same for the baseline and alternate designs.

For refined Design Alternates No. 2A and 2F it can be concluded that their flutter characteristics would fall within the flutter speed band demonstrated in Figure 26.

It is recognized that a wing designed to twist could have a significant effect on areas of flight dynamics other than flutter, such as aileron effectiveness and roll reversal. However, these aspects were not included in this study.

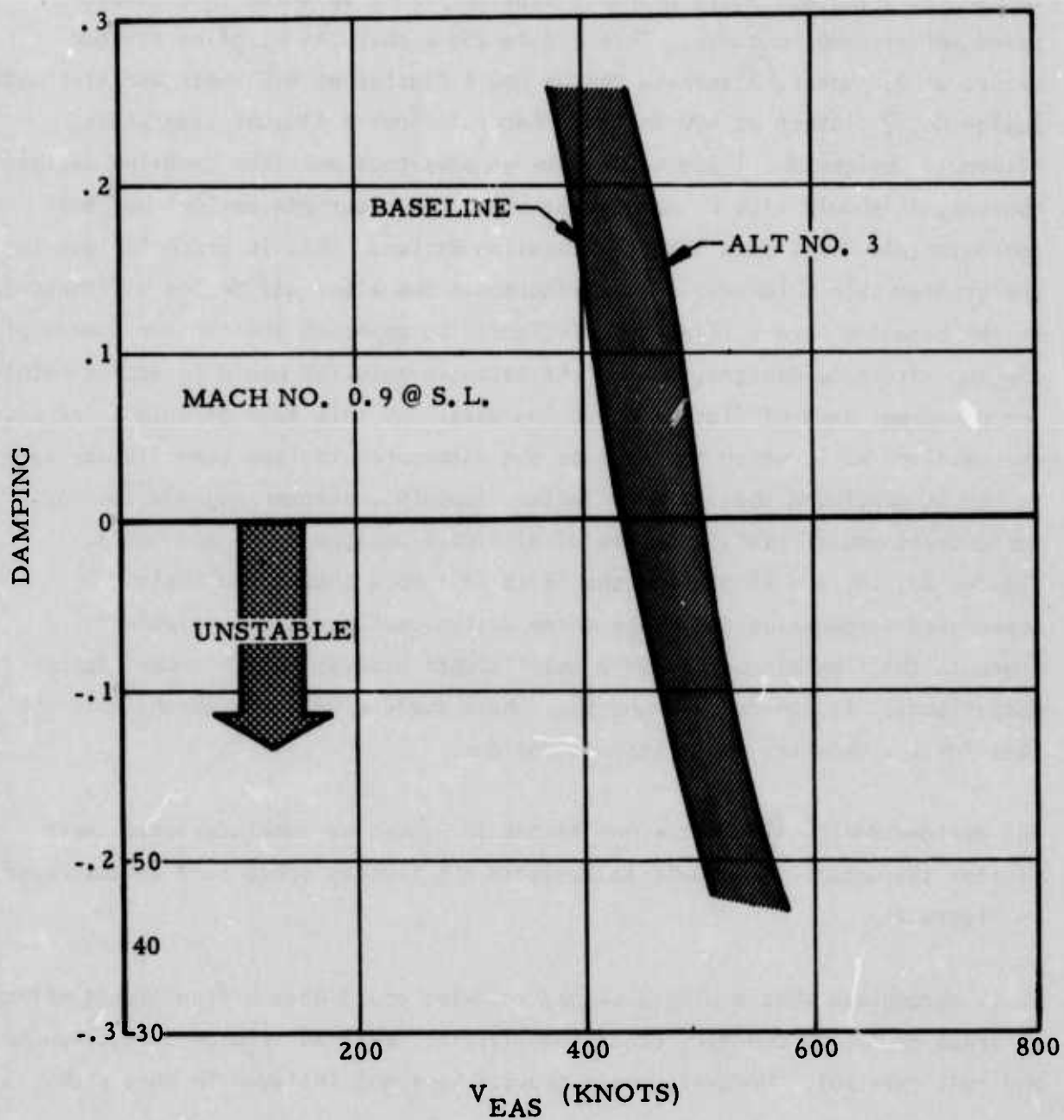


FIGURE 26: FLUTTER SPEED VS. DAMPING FOR THE BASELINE DESIGN AND ALTERNATE DESIGN NO. 3

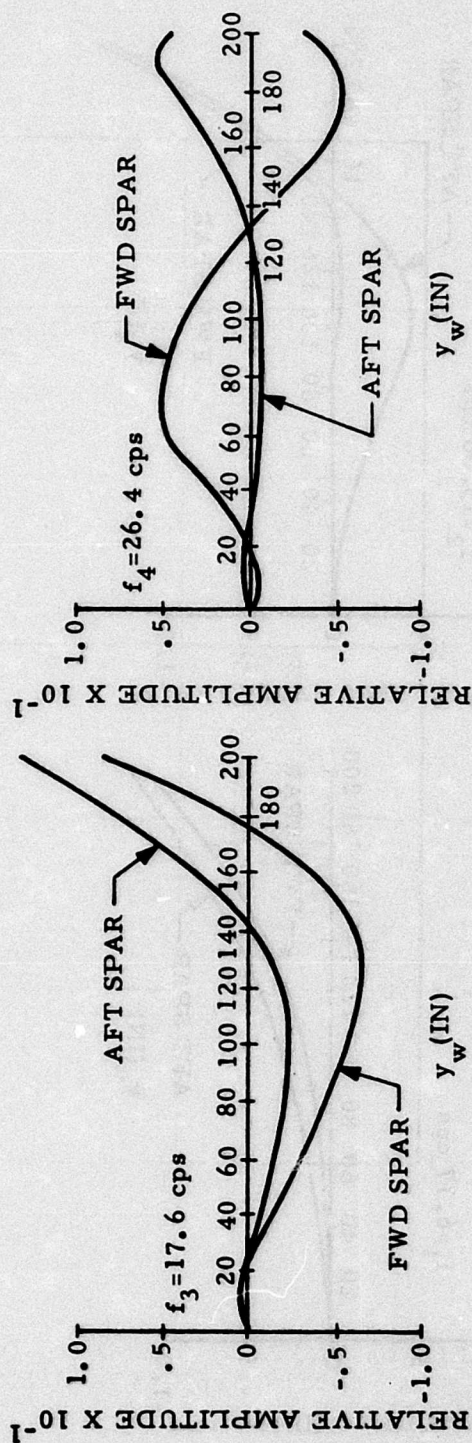
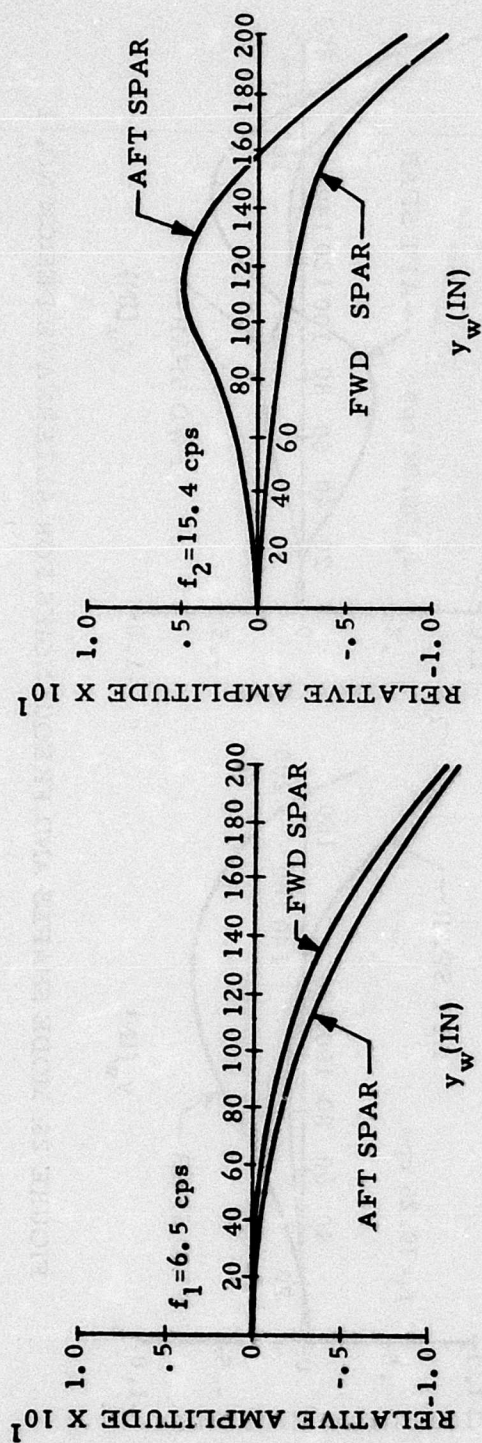


FIGURE 27: MODE SHAPES AND FREQUENCIES FOR THE BASELINE DESIGN

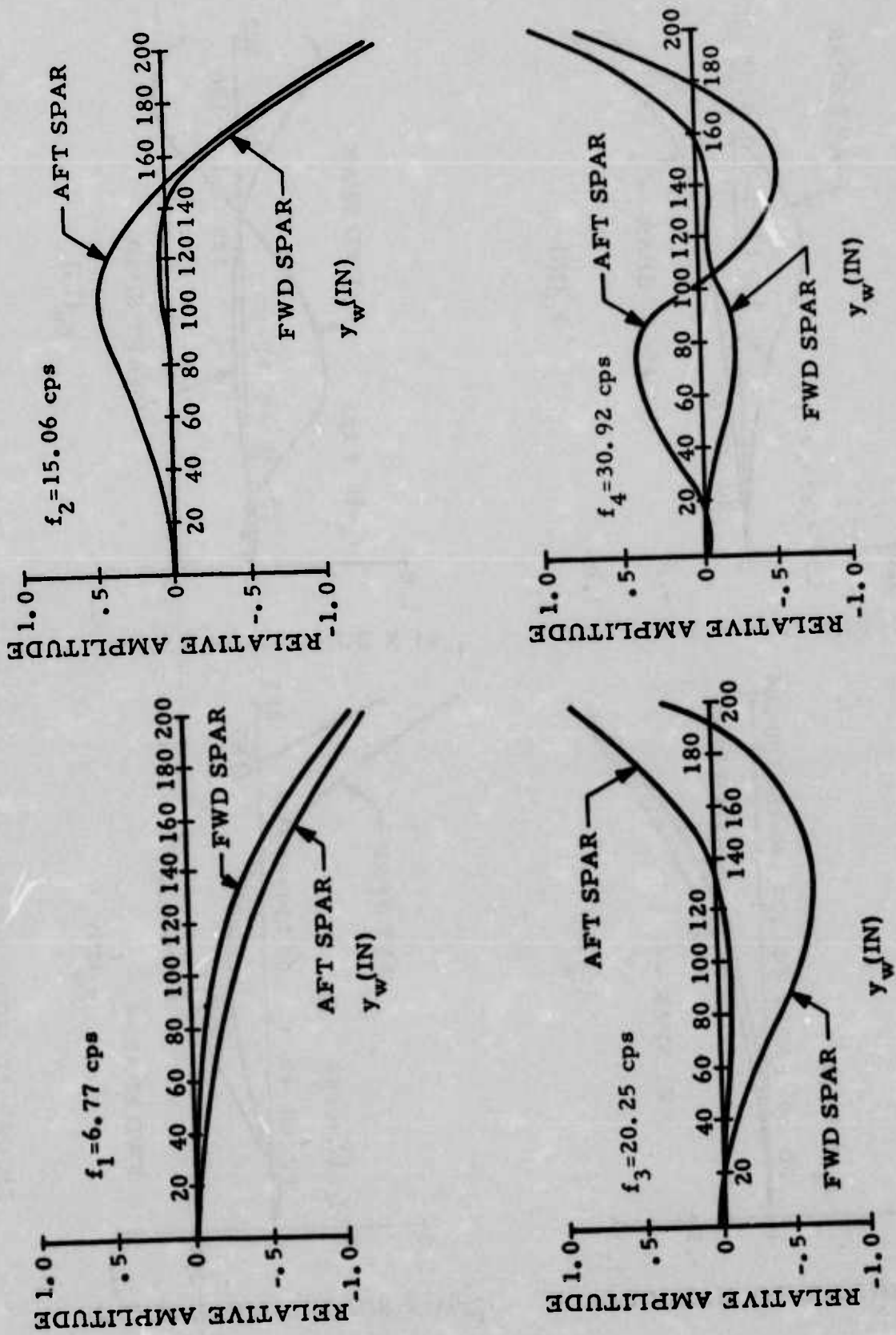


FIGURE 28: MODE SHAPES AND FREQUENCIES FOR ALTERNATE DESIGN NO. 1

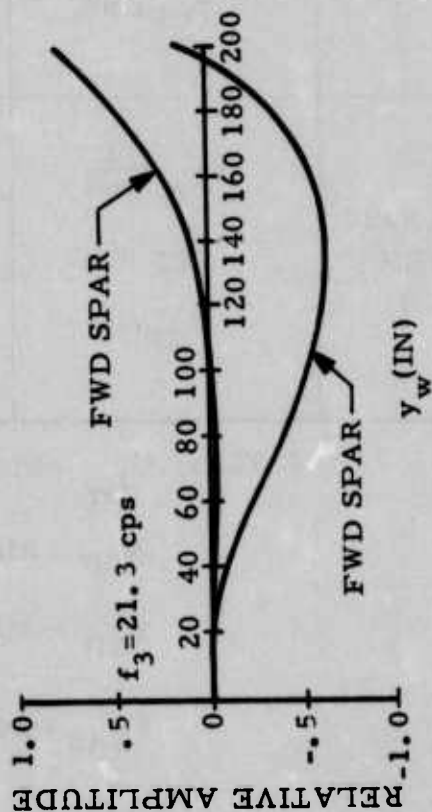
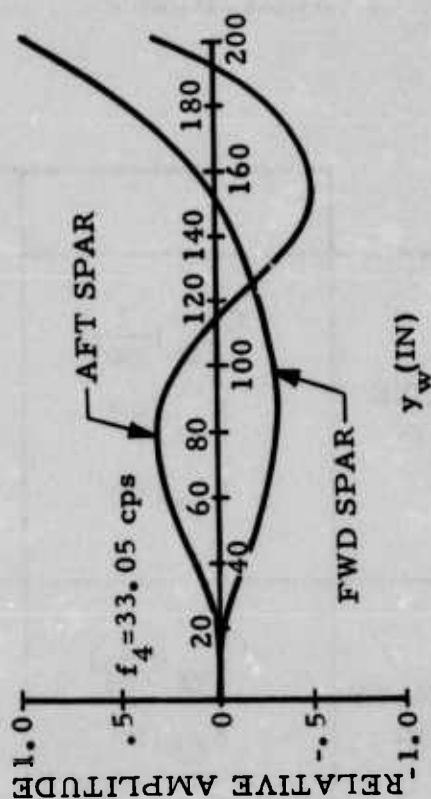
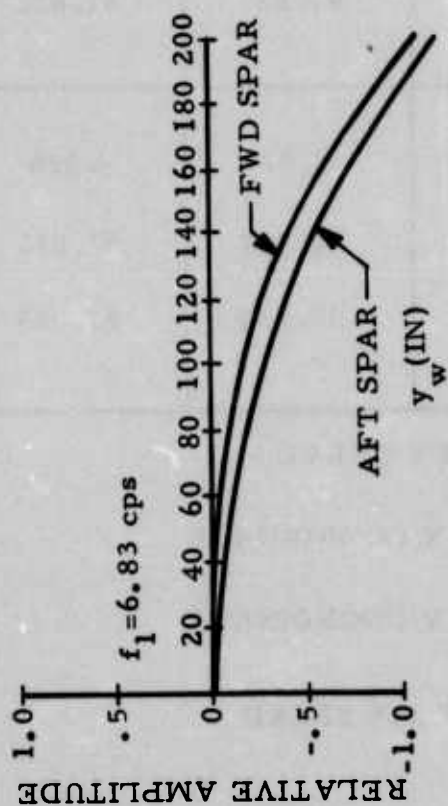
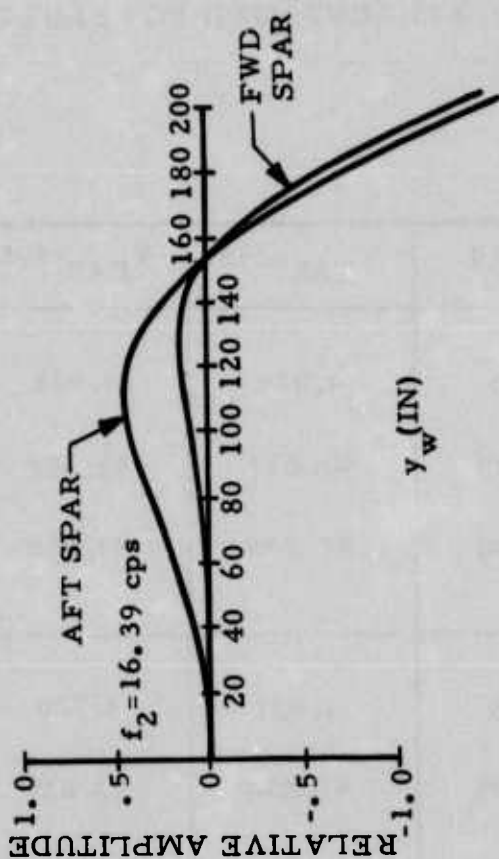


FIGURE 29: MODE SHAPES AND FREQUENCIES FOR ALTERNATE DESIGN NO. 3

TABLE V: FLEXIBLE AERODYNAMIC COEFFICIENT USED FOR FLUTTER EVALUATIONS

		$V_{EAS}=0$	$V_{EAS}=298$	$V_{EAS}=595$
BASELINE DESIGN	$C_L \alpha \left(\frac{1}{\text{rad}} \right)$	4.928	4.929	4.933
	$X_{CP}(\text{in})$	92.039	92.037	92.052
	$Y_{CP}(\text{in})$	87.832	87.833	87.850
ALTERNATE DESIGN NO. 1	$C_L \alpha \left(\frac{1}{\text{rad}} \right)$	4.928	4.927	4.926
	$X_{CP}(\text{in})$	92.039	92.034	92.029
	$Y_{CP}(\text{in})$	87.832	87.827	87.822
ALTERNATE DESIGN NO. 3	$C_L \alpha \left(\frac{1}{\text{rad}} \right)$	4.928	4.927	4.926
	$X_{CP}(\text{in})$	92.039	92.037	92.031
	$Y_{CP}(\text{in})$	87.832	87.830	87.824

NOTE: $C_L \alpha$ - SLOPE OF LIFT CURVE

X_{CP} - AIRLOAD CP X COORDINATE

Y_{CP} - AIRLOAD CP Y COORDINATE

V_{EAS} - EQUIVALENT AIR SPEED

4.4 COST COMPARISONS

The comparison of cost for CCS versus conventional wing main box structure was accomplished by determining recurring and non-recurring cost for:

- o A conventional contoured wing main box with built-in twist (the study baseline)
- o A CCS contoured airfoil main box (Alternate 2F)
- o A CCS flat sided main box (Alternate 2F)

The generation of these cost trends allowed a view of CCS with no built-in twist in both contoured and flat sided main boxes as compared to a twisted conventional wing box with airfoil contour. Table VI illustrates these comparative cost trends. This table demonstrates that on a total cost basis a contoured airfoil shaped CCS main box showed cost essentially the same as that of a conventional contoured main box with built-in twist. However, when a CCS wing main box with flat sides was compared with a conventional contoured airfoil with built-in twist a small total cost reduction is projected (7%). The cost trends in Table VI are based on an aircraft buy size of 200 and on this basis a break even point would occur only when advantages of the flat sided construction was employed. However, the CCS concept does provide the designer with the prerogative of using a flat sided main wing box to produce desirable wing twist where this less costly flat structure is not possible using conventional arrangements with built-in twist.

Costs for each detail part for all wing types were formulated based on:

- o Aluminum plate and forgings
- o Machining of parts from plate or forging
- o Conventional mechanical fastening

Integral stiffeners on the CCS skins increased cost as compared to the conventional skin which didn't have integral stiffeners. Main spars (front

TABLE VI: COST COMPARISONS OF CONTROL CONFIGURED STRUCTURE (CCS)
MAIN WING BOXES WITH A CONVENTIONAL WING BOX

COST ELEMENTS	CONVENTIONAL WING BOX WITH A BUILT-IN TWIST (BASELINE)	CCS WING BOX WITH A CONTOURED MAIN BOX (ALTERNATE 2F)	CCS WING BOX WITH A FLAT SIDED MAIN BOX (ALTERNATE 2F)
SKINS	1.0	1.35 (30%)	1.33 (30%)
SPARS	1.0	0.77 (40%)	0.71 (42%)
RIBS	1.0	0.65 (12%)	0.65 (13%)
ASSEMBLY	1.0	0.73 (18%)	0.73 (15%)
TOTAL COST (RECURRING ONLY)	1.0	0.92	0.89
TOTAL COST (RECURRING PLUS NON-RECURRING)	1.0	1.02	0.93

NOTES:

1. BASELINE COSTS ARE SHOWN AS UNITY
2. ALTERNATE CCS COSTS CAN BE COMPARED DIRECTLY TO
BASELINE
3. COSTS ARE AVERAGE BASED ON 200 AIRCRAFT
4. NUMBERS IN () ARE PERCENTAGES OF TOTAL WING
RECURRING COST ON 200 AIRCRAFT BUY.

and rear) were assumed to be machined from forgings. A cost increase was observed on these two spars since they weighed more due to higher loads as compared to the conventional box main spars. The intermediate spar length was 28% less on the CCS configuration than the conventional wing box which resulted in a cost reduction. In addition the CCS configuration had 13 rib segments compared to 20 rib segments on the conventional structure. This saving was comparatively small in total wing cost reductions. The assembly cost for CCS was also lower by approximately 27% due to a shorter skin to spar joint length (28% less). Furthermore, the conventional main box has 48 rib-to-spar joints, while the CCS box had 44.

All cost comparisons were based on conventional practice and state-of-the-art use of materials and fabrication techniques.

5.0 CONCLUSIONS

This study of the effects and data resulting from the comparative evaluation of Control Configured Structure (CCS) wing main boxes with that of a conventional wing main box was based on aerodynamic characteristics, flutter comparisons, weight comparisons and cost trends. The following paragraphs summarize each of these key technical areas and demonstrate that the theory of CCS has significant potential benefits.

- o Aerodynamic Characteristics - A CCS wing main box such as those evaluated in the alternate design (2F) has a lower profile drag and trim drag over the major flight regime as compared to conventional wing structure with built-in twist.
- o Flutter Comparisons - A CCS wing main box such as those evaluated in the alternate designs has the same flutter characteristics as a conventional wing box (the baseline). This conclusion is valid so long as the wing stiffness of the CCS and conventional wings are approximately equal as reflected by the structural influence coefficients that were very comparable in this study. Other dynamic effects such as aileron effectiveness and roll reversal were not considered in this study.
- o Weight Comparisons - A CCS wing main box such as those evaluated in the alternate designs can be fabricated for the same weight value as a conventional wing main box. While a CCS wing main box will have heavier skins and main spars, it will be lighter in weight for intermediate spars and ribs.
- o Cost Trends - A CCS wing main box such as those evaluated in the alternate designs can be fabricated for essentially the same cost as a conventional contoured main box with built-in twist. A small cost reduction may be realized through the use of flat sided CCS main box structure.

- o Structural - The internal wing spar/stiffener orientation can induce beneficial twists for both positive and negative wing bending loads. In addition the structural main box arrangements that were evaluated demonstrated that this beneficial twist was greatest when the intermediate bending elements (spars and stiffeners) were rotated in a forward direction in relation to a line normal to the aircraft centerline.

In summary this study has shown that CCS wing box structure has sufficient potential to warrant additional study. As far as can be determined by the limited studies that have been performed thus far, there appears to be definite performance advantages to be achieved with essentially no penalty. The structure can be obtained at approximately equal weight, flutter speed and cost as compared to the conventional twisted baseline; and still achieve the basic aerodynamic advantage of providing desired wing box twist (reduced drag and inboard C.P. shift) as a function of airload. Therefore, the CCS wing main box structure provides an airload driven twist (passive action) that heretofore had to be built in as original twist to achieve certain aerodynamic characteristics. The consideration of camber effects was not a subject of this contract effort, but further study appears desirable to consider the influence of these effects.

Although not specifically approached in this study, other conclusions could be logically extrapolated from these results. For instance, CCS structure could potentially provide a more stable weapons delivery platform due to its twist characteristics which minimize the gust response encountered during an attack run.

6.0 RECOMMENDATIONS

As seen from the results presented in this report, the twist obtainable with CCS structure can be advantageous for improving aerodynamic characteristics. However, these advantages tend to be relatively small when compared to those available when the CCS twist platform is augmented with some system providing wing camber. The investigation of the twist plus camber possibilities should be the next logical step in the development of the CCS concept. The effect of camber on twist characteristics is illustrated in Figure 30 (although not necessarily at an optimum level) and is significant, showing that this combination of methods offers potentials above that available with twist alone. Table VII illustrates several parameters which can be improved and their projected amount of improvement when the CCS twist platform is supplemented with two types of wing camber.

In light of the advantages offered when passive CCS structure is combined with camber producing systems, it becomes evident that still another application of load induced twist has high prospect. That would be the use of CCS structure for the wing leading edge section to produce a leading edge flap which rotated under load in a direction producing wing camber. This would be a passive system completely dependent on wing loading giving the camber advantages when it is most useful, which is illustrated in Table VII.

An effort to determine the optimum structural parameters most critical to CCS operation should also be considered. These parameters include internal structure orientation angles, wing sweep angle, wing root restraint, root to tip chord ratio and spar/skin area ratio. Optimization of these parameters would lead to the optimization of the total wing including the passive leading edge camber system.

Other areas of importance which should also be evaluated are those specific cases such as aileron effectiveness and reversal characteristics associated with the CCS twist platform and the effect of CCS structure on wing gust response which could influence both the fatigue life and the stability of a weapons delivery platform.

A logical sequence of work for continuing the development of CCS technology is illustrated in Figure 31. This outline shows that this technology is only in the embryonic stage and several continuing steps are required to fully define and explore all the potentials.

TABLE VII: PROJECTED PERFORMANCE IMPROVEMENTS OVER CONVENTIONAL WINGS

SYSTEM PARAMETER	PASSIVE SYSTEM (CCS TWIST PLUS BUILT IN CAMBER)	PASSIVE SYSTEM PLUS ACTIVE SYS (CCS TWIST PLUS DOUBLE L. E. AND T. E. CAMBER DEVICES)
SUSTAINED LOAD FACTOR INCREASE ~ g's	0.5 (OVER CONVENTIONAL WING)	1.0 (OVER PASSIVE SYSTEM ONLY)
		1.5 (OVER CONVENTIONAL WING)
MANEUVER FUEL SAVINGS	5% (OVER CONVENTIONAL WING)	10% (OVER PASSIVE SYSTEM ONLY)
		15% (OVER CONVENTIONAL WING)

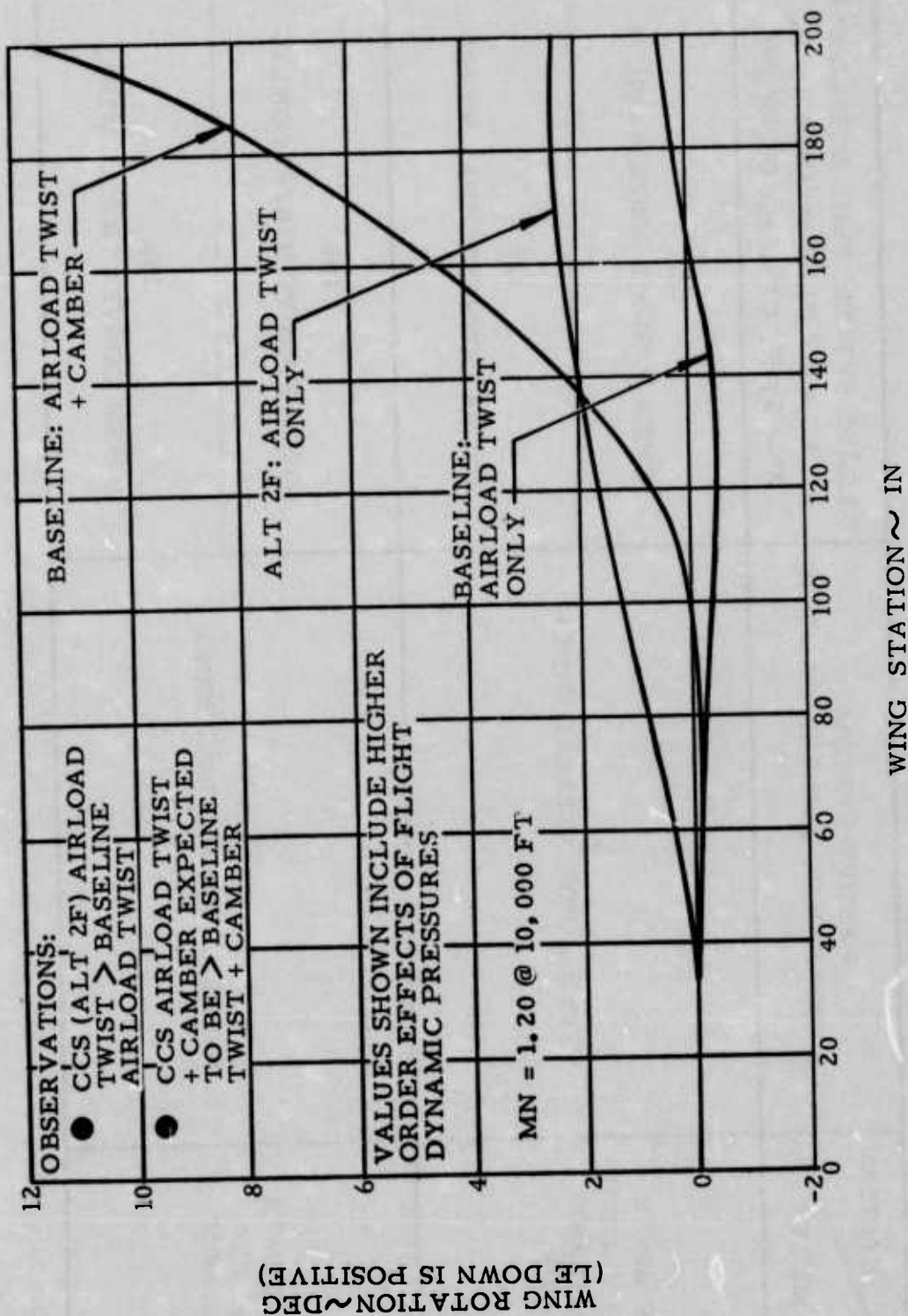


FIGURE 30: EFFECT OF CAMBER ON BASELINE EQUILIBRIUM TWIST ~ 4g CONDITION
AT MACH NUMBER 1.20

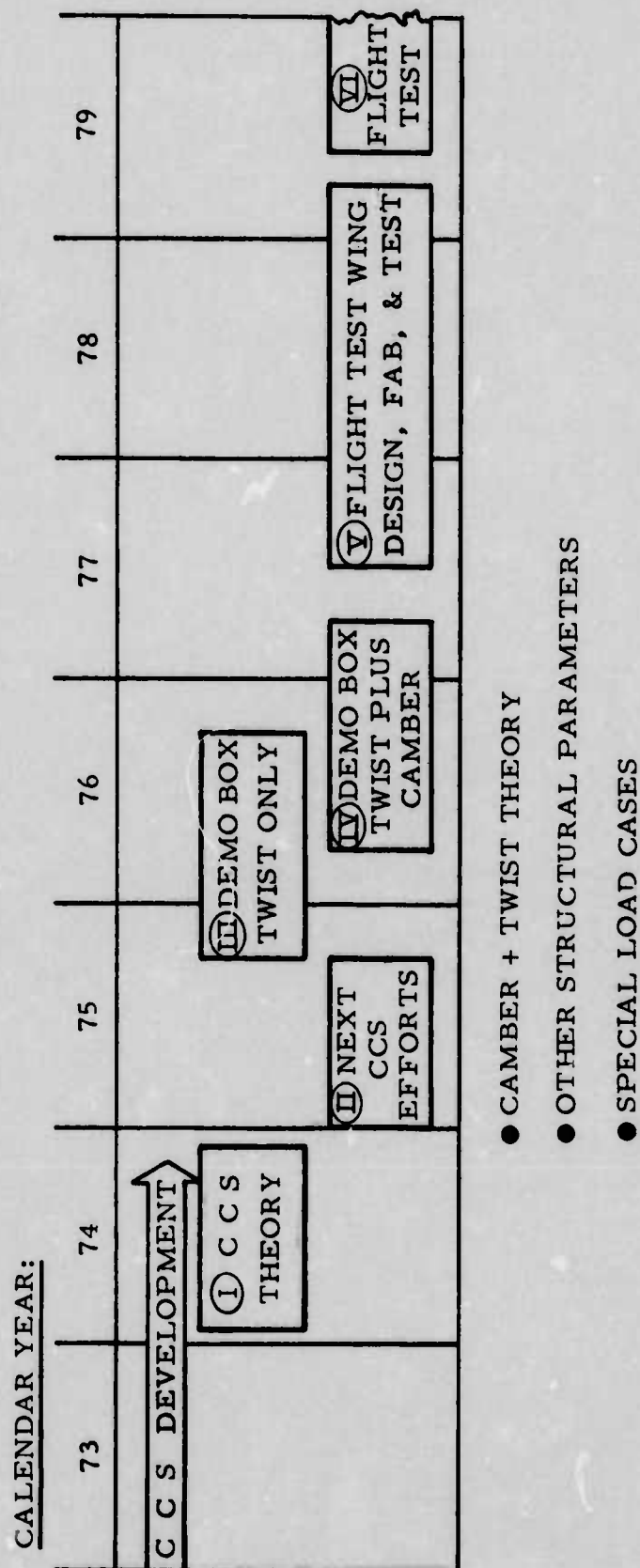


FIGURE 31: CCS TECHNOLOGY DEVELOPMENT SEQUENCE

7.0 REFERENCES

1. Don W. Kinsey, "Analysis of Twist Effects From Available 1/24 Scale F-111/TACT Model Data", Aerospace Vehicle Branch, Flight Mechanics Division, Air Force Flight Dynamics Laboratory, Technical Memorandum AFFDL TM 74-91-FXS dated April 1974.
2. A. L. Curry and E. A. Minter, "Preliminary Airframe Structural Design Load Prediction Techniques for Military Aircraft" (Volumes 1 thru 5), Vought Systems Division, LTV Aerospace Corporation, Technical Report AFFDL-TR-73-157 dated December 1973.

APPENDIX A STRUCTURAL METHODS

The primary structural analysis tool used in this study was the NASTRAN (NAsa STRuctural ANalysis) finite element displacement system. This system used was the McNeal-Schwendler Corporation (MSC) CDC 6600 version 20. Several "pre" and "post" processor routines to NASTRAN were used for the data management of output. The relationship between these processor programs and NASTRAN is shown in Figure 32.

The solution sequence used was to initially define the structural math model grid locations, raw structural element locations (spar web caps, skin membranes, spar and rib shear webs) and the loading conditions (shear, moment and torsion curves). This data was input into the VSD JWWING pre-processor program which output the model finite element bulk data and the distributed grid point load data in the format required for use in NASTRAN. The pre-processor NOPIP initiates the NASTRAN input file and resizing process. Then NASTRAN and the post-processor resizing program NASTOP analyzed and resized the structure using the designated constraint parameters (allowable stresses, minimum thicknesses and areas) using the fully stressed design (stress-ratio) approach. The output consisted of model weight, loads, stresses, reactions and displacements. These data were combined with the mass and aerodynamic slice requirements (panel point locations) input into the GMASS and NASFLEX post processors to generate slice mass data, aerodynamic and dynamic structural influence coefficient (SIC-influence) matrices.

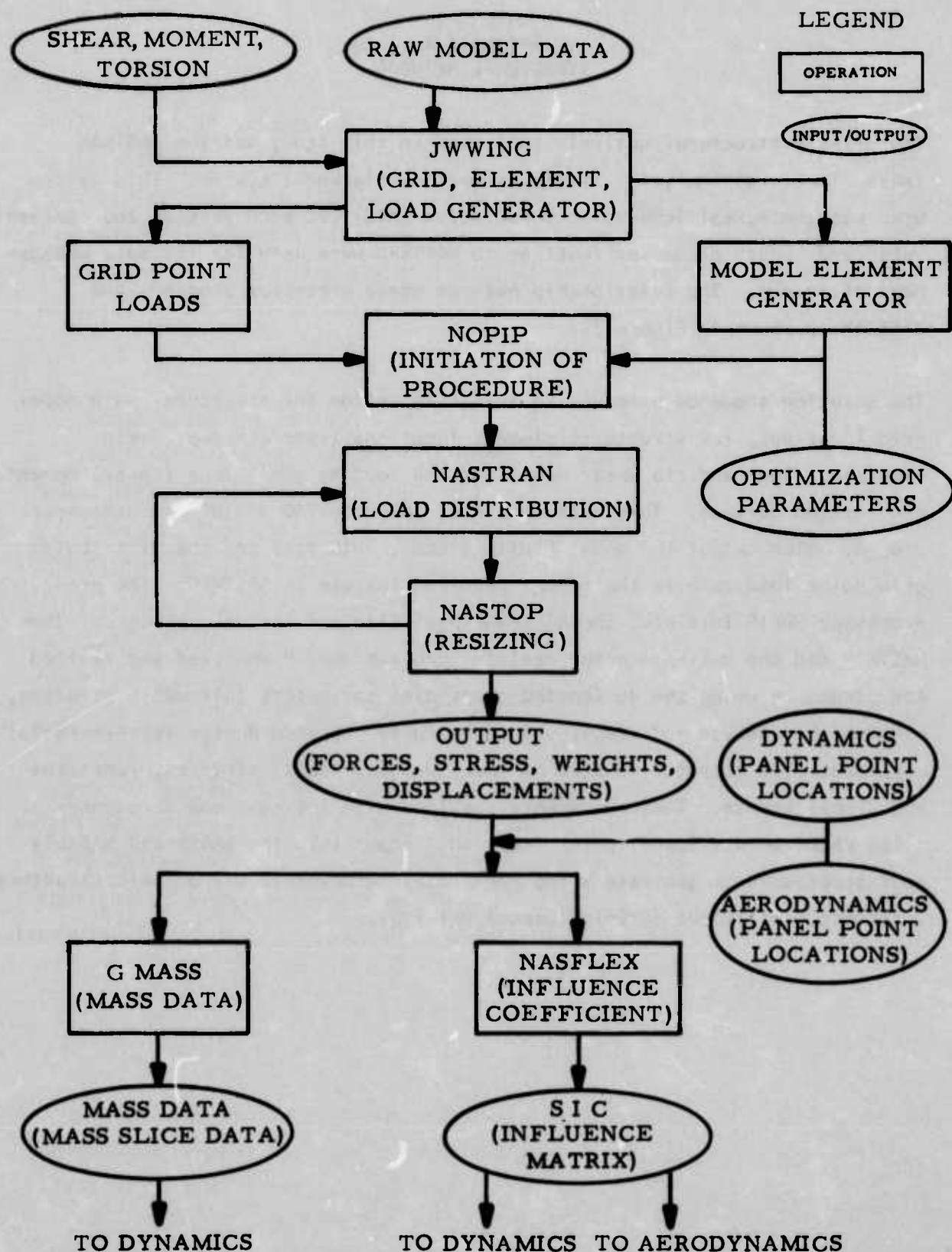


FIGURE 32: FLOW DIAGRAM FOR STRUCTURAL METHODS EMPLOYED IN CCS ANALYSIS

APPENDIX B AERODYNAMIC ANALYSIS METHODS

The aerodynamic effort in support of the Control Configured Structure (CCS) program involved two separate tasks. The preliminary phase consisted of a parametric study of the effects of a spanwise variation of wing twist, chordwise camber and a combination of both effects on the aerodynamic characteristics of a select wing planform. The wing planform was that used in a previous configuration study and variations in twist and camber were chosen based on the same design studies.

The parametric study was conducted to provide a preliminary aerodynamic evaluation base to compare CCS configurations and to provide trends which could be used to project effects for future efforts. The second task under the study involved the aerodynamic analysis of a specific configuration in equilibrium twist at Mach numbers of .80 and 1.20 and an altitude of 10,000 feet. The results of this evaluation were presented in Section 4.0 of this report; however, a brief summary of the methods used in generating load distributions and aerodynamic data are contained in this appendix following the parametric data.

The aerodynamic evaluations were made using theoretical solutions for both the rigid and equilibrium twist load conditions. The procedure was validated by comparing wind tunnel test results to theoretically derived values for the same configuration. These wind tunnel data were obtained on configurations very similar to those used in the study and thus provide additional information for configuration evaluation.

1. PARAMETRIC STUDY

In any airplane design effort, particular emphasis is placed on wing selection. The selection of the basic planform and airfoil section is made considering the effects of wing area, aspect ratio, leading edge sweep, and taper ratio

on overall airplane performance requirements. Once these parameters have been evaluated and the wing selected, some refinement of the airplane drag with lift (drag polar) may still be made by alterations in wing twist, airfoil camber, or combinations of both. A real potential therefore exists for configuring the wing internal structure to deflect under load so as to provide aerodynamic characteristics normally obtained by incorporating built-in twist, camber or possibly a combination of both.

A parametric analysis was made to evaluate the relative effects of these forms of geometric change when compared to a plane, undeflected wing. This analysis was accomplished using theoretical solutions (verified by comparison to experimental data) to provide insight as to the order of magnitude of the aerodynamic effects obtainable using nominal values of both twist and camber. One configuration which incorporated both twist and camber was also investigated. The analysis of all configurations was made for two loading conditions corresponding to a forward loading on the structure, forward C.P., and an aft loading. This was accomplished by evaluating the effects at a Mach number of 0.80 for a forward C.P. and at a Mach of 1.20 for an aft C.P. since the variation in aerodynamic loadings due to Mach number followed this trend.

(1) Experimental Data Verification

To correlate the theoretical methods with experimental results, two configurations were evaluated for which wind tunnel data were available. The review was made to examine the trends of aerodynamic data with angle of attack and to compare the relative orders of magnitude. Comparisons were made for supersonic and subsonic conditions to establish the suitability of the theoretical methods. A portion of these comparisons was formalized and is presented in Figures 33 thru 35 for a plane wing (no built-in twist) and one which incorporated a spanwise variation in twist.

The results of a more comprehensive study on the effects of twist on aerodynamic characteristics was reported in Reference 1. These data were obtained on a model of the F-111 with a supercritical airfoil section

incorporated in the wing geometry. The tests were conducted to show: (1) the effects of twist at different lift coefficients, (2) the effects of twist at different Mach numbers, and (3) the effects of twist at different sweep angles. The range of twist angles tested and the spanwise variations were similar to that used in the subject parametric study. These data were in agreement with the results of the program parametric study in trend and order of magnitude. This lends strong support to the theoretical simplification of solutions for incremental wing effects without the complications of a body or wing thickness since the two wind tunnel test results (VSD and Ames) were for models having widely differing configurations.

o Drag - Differences in absolute values between experimental and theoretical data are apparent. These differences were due to geometric variables and do not invalidate the incremental effects of twist or the trends of these effects with angle of attack and Mach number. These wind tunnel data were obtained using a model which incorporated a fuselage and vertical tail. Since these items will produce drag at zero wing lift, the drag polar was displaced from zero. In addition the wing has a finite thickness which is not duplicated in the theoretical calculations. Thus for the plane untwisted wing, no drag value is shown at zero C_L since the wing was simulated by a plane of zero thickness; but having the planform geometry of the wing tunnel test article. These differences were not important however, since the effects of geometry on wing aerodynamic characteristics are additive. This was confirmed by the data presented in Figure 33 which show the relative effects of twist on the incremental value of C_D at C_L of zero and the trends with increasing C_L to be comparable.

If absolute magnitudes are important in configuration evaluations, the drag polar may be more accurately calculated using a combination of theoretical and empirical methods. A method was available at VSD which was used to calculate the drag polar for a plane wing starting from the initial C_D value at zero lift, for the wing/body/tail configuration, and the non-linear C_L variation with angle of attack as measured in the wind tunnel. The computed values are shown in Figure 34 and agree very well with the measured

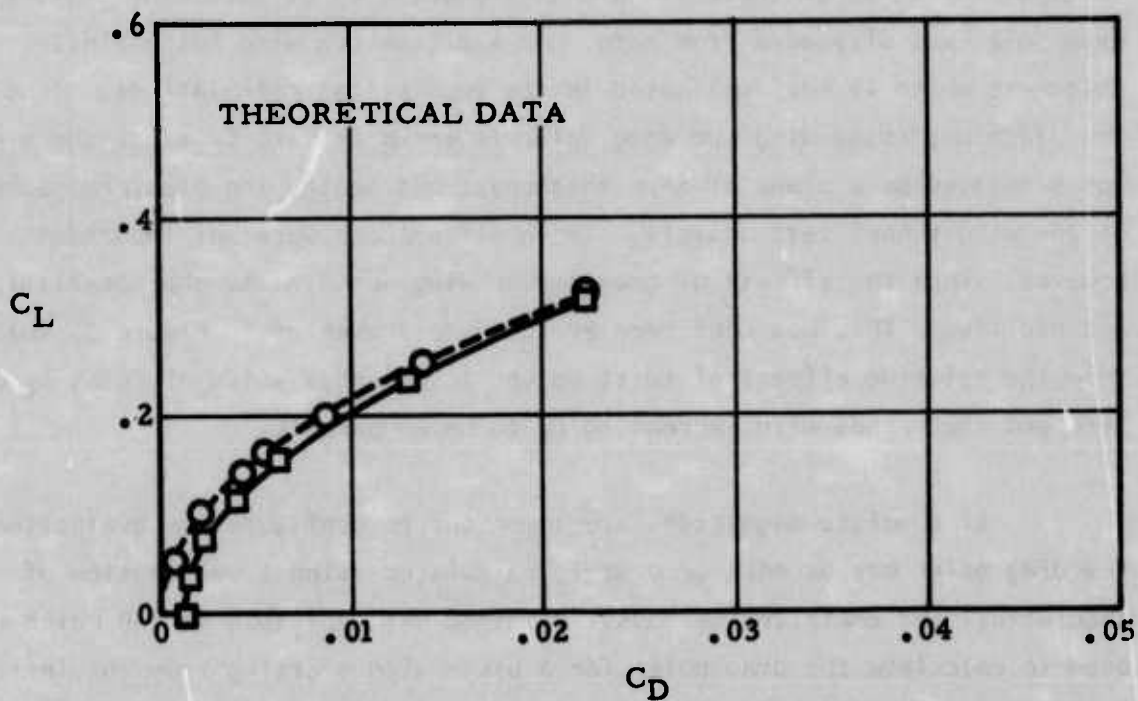
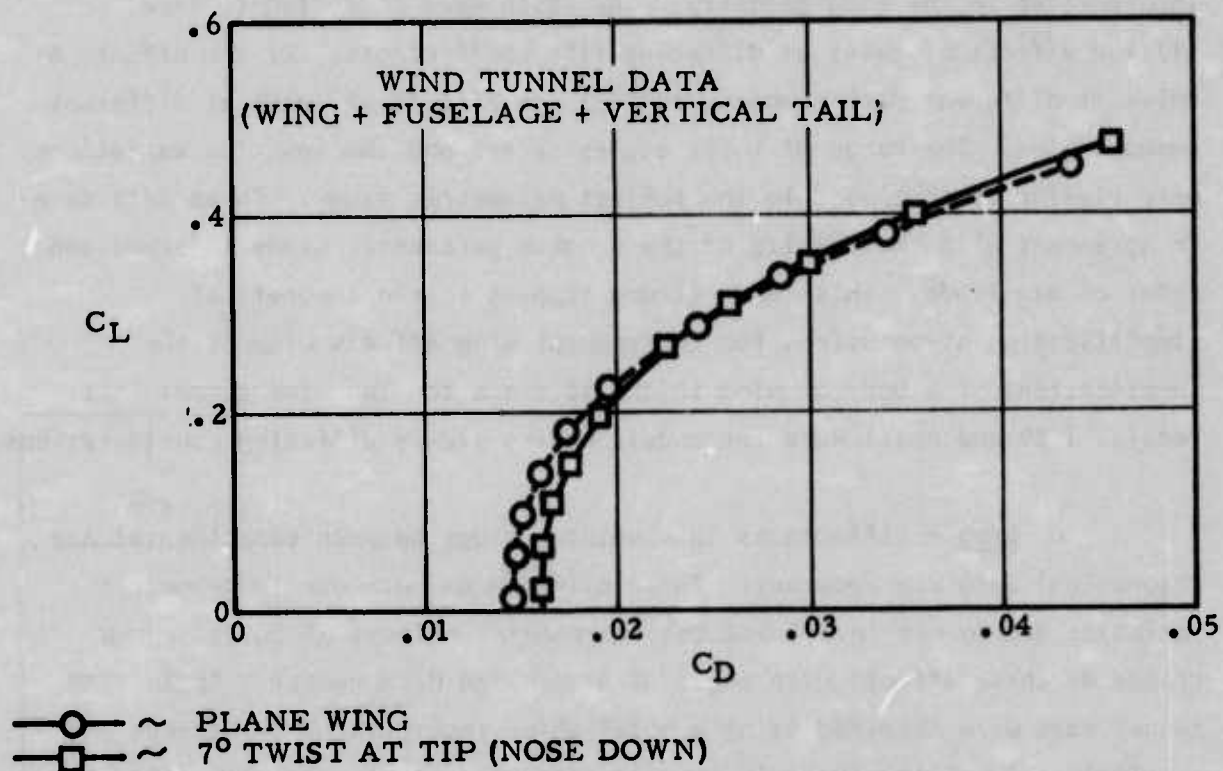


FIGURE 33: COMPARISON OF THEORETICAL PREDICTIONS WITH WIND TUNNEL DATA $M = .80$

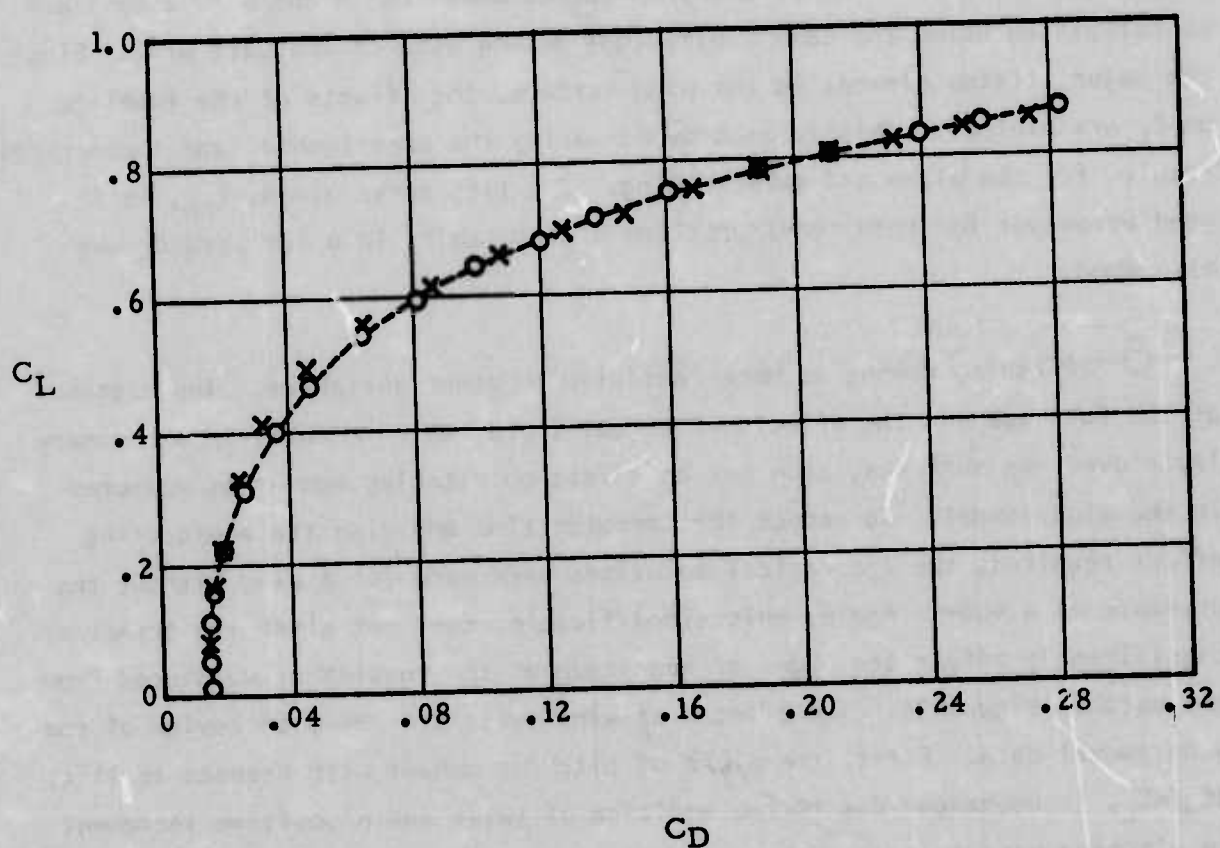
ZERO TWIST

$$R = 3.8$$

$$\lambda = .296$$

$$\Lambda = 35^\circ$$

$$M = .80$$



○ ~ HSWT TEST 433 (RUN 47)
X ~ COMPUTER ROUTINE

FIGURE 34: NON-LINEAR DRAG POLAR

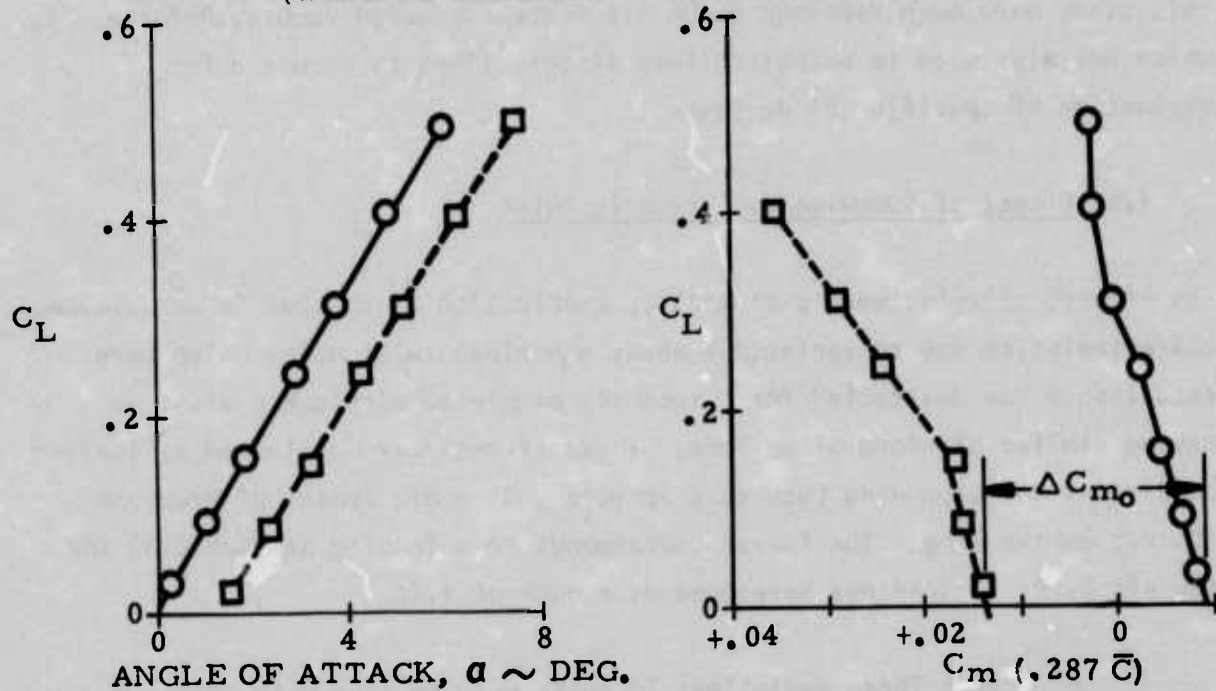
wind tunnel values. This procedure was initiated with the intention of using it for all drag studies, but was found to be too time consuming and was not required to provide a preliminary evaluation of the effect of variations in wing geometry. For this reason drag evaluations, within the program study, were made on the basis of theoretical linear solutions only.

o Lift and Pitching Moment - The effects of wing twist are presented in Figure 35 for lift and pitching moment as measured in the wind tunnel and as calculated using the same theoretical method used to evaluate drag. Since the major lifting element is the wing surface, the effects of the fuselage on C_L are minimal. This is seen by comparing the experimental and theoretical results for the plane and twisted wing. The lift curve slope, $C_{L\alpha}$, is in good agreement for both configurations and the shift in α for zero C_L was also good.

Pitching moment is more sensitive to other variables. The presence of the fuselage and the effects of a real fluid, which results in a boundary layer over the surfaces, each has an effect on pitching moment as measured in the wind tunnel. To reduce the computer time and also the engineering effort required, the theoretical solutions were made for a wing without the presence of a body. Again, this simplification does not alter the trends or significantly affect the order of magnitude of the results as evidenced from the data in Figure 35. Two effects of wing twist are noted on review of the wing tunnel data. First, the slope of pitching moment with respect to lift, dC_m/dC_L , is unchanged due to the addition of twist and a positive increment in pitching moment is introduced. These were the same results shown from a review of the theoretical data, however, absolute values of dC_m/dC_L and ΔC_{m0} are altered due to viscous effects and the presence of a fuselage on the wind tunnel model.

From a review of these data and other comparisons made during the informal review of all data examined during the course of this study, it was concluded that valid conclusions may be drawn as to the aerodynamic trends and incremental effects due to configuration changes as calculated using

WIND TUNNEL DATA
(WING + FUSELAGE + VERTICAL TAIL)



—○— ~ PLANE WING
--□-- ~ 7° TWIST AT TIP (NOSE DOWN)
THEORETICAL DATA

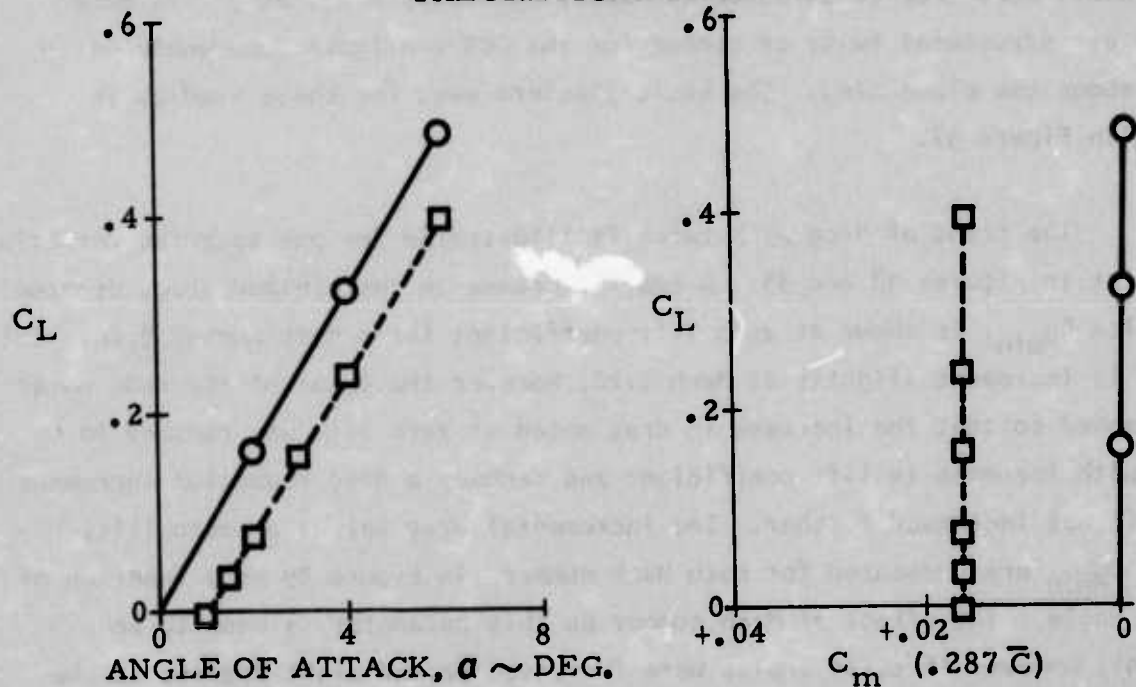


FIGURE 35: COMPARISON OF THEORETICAL PREDICTIONS WITH WIND TUNNEL DATA $M = .80$

theoretical solutions for the wing alone. The theoretical method used for this study have been reported in an Air Force sponsored report, Reference 2, which was also used to establish load distributions as required for evaluation of specific CCS designs.

(2) Effect of Spanwise Variation in Twist

The effects of twist were evaluated by examination of changes in aerodynamic characteristics due to variations about a nominal twist value which were established "as desirable" for a recently completed airplane evaluation having similar planform dimensions. These effects were evaluated at loading conditions corresponding both to a forward and an aft Center of Pressure (C. P.) on the wing. The former corresponds to a loading at Mach 0.80 and the aft C. P. to loadings developed at a Mach of 1.20.

o Drag - Three variations in twist were defined with span. A sample twist variation is shown in Figure 36. The other distributions were defined using the same basic spanwise variation. The resulting aerodynamic parameters were then compared to the base, untwisted wing, as a reference since all structural twist or camber for the CCS configurations would be made about the plane wing. The basic planform used for these studies is shown in Figure 37.

The trend of drag with twist is illustrated for one spanwise variation of twist in Figures 38 and 39. A small increase in the minimum drag, denoted by $\Delta C_{D_{min}}$, is shown at zero lift coefficient for a Mach number 0.80. This value is increased slightly at Mach 1.20, however the shape of the drag polar is changed so that the increase in drag noted at zero lift was reduced to zero with increase in lift coefficient and becomes a drag reduction increment as lift was increased further. The incremental drag values at zero lift, $\Delta C_{D_{min}}$ are presented for both Mach numbers in Figure 39 as a function of twist angle. The effect of Mach number on this parameter is seen to be minimal, however if twist angles were increased beyond eight degrees at the tip the $\Delta C_{D_{min}}$ values would rise quite rapidly. Thus considering only the untrimmed drag polar, values of twist beyond eight degrees would not be

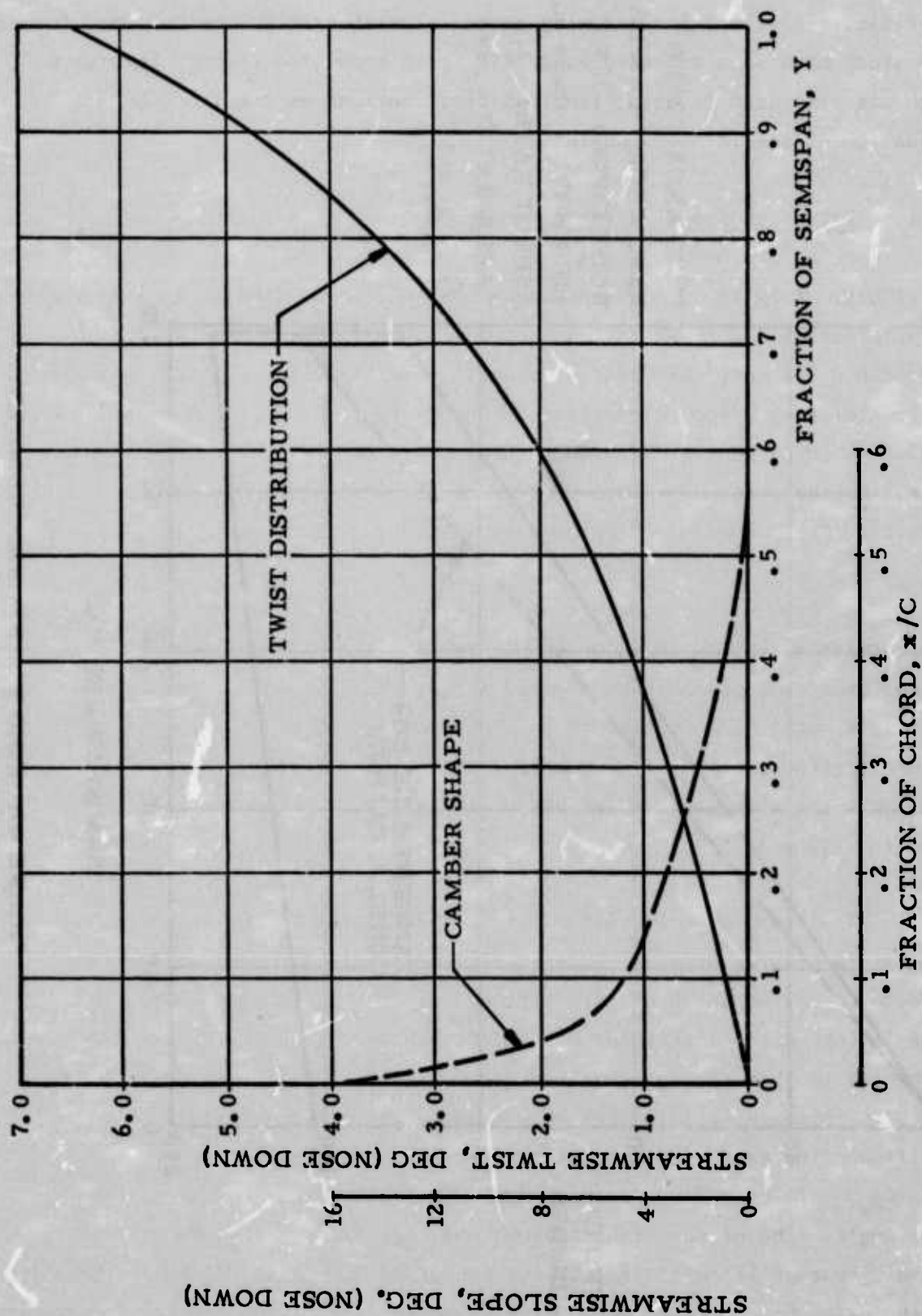


FIGURE 36: NOMINAL VALUES OF TWIST & CAMBER USED IN PARAMETRIC VALUES

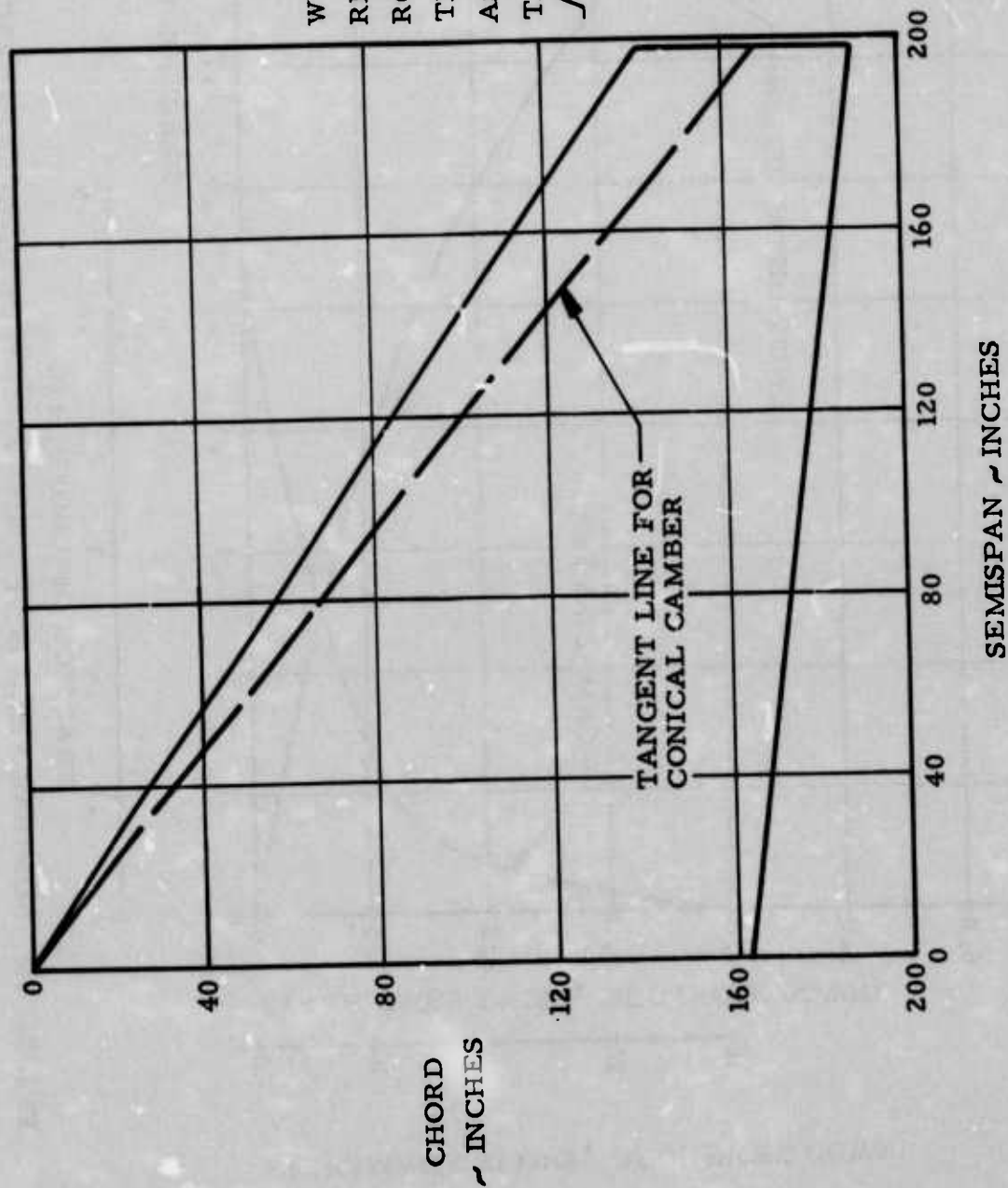
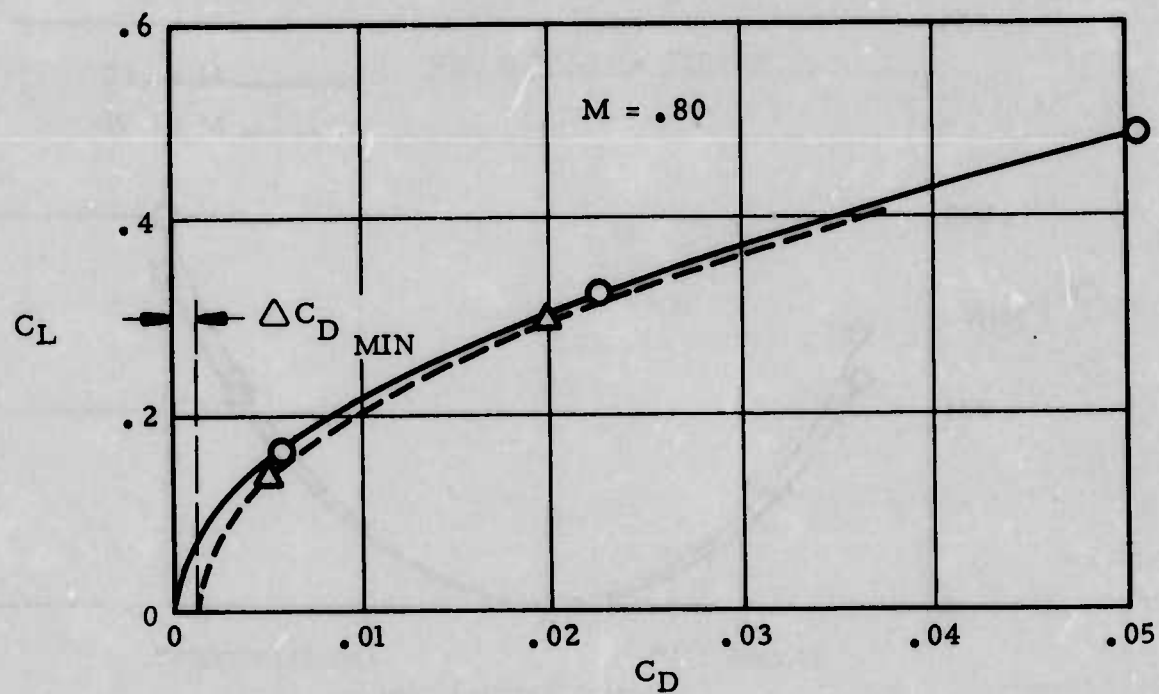


FIGURE 37: WING PLANFORM GEOMETRY



—○— ~ PLANE WING
 - -△- - ~ 6.5° TWIST @ TIP

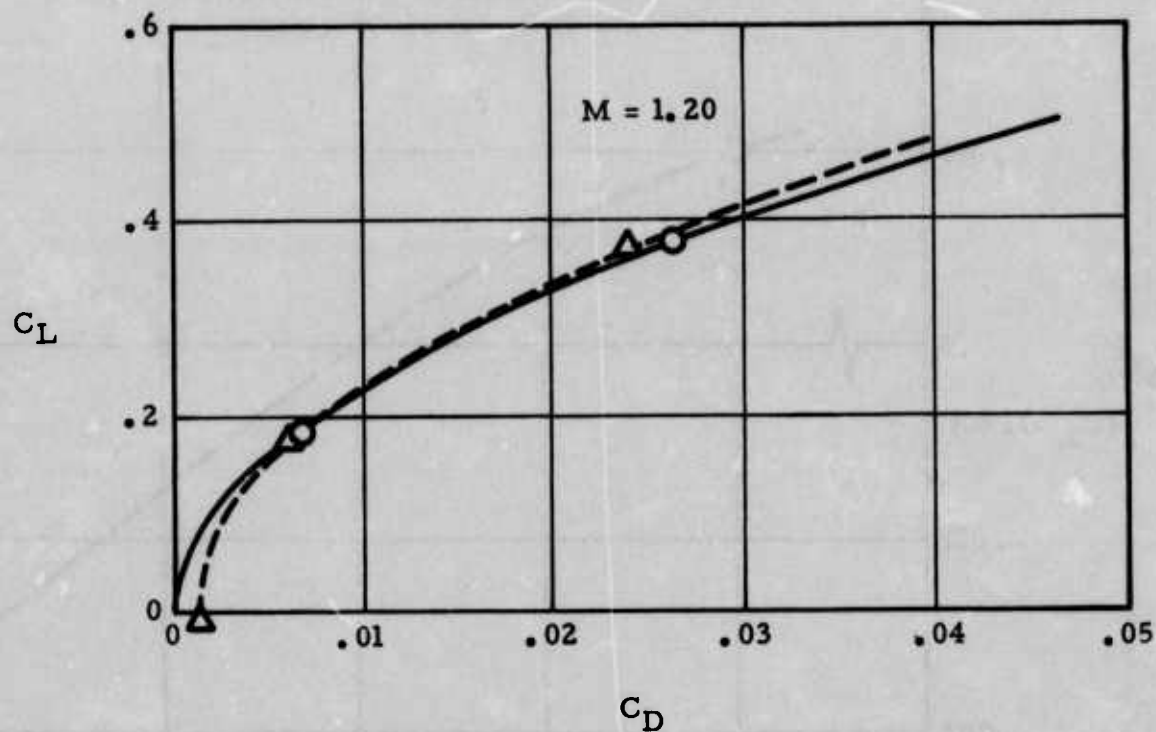


FIGURE 38: EFFECT OF SPANWISE TWIST VARIATION ON DRAG POLAR SHAPE

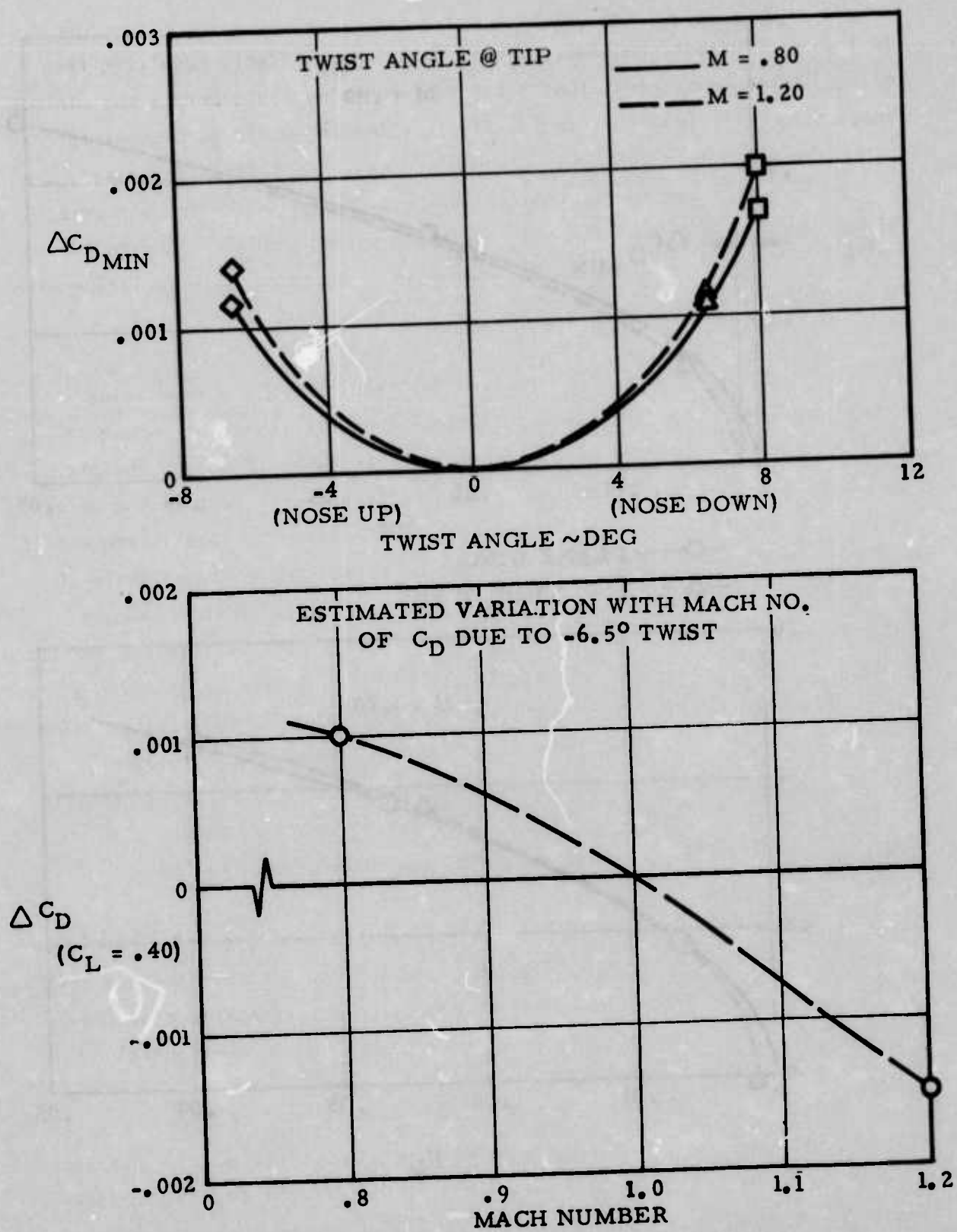


FIGURE 39: EFFECT OF TWIST ON DRAG VALUES

desirable. Further, considering only $\Delta C_{D_{min}}$ effects resulting from twist, it became apparent that a CCS configuration would permit the minimum drag at low lift levels since insufficient loading would be present to twist the wing, thus $\Delta C_{D_{min}}$ would be zero. As lift is increased, the structure twists and the incremental drag values are a smaller percentage of the total. In the supersonic case these values actually tend to reduce the wing drag over the untwisted value. An estimate of this variation with Mach number is shown in Figure 39.

o Lift and Pitching Moment - The results for the same twist variations on the aerodynamic longitudinal characteristics are shown in Figure 40 for the forward C. P. loading at Mach number 0.80 and the aft C. P. loading at Mach number 1.20. The primary effect was a shift in the aerodynamic parameters at zero angle of attack. Because of the displacement of lift with angle of attack, the wing must be rotated to a higher angle of attack to achieve the same lift. This same twist results in a nose up pitching moment, ΔC_{m_0} , which is constant with lift coefficient for both Mach numbers investigated. This characteristic is an aid in trimming a stable airplane configuration since less trim force is required for a given value of lift. The magnitude of the reduction is a function of the airplane configuration. The ΔC_{m_0} values are plotted as a function of wing tip twist in Figure 41, and appear to be a linear function of twist. The variation with Mach number was small for the values investigated.

In a CCS configuration, this increment in pitching moment would be absent at the lower values of lift and would increase in magnitude as lift is increased. This trend introduces a reduction in the static stability parameter, dC_m/dC_L , which would have to be considered in configuration evaluation.

o Spanwise Location of Wing C. P. - A composite plot of the spanwise location of wing loading C.P. with lift coefficient for all configurations evaluated are presented in Figure 42 for a Mach number of 0.80 and in Figure 43 for a Mach number of 1.20. At the lower lift coefficients the C.P. of loading approaches zero lift asymptotically; since for the twist

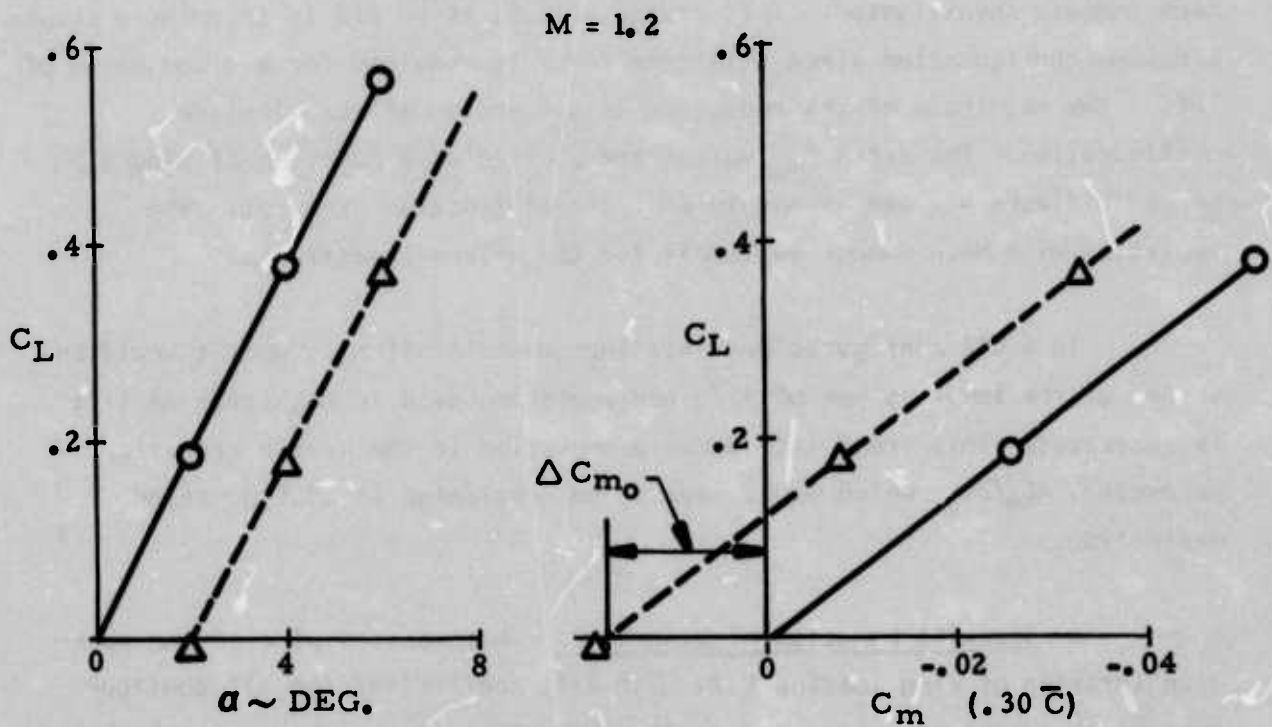
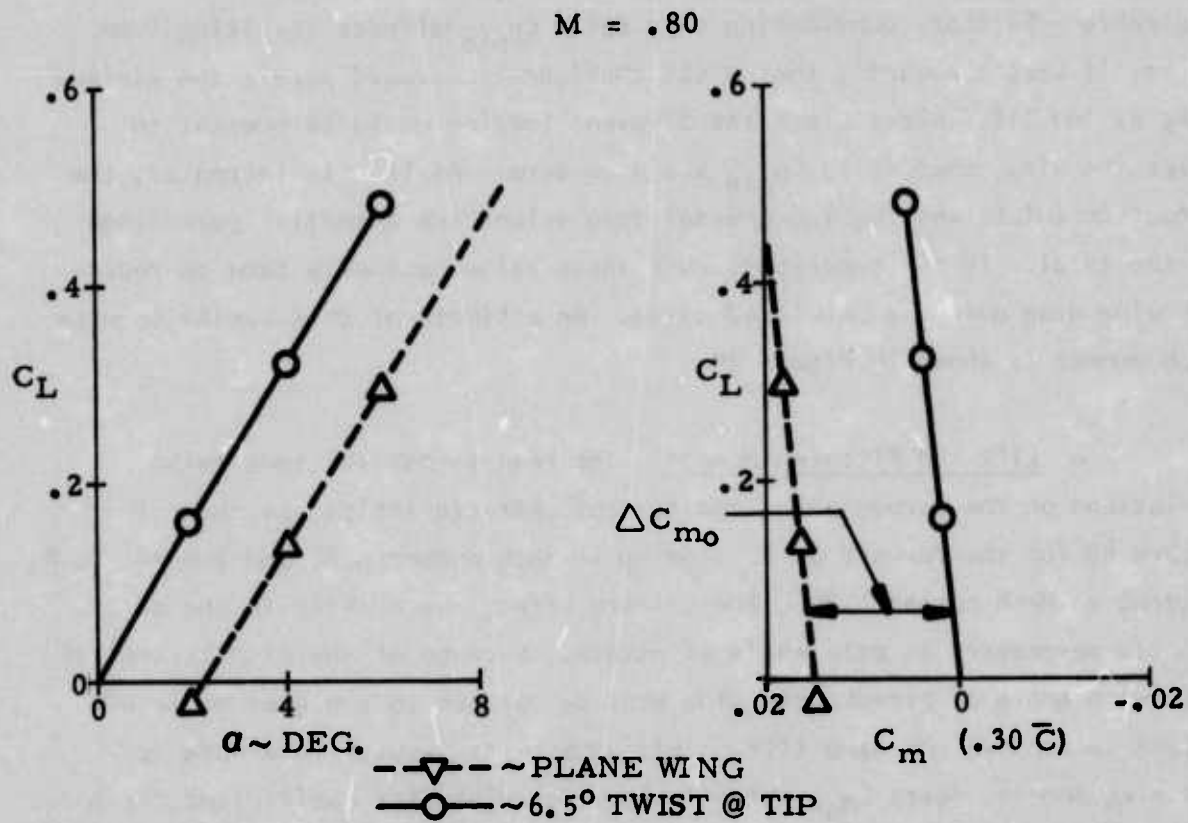


FIGURE 40: EFFECT OF SPANWISE TWIST VARIATION ON LIFT AND PITCHING MOMENT

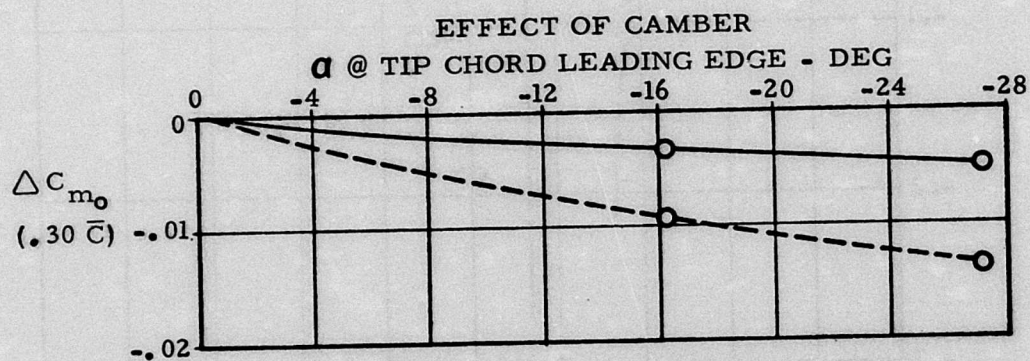
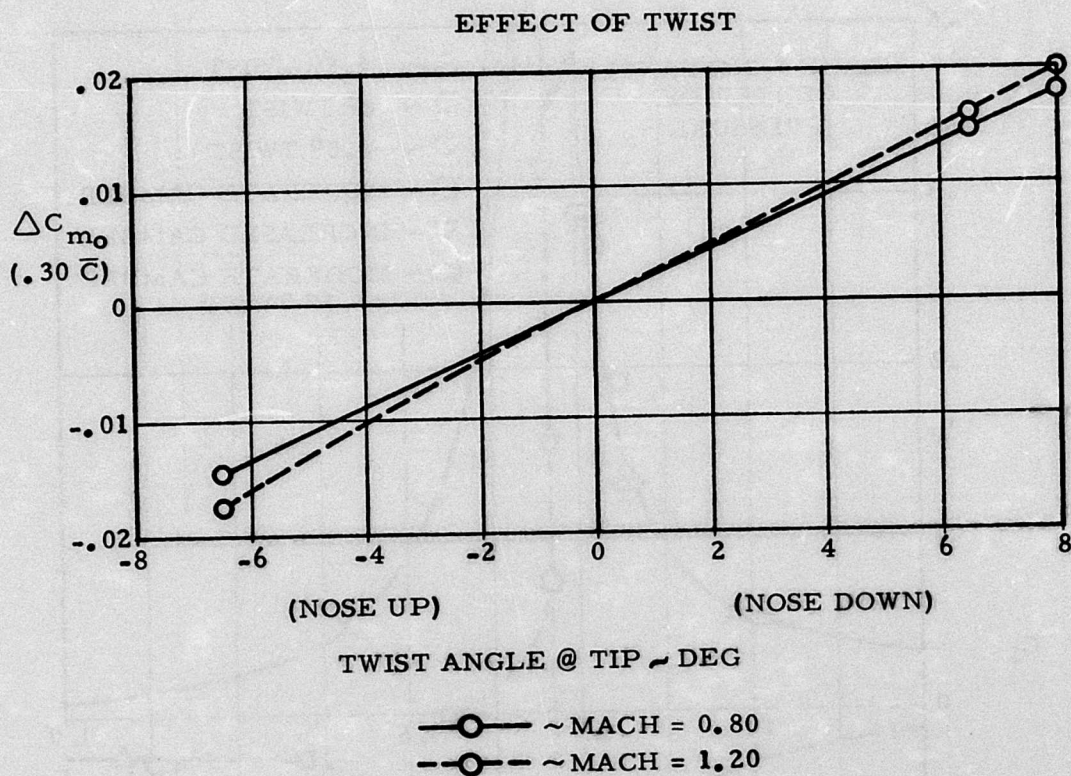


FIGURE 41: EFFECT OF TWIST AND CAMBER ON ZERO LIFT PITCHING MOMENT

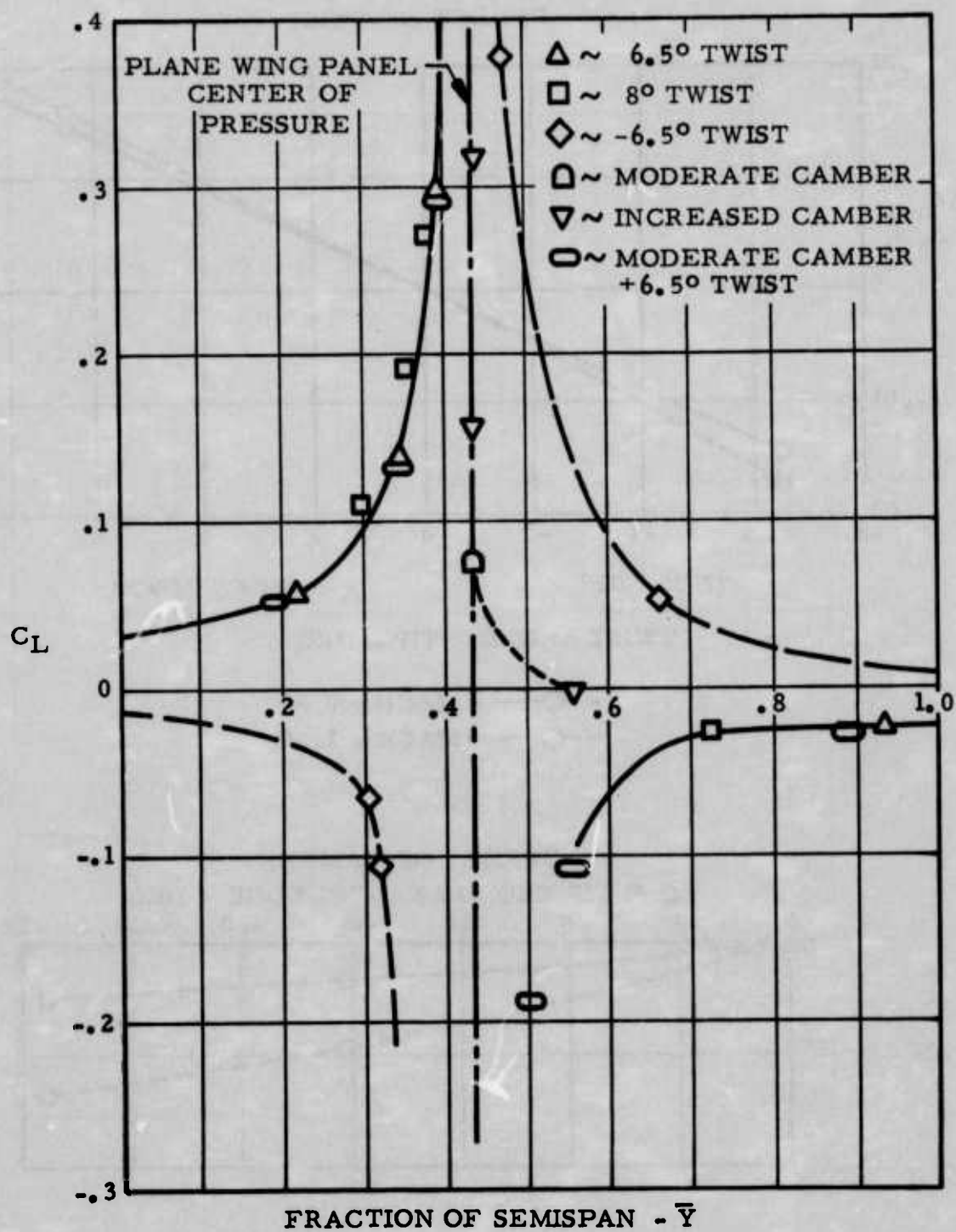


FIGURE 42: SPANWISE LOCATION OF PANEL LOADING $M = .80$

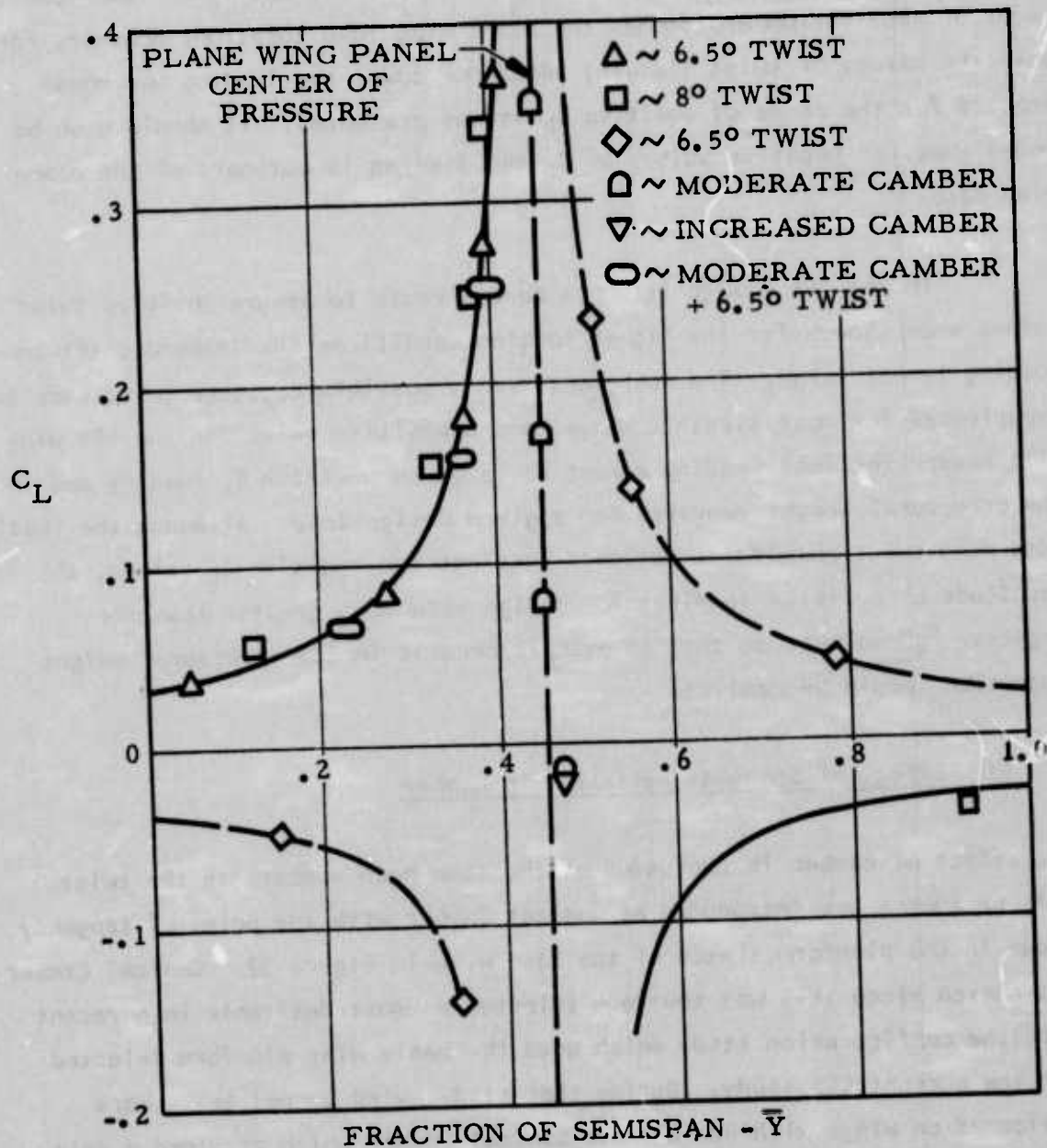


FIGURE 43: SPANWISE LOCATION OF PANEL LOADING $M = 1.20$

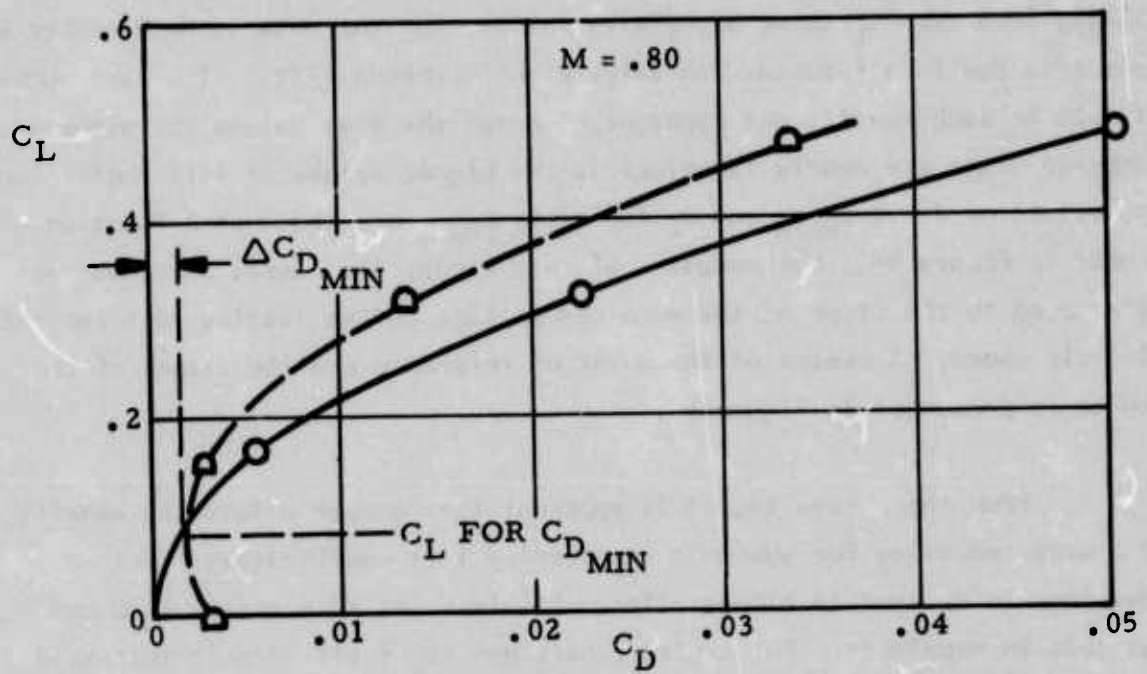
case, zero lift consists of an up load on the inboard portion of the wing and a down load on the outer panels. The combination of these two loadings produces a pure couple with zero lift. For either a net up or down load the point of application approaches the plane wing load location; however, for positive values of twist (leading edge nose down) the loading was moved inboard for the range of positive C_L values presented. It should also be noted that for negative values of C_L the loading is outboard of the plane wing case.

In the CCS design it would be desirable to assure positive twist values even though for the higher loading conditions the inboard shift in loading is not large. The increment from a possible negative twist case as experienced for most flexible wings, and a positive twist for the CCS wing will reduce the root bending moment for a given positive C_L loading and thus the structural weight required for a given design load. Although the leading edge down twist results in outboard loadings for negative C_L values, the magnitude of positive loadings for design were much greater than for negative "g" values, so that an overall benefit in CCS structural weight reduction should be realized.

(3) Effect of Spanwise Variation in Camber

The effect of camber is evaluated at the same Mach numbers as the twist. This parameter was introduced as Conical Camber with the point of tangency shown in the planform sketch of the base wing in Figure 37. Conical Camber was chosen since this was the form selected as most desirable in a recent airplane configuration study which used the basic wing planform selected for the current CCS study. During that study, wind tunnel tests were performed on wings with and without Conical Camber which provided a data base for evaluating the trends noted in the aerodynamic data which are calculated using theoretical methods.

o Drag - Camber has a dual effect on the drag polar as seen in Figure 44. As in the case of twist addition, the minimum drag is increased over the plane wing used as a base. In addition, the C_L for C_{Dmin} is



—○— ~ PLANE WING
 —□— ~ MODERATE CAMBER (16.2° @ TIP)

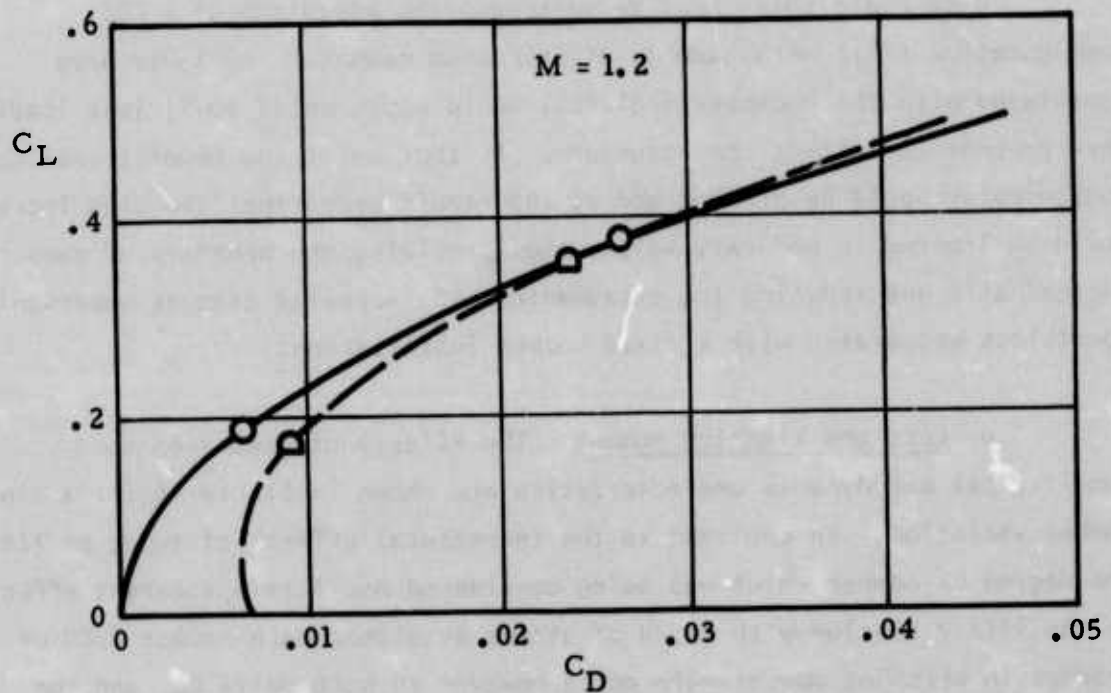


FIGURE 44: EFFECT OF CONICAL CAMBER ON DRAG POLAR SHAPE

case, zero lift consists of an up load on the inboard portion of the wing and a down load on the outer panels. The combination of these two loadings produces a pure couple with zero lift. For either a net up or down load the point of application approaches the plane wing load location; however, for positive values of twist (leading edge nose down) the loading was moved inboard for the range of positive C_L values presented. It should also be noted that for negative values of C_L the loading is outboard of the plane wing case.

In the CCS design it would be desirable to assure positive twist values even though for the higher loading conditions the inboard shift in loading is not large. The increment from a possible negative twist case as experienced for most flexible wings, and a positive twist for the CCS wing will reduce the root bending moment for a given positive C_L loading and thus the structural weight required for a given design load. Although the leading edge down twist results in outboard loadings for negative C_L values, the magnitude of positive loadings for design were much greater than for negative "g" values, so that an overall benefit in CCS structural weight reduction should be realized.

(3) Effect of Spanwise Variation in Camber

The effect of camber is evaluated at the same Mach numbers as the twist. This parameter was introduced as Conical Camber with the point of tangency shown in the planform sketch of the base wing in Figure 37. Conical Camber was chosen since this was the form selected as most desirable in a recent airplane configuration study which used the basic wing planform selected for the current CCS study. During that study, wind tunnel tests were performed on wings with and without Conical Camber which provided a data base for evaluating the trends noted in the aerodynamic data which are calculated using theoretical methods.

o Drag - Camber has a dual effect on the drag polar as seen in Figure 44. As in the case of twist addition, the minimum drag is increased over the plane wing used as a base. In addition, the C_L for $C_{D_{min}}$ is

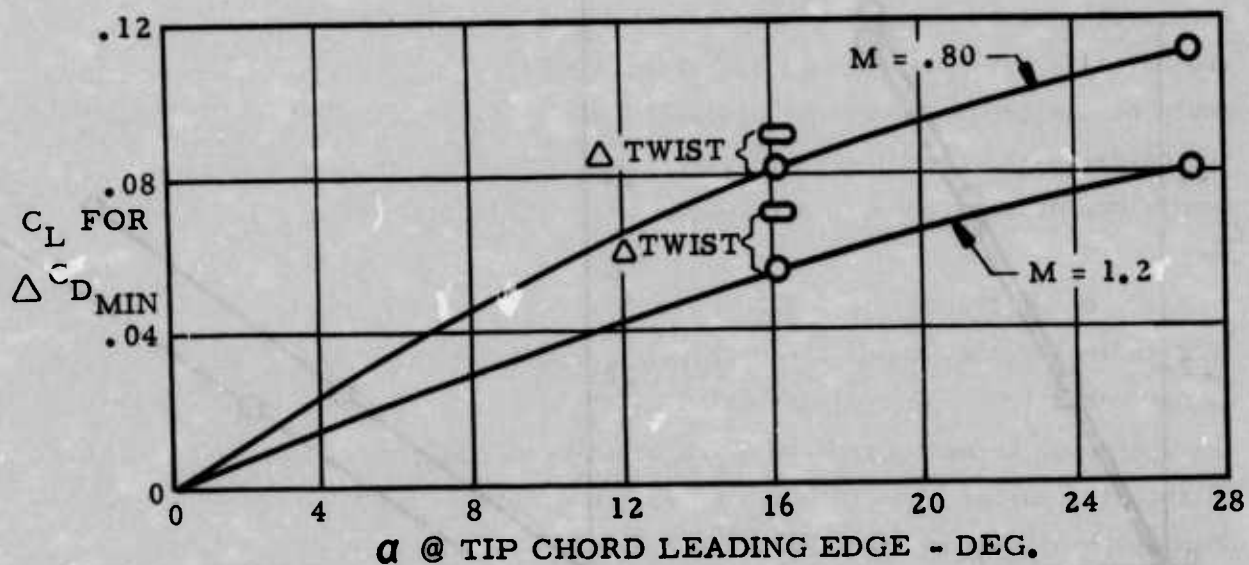
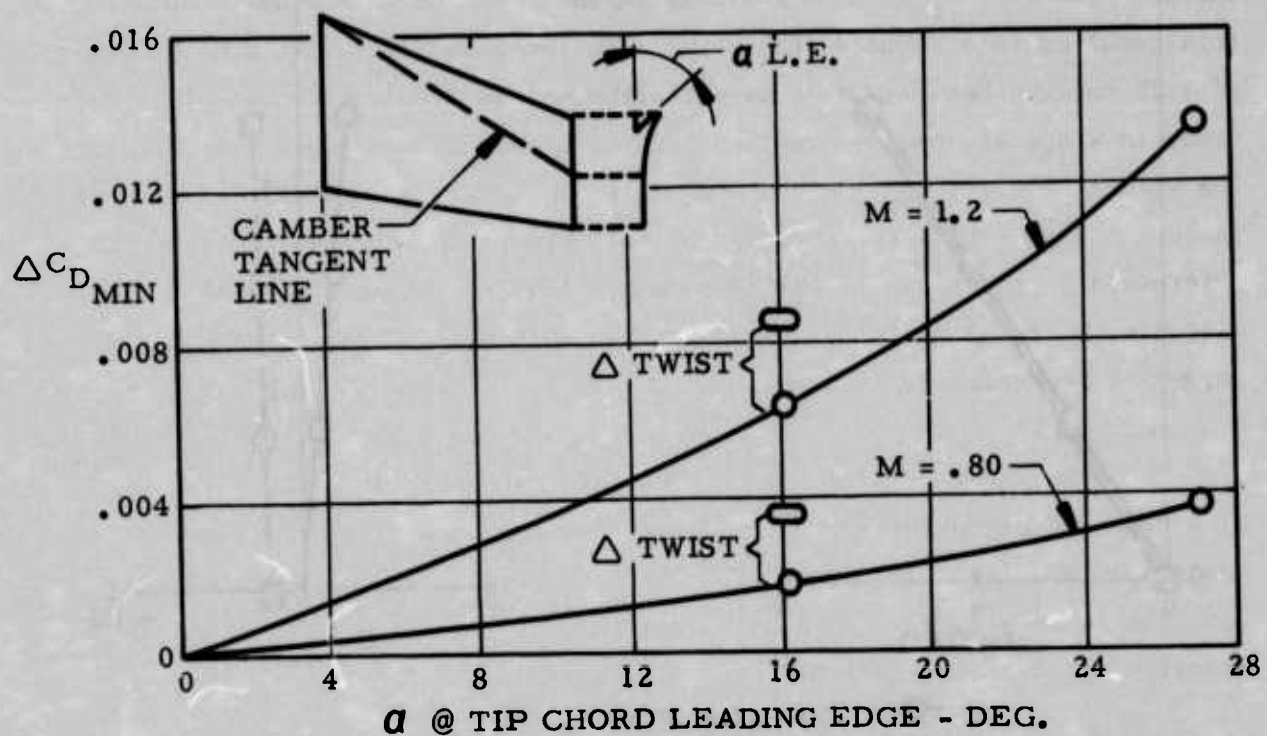


FIGURE 45: EFFECT OF CONICAL CAMBER ON MINIMUM DRAG VALUES

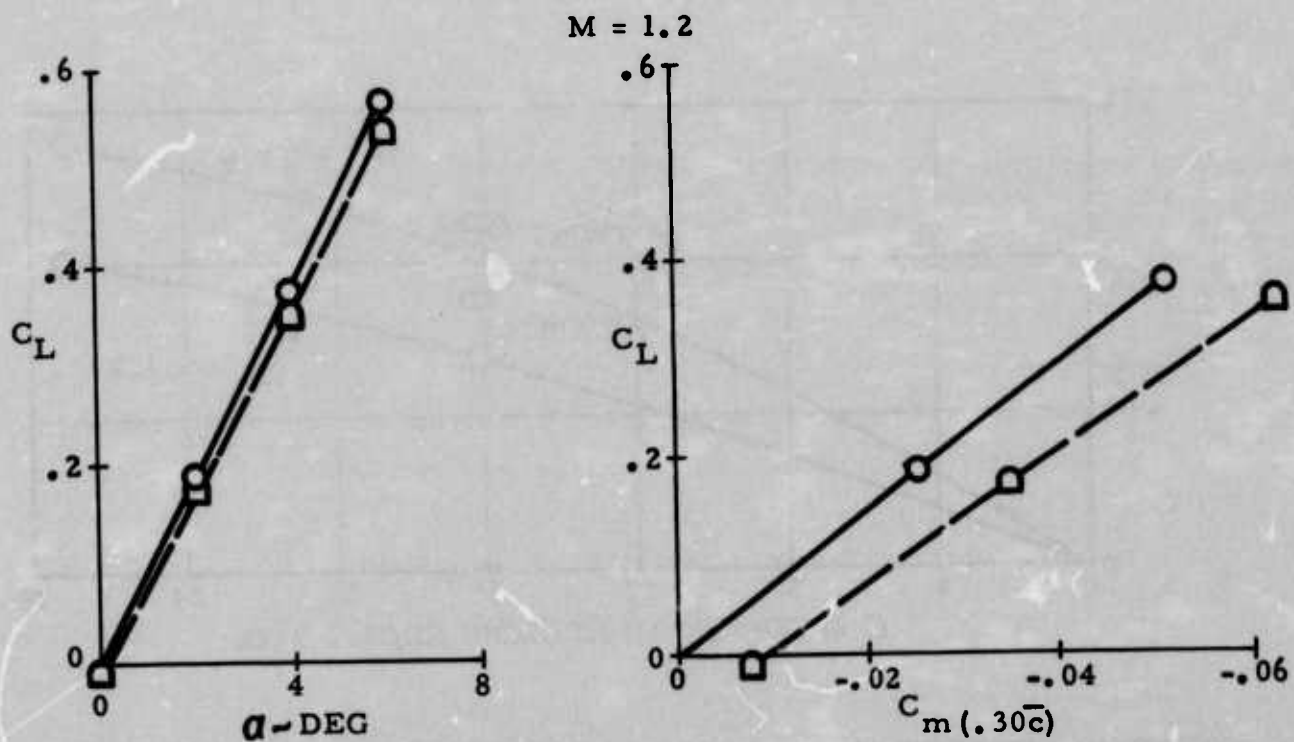
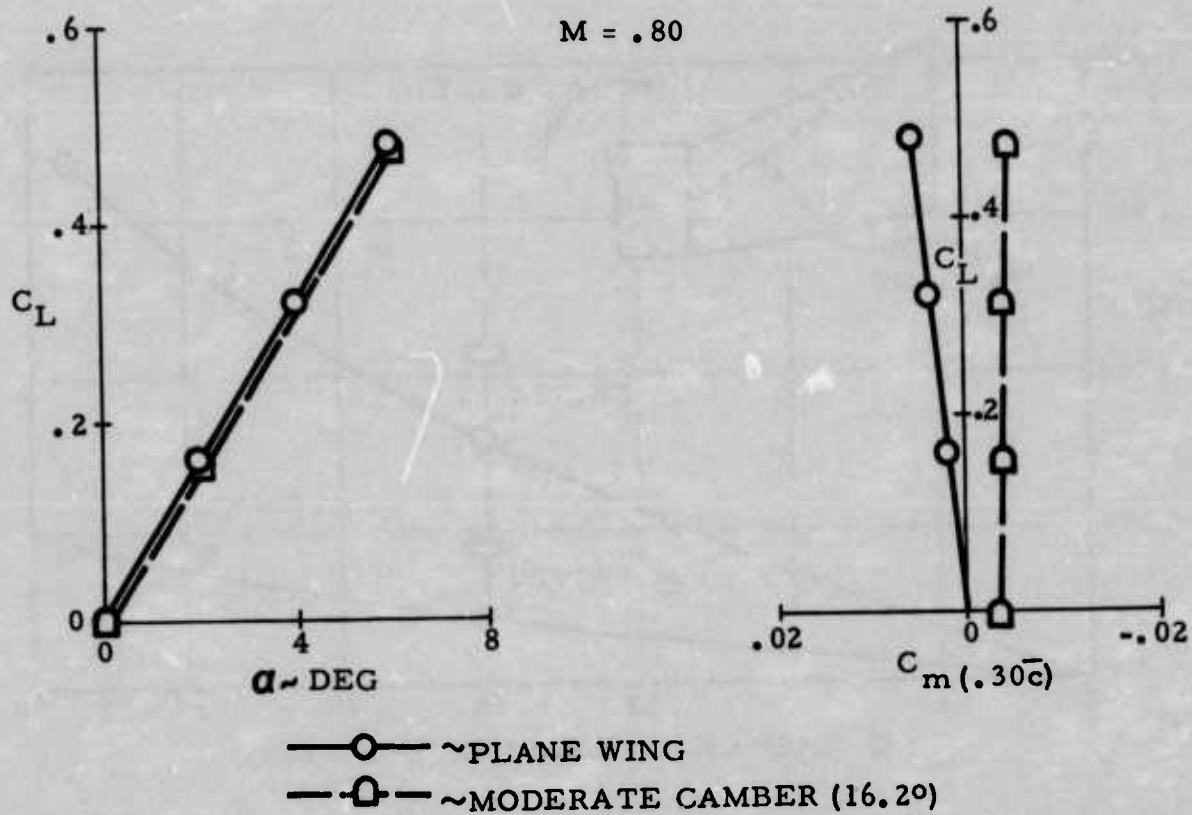


FIGURE 46: EFFECT OF CONICAL CAMBER ON LIFT AND PITCHING MOMENT

moment are undesirable since more horizontal tail incidence is required to trim thus increasing total airplane drag. The increase in static stability, negative dC_m/dC_L , is desirable under certain conditions since a more stable configuration permits reduced trim forces. Stability effects are not shown in summary plot form since this is a secondary effect and was not used in the preliminary evaluation of the effects of CCS configurations on the aerodynamic characteristics. This parameter would play a part in evaluation of a complete balanced airplane system.

If a CCS configuration were to be designed to produce wing leading edge camber, the effects on pitching moment would require detailed review of overall effects on a complete airplane configuration. At low lift levels, the negative ΔC_{m_0} effect would be minimal since the structure would not be deflected; however, the value would increase with increasing load. This increases the horizontal tail trim requirement both as an increase in negative ΔC_{m_0} and as a result of increasing static stability, negative dC_m/dC_L . For this reason it is difficult to make any definitive comment on the effect of camber on the pitching moment characteristics independent of other considerations.

o Spanwise Location of Wing Center of Pressure - Summary plots of loading center of pressure were presented earlier in Figures 42 and 43 when discussing the effects of twist. From a review of these figures, it can be seen that camber does not materially alter the loading center on the wing panel over the base plane wing except at very low lift coefficients. Thus variations in spanwise loading due to camber resulting from a CCS would not be an important consideration in configuration selection.

(4) Combined Camber and Twist

To complete the parametric study, one case of combined camber and twist was analyzed. The spanwise variation of twist, denoted as 6.5 degrees at the wing tip, was added to the "moderate" camber configuration and the aerodynamic data compared to the results discussed previously.

o Drag - A specific drag polar is not presented, however, the trends may be noted by referring to Figure 45. It appears the incremental drag denoted on the plots as "delta twist" is about the value obtained due to twist alone. The C_L for $C_{D_{min}}$ is increased slightly, however, it is not a large value and thus does not shift the drag polar enough to offset the drag increase due to the addition of twist. It would appear that from a drag standpoint no gain is realized over the camber alone case at either Mach number 0.80 or 1.20.

o Lift and Pitching Moment - Comparative plots of lift and pitching moment coefficients are presented in Figures 47 and 48 for Mach numbers of 0.80 and 1.20. These data show the effect of adding a spanwise twist distribution to a wing having a "moderate" amount of camber. For comparison, data for the basic plane wing are also shown so that trends with configuration changes may be seen. From these plots it appears that the effects of twist and camber are additive, with twist responsible for zero shifts in C_L and C_m and camber affecting the static stability parameter dC_m/dC_L . From this standpoint it would appear that a configuration might be tailored to achieve the reduction in trim requirements resulting from the positive C_m due to the addition of twist and a moderate increase in static stability shown due to the addition of camber.

o Spanwise Location of Wing C.P. - In reviewing again the center of pressure location of the various wing configurations in Figures 42 and 43, it becomes apparent that for the combination of camber and twist, the loading distribution is dominated by twist and does not show the trends associated with camber alone. For positive wing loadings this assures a more inboard loading if nominal amounts of twist are incorporated in the wing.

In summary, a parametric study of wing variables which could be altered by externally applied aerodynamic forces has been made to determine their effect on the aerodynamic characteristics of a wing. The major benefits are in the area of drag reduction by alterations to the drag polar, and in reducing the effects of drag due to trim. An additional benefit is possible if the structural deflections result in a properly controlled spanwise variation of

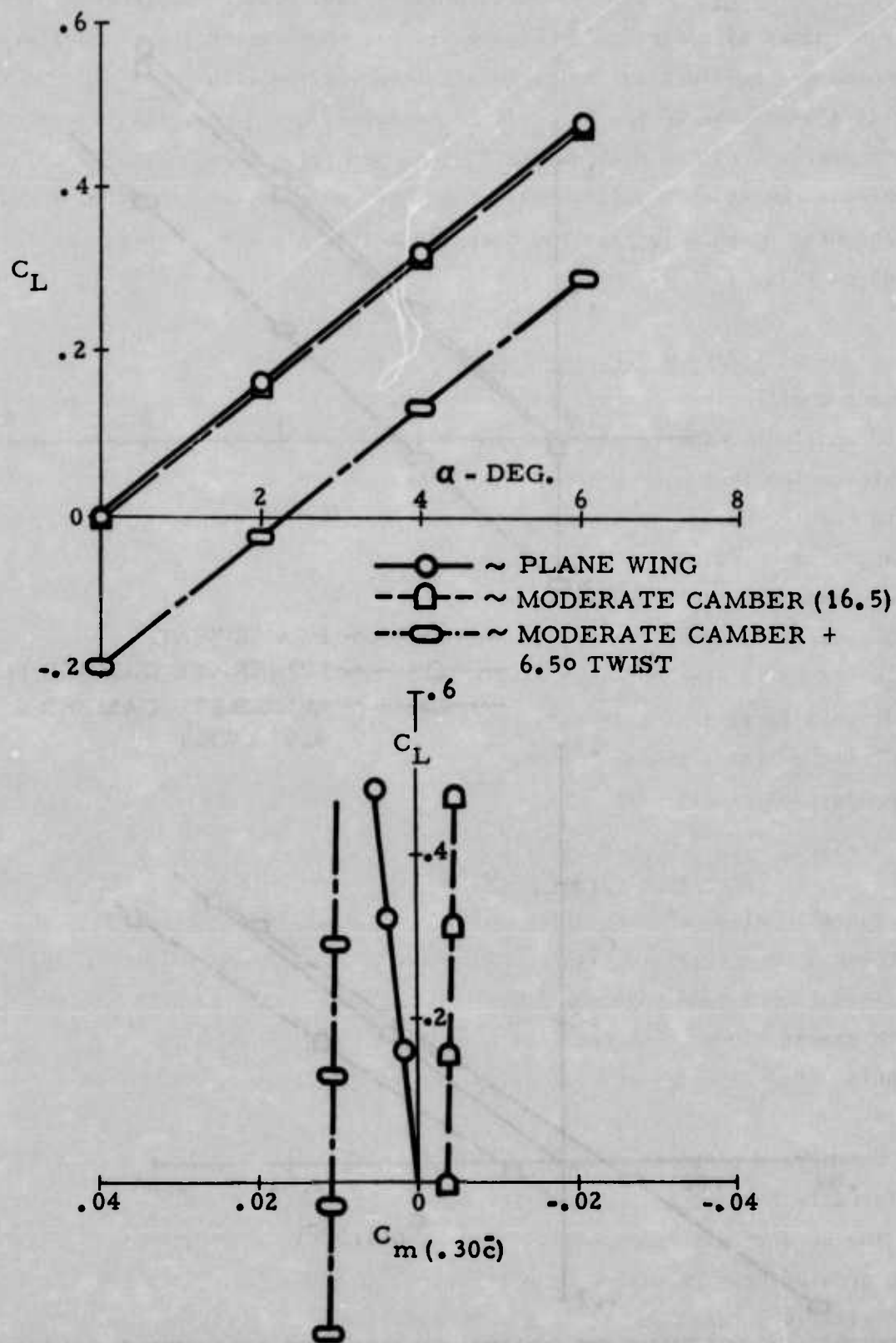


FIGURE 47: EFFECT OF COMBINED CAMBER AND TWIST ON LIFT AND PITCHING MOMENT $M = .80$.

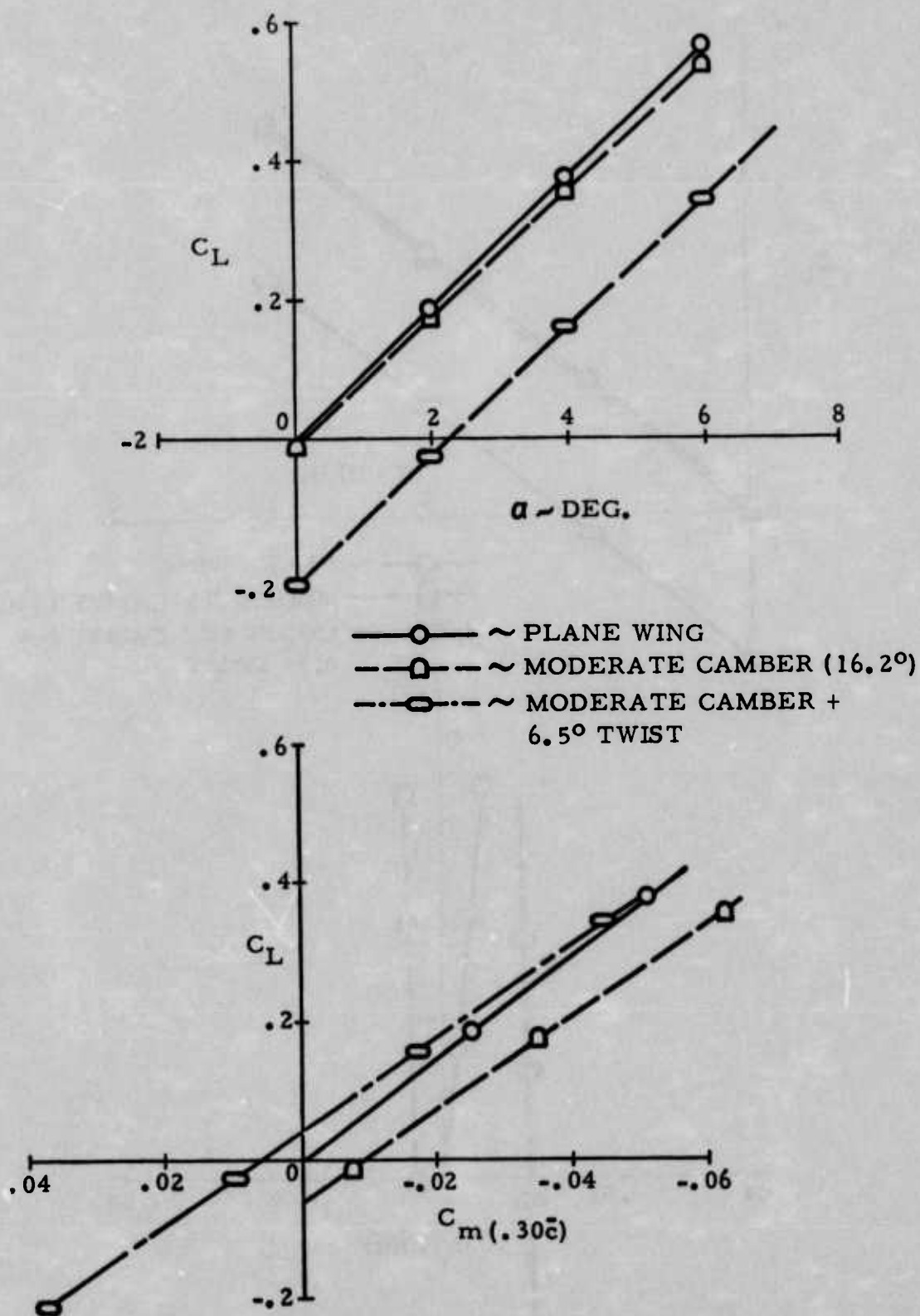


FIGURE 48: EFFECT OF COMBINED CAMBER AND TWIST ON LIFT AND PITCHING MOMENT $M = 1.20$

twist which will produce an inboard shift of loading with an increase in lift due to "g". This permits a reduced structural weight due to the reduced wing root bending for a given aerodynamic lift requirement.

2. ANALYSIS METHODS

The methods used to coordinate aerodynamic analysis with the Structural analysis is illustrated in the flow diagram presented in Figure 49. For the initial parametric study, aerodynamic data were evaluated for the rigid case with no structural deformation due to loading. Data thus obtained were used to show the desired trend and orders of magnitude of aerodynamic characteristics with geometric and Mach number variables. This was the standard procedure used in preliminary design prior to wing structural definition.

With the wing internal structure defined, a panel point definition could be made. This was then used to generate structural influence coefficients. Using this same panel point definition, aerodynamic influence coefficients were calculated independently using the Woodward-Carmichael routine previously reported in Reference 2. These data were then used in a finite element flexible solution which provided aerodynamic data for equilibrium twist conditions at any preselected flight condition. For the purposes of this analysis, the aerodynamic data were calculated at Mach numbers of .80 and 1.20 for 4 "g" flight at 10,000 feet. The routine also calculated spanwise loading information which was fed into FASTLOADS to yield the spanwise variation in shear, bending and torsion moment. These data were used for final evaluation of the proposed configurations.

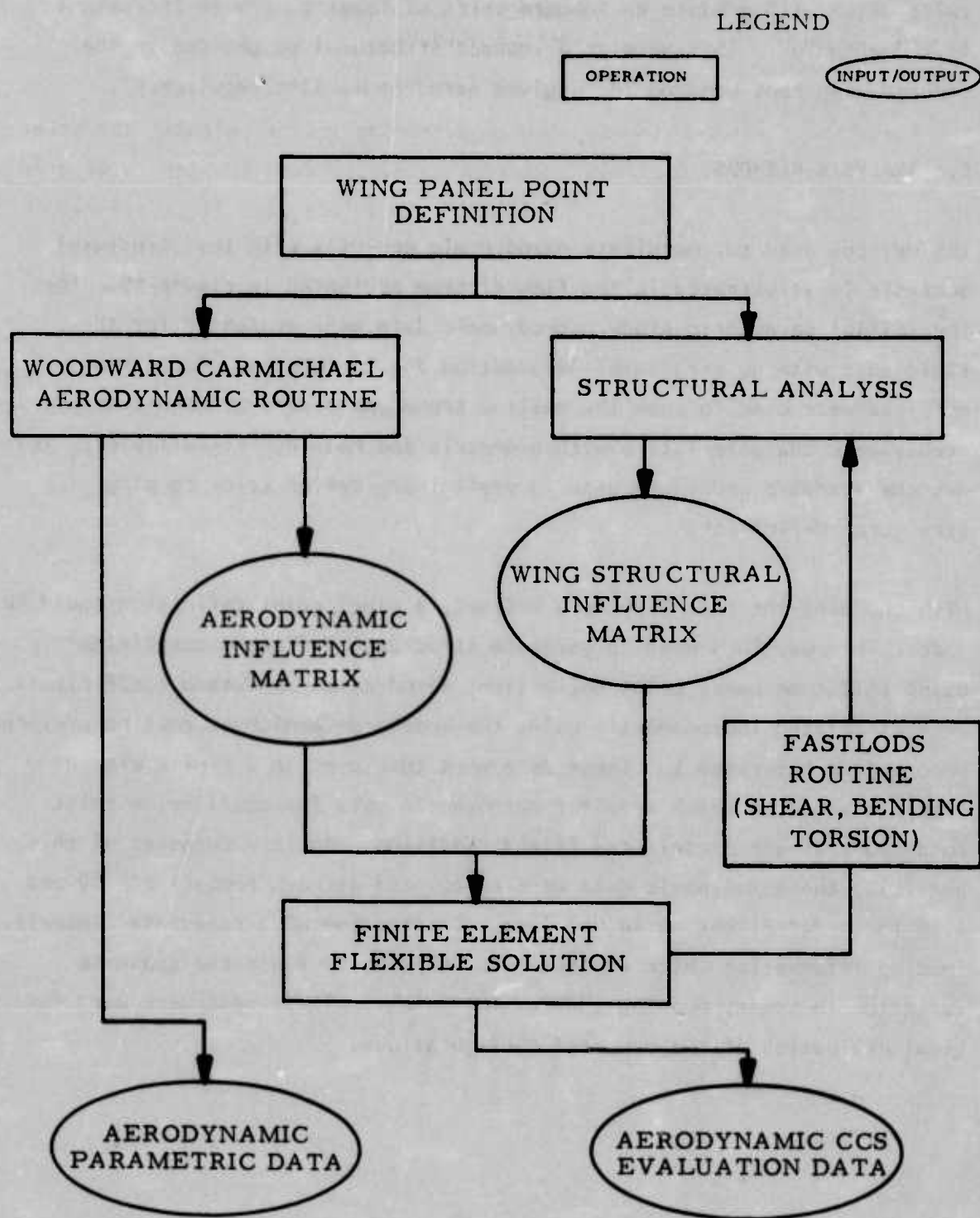


FIGURE 49: FLOW DIAGRAM FOR AERODYNAMIC METHODS EMPLOYED IN CCS ANALYSIS

APPENDIX C DYNAMICS METHODS

Stiffness and inertia data was used to determine the aeroelastic characteristics of the various wing design configurations. Desired structural grid point locations and inertia slice boundary locations were first defined. Then a main wing box influence coefficient matrix was defined for the Dynamics grid points and main wing box inertia slice data was defined for the Dynamics slice boundaries.

These data were then used to perform modal analyses of the different configurations, and the model data was used then to perform airforce analysis on the wings. The airforce matrices obtained were those determined by the Doublet Lattice Method.

The modal and airforce data were then used to write the equations of motion in generalized form, and these equations were then solved to determine at what speeds instabilities (flutter) should be expected. These analyses result in flutter speed versus damping curves. The flow diagram illustrating the interface and function activities related to the dynamics analysis is shown in Figure 50.



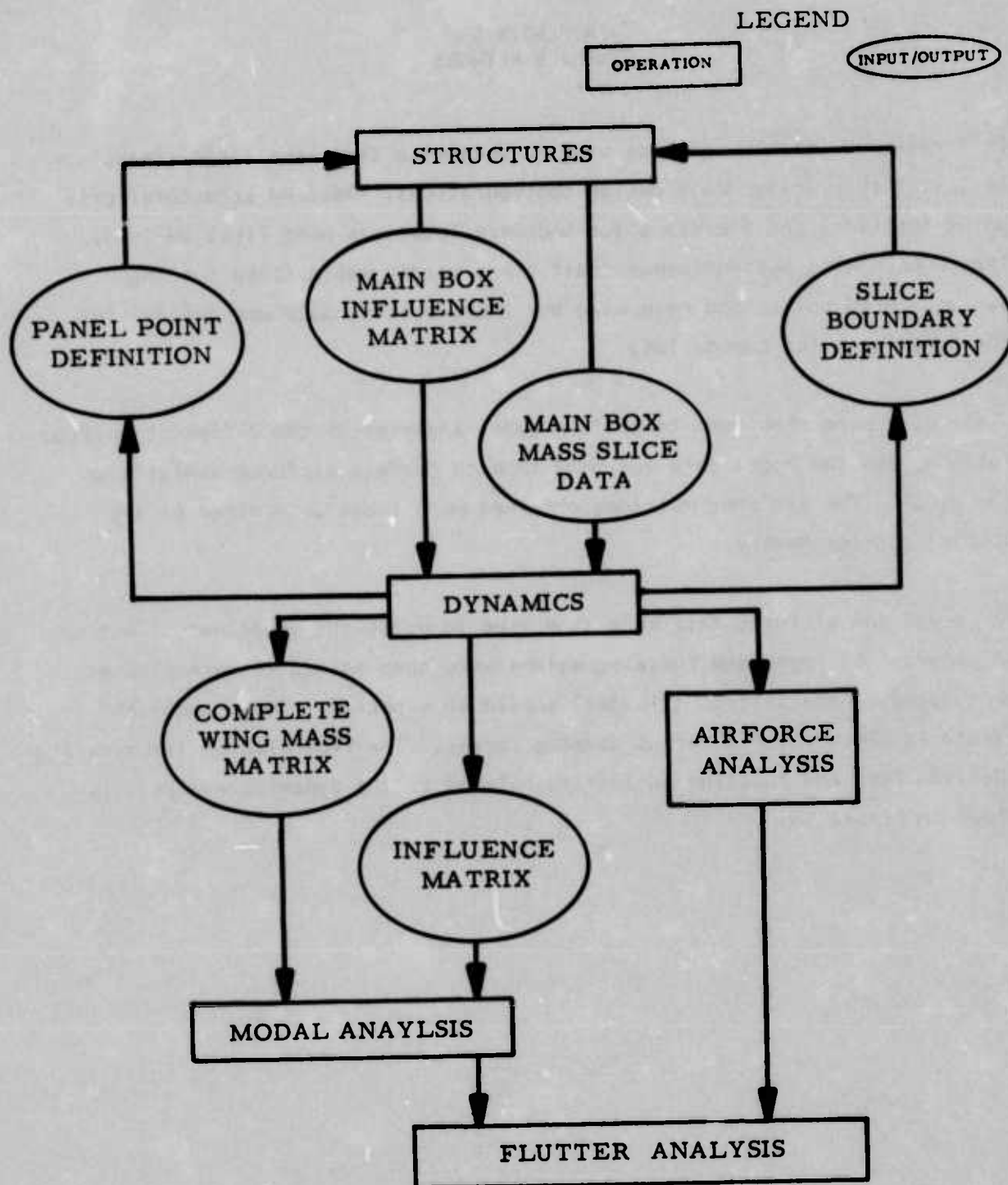


FIGURE 50: FLOW DIAGRAM FOR DYNAMICS METHODS EMPLOYED IN CCS ANALYSIS